UNIVERSITY OF CALIFORNIA
SANTA CRUZ

IDENTIFYING A MUTANT RESPIRATORY SYNCYTIAL VIRUS G IMMUNOGEN AS A VACCINE CANDIDATE

A dissertation submitted in partial satisfaction
of the requirements for the degree of

DOCTOR OF PHILOSOPHY

in

MICROBIOLOGY and ENVIRONMENTAL TOXICOLOGY

by

Ana Maria Nuñez Castrejon

September 2022

The Dissertation of
Ana Maria Nuñez Castrejon is approved:

_____
Rebecca DuBois, Ph.D.

_____
Victoria Auerbuch-Stone, Ph.D.

_____
Jacqueline Kimmey, Ph.D.

_____
Peter Biehl
Vice Provost and Dean of Graduate Studies

Table of Contents

List of Figures

Chapter 2

Chapter 3

List of Tables

Chapter 2

Chapter 3

Abstract

Identifying a Mutant Respiratory Syncytial Virus G Immunogen as a Vaccine Candidate

Ana Maria Nuñez Castrejon

Respiratory syncytial virus (RSV) is the top cause of severe lower respiratory disease in infants and children and causes over 100,000 deaths in children worldwide each year. RSV is also a leading cause of respiratory disease in immunocompromised and elderly populations. However, no FDA approved vaccine exists to protect against RSV infection. RSV contains two immunogenic proteins on its envelope, RSV F and RSV G, that have been the targets of vaccine developmental strategies. Most current efforts to create a vaccine against RSV focus on RSV F, and several candidates are in phase III clinical trials. The only current prophylaxis available for RSV is a monoclonal antibody against RSV F, yet it does not prevent infection. RSV G as a vaccine immunogen is linked to vaccine enhanced disease and is poorly immunogenic, however anti-RSV G antibodies have been shown to be protective in animal models of RSV disease and correlate with protection in humans. In this thesis, I present the history of an inactivated RSV vaccine that caused vaccine enhanced disease in children, a summary of studies using RSV G as a vaccine antigen, and an overview of the RSV G vaccine antigens currently in clinical trials. I present data showing that the structure-based design of an RSV G immunogen with a mutation in the central conserved domain is a promising vaccine candidate. Finally, I present studies to investigate RSV G binding and activation of the human chemokine receptor

CX3CR1 on mammalian cells. Overall, these studies provide a foundation for the further development of the RSV G immunogen as a vaccine candidate to protect against RSV disease.

Acknowledgements

First, I would like to thank my advisor, Dr. Rebecca DuBois, for the guidance and mentorship I received these last five years. Thank you for allowing me to grow and discover my skills. Thank you for the patience, understanding, and giving me the time I needed for writing my literature review, studying for two qualifying exams, writing my first author paper, and now for writing my thesis. Thank you for allowing me to have a work-life balance. I would also like to thank my thesis committee members, Dr. Vicki Auerbuch-Stone and Dr. Jacqueline Kimmey for your support and advice.

I would also like to thank the DuBois lab members past and present. Thank you to Dr. Sara O'Rourke for showing me the ropes with mammalian protein expression, helping me troubleshoot my cell-based assays, and reassuring me when my imposter syndrome was getting the best of me. Thank you to Dr. John Dzimianski for helping me through the X-ray crystallography process from answering questions about setting up drops to showing me how to use the microscope, helping me scoop and freeze my crystals, helping me shoot my crystals, helping me process my data, and helping me learn the X-ray crystallography software. Thank you, Nicholas Lorig-Roach, for helping me troubleshoot my experiments, letting me bounce ideas, and being there to help me interpret my data. I would like to thank Dr. Stanislav

Fedechkin, Natasha George, and Joshua Dillen for training me during my rotations and my first year in the DuBois lab. Thank you for helping me learn *E. coli* protein expression and purification and helping me feel more confident in cell culture. Thank you to all other lab members that have at some point helped me use the floor centrifuge that I hated so much.

Thank you to the Microbiology and Environmental Toxicology department and the PBSE program. Thank you to our collaborators Trellis BioScience and Dr. Ralph Tripp's lab for the reagents that made our experiments possible. Thank you to the Eugene Cota-Robles Fellowship that provided three years of funding for me. Thank you for seeing the potential in me and allowing me to focus on my learning and developing my skills.

Next, I would like to thank my family for all the love and support I have received from everyone. Thank you to my parents Maria and Nereo Nuñez, to my sisters Nely, Lina, Luz, Dulce, Joci, and Chels, to my brothers Arnold and Lando, to my brother in laws Oscar, Oscar, Lalo, Camilo, and Elber and my sister in laws Maria and Marci, and to my nieces and nephews. I love you all and am grateful to have such a big village.

Finally, thank you to all the friends I have made along the way. Thank you to my cohort and the cohort before mine. I appreciate all the love and support I have received from all of you as well. I would especially like to thank Nicholas Santiago and Juliana Nzongo for your friendship and helping me through the wild times that happened alongside getting this Ph.D.: the power outages, the COLA strike, the

COVID shut down, the wildfires, and two separate quarantine isolation times. Thank you to the dinner party/ camping team Nick, Ash, and Maryam.

Chapter 1:

Development of an RSV vaccine targeting the RSV G antigen: history and current views

1.1 Introduction

Respiratory syncytial virus (RSV) is the leading cause of severe lower respiratory tract disease in children under two years of age and is also a major contributor of respiratory disease in elderly and immunocompromised individuals (1, 2). There are between 57,500 to 100,000 hospitalizations of children under five years of age and about 11,000 deaths of elderly individuals due to RSV infection in the US annually (3–5). Worldwide, RSV causes over 100,000 deaths in children under 5 each year, mostly in lower-income countries (4).

RSV is an enveloped RNA virus in the pneumoviridae family. RSV contains a negative-sense single-stranded RNA genome that encodes 11 proteins (6). The surface of the RSV virion is studded with two major immunogenic envelope glycoproteins, RSV F and RSV G, which are targets of neutralizing antibodies (7, 8).

The RSV F fusion glycoprotein is used to fuse viral and host cell membranes (9). RSV F is conserved, highly immunogenic, and required for infectivity, thus has been the target of most vaccine developmental strategies (9–12). The monoclonal antibody palivizumab (Synagis) targets the F protein and is the only current prophylaxis available to reduce hospitalizations due to RSV (13–15). Palivizumab is

administered only to at-risk patients, who include premature infants and infants with chronic lung disease or congenital heart disease (13). This antibody must be injected once a month throughout the RSV season, and the cost of treatment with palivizumab can range from $1,500 to $4,300 per dose (13). Motavizumab is a higher-affinity monoclonal antibody derived from palivizumab, however it was not FDA approved because it did not provide better protection than palivizumab against RSV infection (16). Additionally, motavizumab resulted in hypersensitivity in clinical trials (16, 17).

In addition to RSV F fusion glycoprotein, RSV utilizes the RSV G glycoprotein to attach to respiratory epithelial cells and certain immune cells. RSV G's overall sequence is highly variable and contains abundant glycosylation modifications in its two mucin-like regions which contribute to RSV G's variability (9). Despite RSV G's central role in RSV infection, it has been overlooked as a potential vaccine target due to its sequence variability, poor immunogenicity, and safety concerns described in the next section. However, RSV G contains a highly conserved unglycosylated region called the central conserved domain (CCD) (18). Several lines of evidence support that the RSV G's CCD, which contains a CX3C motif, binds to the human chemokine receptor, CX3CR1, on respiratory epithelial cells to promote virus infection and dampen the host anti-viral response (19–22). Additionally, a secreted, soluble form of RSV G binds to CX3CR1+ immune cells and interferes with the activities of the natural ligand of CX3CR1, CX3CL1 or fractalkine (23–26).

However, broadly neutralizing monoclonal antibodies against RSV G's CCD, such as the antibodies 3D3 and 3G12, reduce viral loads and symptoms of disease more extensively than palivizumab *in vivo* (discussed further in section 1.4) (27–29). Furthermore, higher anti-RSV G antibody levels correlated with less severe disease in children and infants upon RSV infection (30).

While RSV vaccine strategies have historically focused on the RSV F antigen, many studies reveal the importance of the RSV G antigen in generating protective immunity. Here, we review the history of RSV G-containing vaccines and highlight recent studies supporting RSV G as an essential RSV vaccine antigen.

1.2 Formalin-inactivated RSV vaccine

The first RSV vaccine candidate, formalin inactivated RSV (FI-RSV), lead to vaccine enhanced disease (VED) in immunized subjects. Eighty percent of FI-RSV immunized children were hospitalized after natural infection with RSV (31, 32). Two deaths occurred as a result of FI-RSV immunization due to VED (32, 33). The original autopsy described excess eosinophil infiltration into the lungs, making eosinophilia a key endpoint for VED in subsequent studies in animal models (32). However, rereview of autopsy reports revealed neutrophilia. More recent studies suggest that eosinophils do not have a role in VED, and instead Th2-biased cytokine/chemokine responses to infection, and the induction of non-neutralizing antibodies, are better markers of VED (34–38). This evolving view on the mechanisms of VED should be kept in mind when reviewing previous literature on vaccine studies with RSV G immunogens.

Studies have shown that immunizing animal models with RSV G prior to RSV challenge leads to some features of vaccine enhanced disease, resulting in a long-lasting impression that RSV G is an unsafe vaccine immunogen (39–41). One study investigated the different immune responses of mice immunized with vaccinia virus (vv) expressing WT RSV G (vvWTG), membrane-anchored only RSV G (vvM48I), or secreted only RSV G (vvM48) (42). This study found that mice immunized with vvM48 had more severe disease, higher lung viral loads, and the highest concentration of eosinophils in the lungs compared to mice immunized with vvWTG or vvM48I after RSV challenge. Mice immunized with vvM48 and vvM48I co-administered with purified secreted RSV G and challenged with RSV had the highest levels of the Th2 cytokine IL-5. Antibody titers were highest in mice immunized with vv containing membrane-anchored RSV G (42). This study shows that RSV G can induce eosinophilia and a Th2-biased response that leads to more severe disease upon RSV infection.

A separate study suggested that the VED associated with FI-RSV immunization was due to RSV G, specifically the CX3C motif within RSV G (26). Mice immunized with formalin inactivated RSV A2 and administered with an anti-CX3CR1 antibody challenged with RSV did not develop eosinophilia. Additionally, mice immunized with an RSV strain with a point mutation at amino acid 186 (Cysteine to Arginine) within the CX3C motif that was formalin inactivated and challenged with that same strain also did not develop eosinophilia, which suggests that the CX3C motif of RSV G promotes eosinophilia upon RSV infection (26).

To further investigate the mechanism of vaccine enhanced disease due to FI-RSV immunization, additional studies have been carried out using BALB/c mice and cotton rats. While mice immunized (primed) with FI-RSV or vvGs and challenged with RSV both lead to VED with lung eosinophilia, differences in Th2 cytokines such as IL-4 (differentiates T cells into Th2 T cells), IL-5 (activates eosinophils), IL-13 (can lead to the overproduction of mucin), and eotaxin (eosinophil recruitment), suggest the mechanism of VED is different (34, 35, 43). Priming with FI-RSV that leads to VED is dependent on IL-4 and lung eosinophilia is reduced in IL-4 depleted mice immunized with FI-RSV, however IL-4 depleted mice primed with vaccinia virus expressing the secreted form of RSV G (vvGs) had similar eosinophil recruitment into the lungs as control mice immunized with vvGs, which suggests that eosinophilia induced by RSV G is IL-4 independent (34).

Notably, one study showed that eosinophil deficient mice immunized with FI-RSV and challenged with RSV had similar lung viral loads, histopathology scores, and airway function as wild-type mice, which suggests that eosinophil infiltration into the lungs is not the cause of VED (36). This study also showed that STAT6 (a transcription factor needed to differentiate CD4 T cells into Th2 cells) deficient mice immunized with FI-RSV and challenged with RSV had overall lower levels of the Th2 cytokines IL-4 and IL-13 in the lungs, less eosinophil infiltration into the lungs, less airway hyperreactivity, mucus hypersecretion, and lower histopathology scores compared to wild-type mice, which demonstrates that CD4 T cells play a role in VED (36).

A separate study used various forms of formalin inactivated recombinant RSV to immunize mice: wild-type RSV, RSV without RSV G, RSV without the heparin-binding domain of RSV G, or RSV without the SH envelope protein (35). This study showed that mice immunized with any of these versions of FI-RSV and challenged with RSV all led to weight loss, eosinophilia, similar histopathology scores, the induction of Th2 cytokines, and that mice immunized with mutant FI-RSV had higher lung viral loads four days after RSV challenge (35). These data suggest that vaccine enhanced disease still develops in mice immunized with FI-RSV even in the absence of RSV G.

Furthermore, immunizing mice with FI-RSV or with recombinant vaccinia virus expressing secreted RSV G (vvGs) predisposes naïve mice to enhanced disease in the form of eosinophil infiltration into the lungs and excessive Th2 cytokine and chemokine production (43). This study demonstrated that the CD4+ T cells that are stimulated by RSV G are predominately Vβ14+ in T cell receptor (TCR), and that depleting Vβ14+ T cells lead to less severe disease in immunized mice (43). To determine whether vaccine enhanced disease caused by FI-RSV and RSV G is caused by the same mechanism, mice were immunized with vaccinia virus expressing secreted RSV G (vvGs) or FI-RSV and Vβ14+ T cells were depleted by treatment with an antibody against Vβ14 and challenged with RSV (43). Vβ14+ T cells were found to play a role in recruiting eosinophils to the lungs of mice immunized with vaccinia virus expressing secreted RSV G but not when they are immunized with FI-

RSV. Additionally, Vβ14+ T cells play a role in producing Th2 biased cytokines and chemokines in mice immunized with vvGs but not FI-RSV (43).

Overall, these results suggest that although immunization with FI-RSV and RSV G result in similar pathologies, the mechanism by which vaccine enhanced disease occurs is different and is still under investigation. Nevertheless, the vaccine-enhanced disease pathologies observed after immunization with vvGs or recombinant RSV G protein (described below) illuminated safety concerns about the RSV G antigen and supported the development of new strategies to reduce known markers of VED in pre-clinical animal models of RSV infection and disease.

1.3 Factors to consider in the development of an RSV vaccine

One factor to consider in RSV vaccine development is that there are multiple target populations including pregnant individuals, RSV-naïve infants, RSV-exposed children, and elderly individuals, and different populations may benefit from different vaccines. It should be noted that vaccine enhanced disease only occurred in RSV-naïve children that were vaccinated with FI-RSV and not in RSV-exposed children (31, 44). Thus, animals models that are used to study vaccine enhanced disease should be naïve to RSV infection prior to vaccination (31). FI-RSV mediated VED has now been modeled in RSV-naïve mice, cotton rats, and nonhuman primates.

1.4 Anti-RSV G antibody as a prophylaxis or treatment

An approach to develop an RSV vaccine involves using anti-RSV G antibodies prophylactically or as treatment after RSV infection.

The anti-RSV G antibody, CB017.5, has been shown to reduce inflammation and viral loads in a cotton rat prophylactic and treatment model (45).

Human anti-RSV G antibodies 3G12 and 3D3 have been shown to reduce pulmonary inflammation, lung airway resistance (28) and lung viral loads in a mouse prophylactic and treatment model (27, 28). Human anti-RSV G antibody 2B11 and 3D3 have also been shown to reduce lung viral loads, BAL cell influx, and histopathology scores in a mouse prophylactic and treatment model (29).

An additional anti-RSV G antibody that was explored for its ability to protect against RSV disease is the mouse anti-RSV G 131-2G. 131-2G was used to immunize naïve mice and mice immunized with FI-RSV to determine whether it could decrease pulmonary inflammation (46). Mice immunized with 131-2G had a reduction of cell infiltration in their bronchoalveolar lavage fluid, decreased levels of IFN-γ, and inhibited virus replication in the lungs (46). Mice immunized with FI-RSV and then treated with 131-2G had decreased weight loss and pulmonary cell infiltration compared to FI-RSV immunized mice and treated with an antibody Ig control (46). These results suggest that 131-2G decreased FI-RSV induced pulmonary inflammation and weight loss. A few other studies have shown that 131-2G can reduce lung viral loads, mouse weight loss, and pulmonary inflammation (47–53).

These studies show that anti-RSV G antibodies are protective in animal models as a prophylaxis and treatment after RSV challenge. No anti-RSV G antibody has been tested in clinical trials. Currently, the only prophylaxis available to protect against RSV is palivizumab an anti-RSV F antibody. Another anti-RSV F antibody,

nirsevimab, has recently finished phase III clinical trials and was shown to have an efficacy of 74.5% against medically attended RSV infection, and a 62% efficacy against hospitalization for RSV infection (54).

1.5 Live RSV vaccines

Live attenuated RSV vaccines have been prioritized for vaccines tested in infants due to the adverse effects and deaths that resulted from the FI-RSV vaccine of the 1960s. A previous study used two RSV strains (RSV A2 and r19F) with a mutated CX3C motif to immunize mice to determine the efficacy and immunogenicity of a live RSV vaccine because a limitation of live attenuated vaccines is a balance between attenuation and immunogenicity (11, 55). Immunizing mice with RSV strains containing a mutated CX3C motif did not lead to enhanced disease and elicited protective antibodies suggesting that disrupting RSV G's interaction with CX3CR1 can be protective in mice (55).

An additional study used recombinant live attenuated influenza vaccine (LAIV) as the vaccine platform for RSV G aa 131-230 fused to hemagglutinin (LAIV-G1 or LAIV-G2) to immunize BALB/c mice (56). Mice immunized with LAIV-G1 or LAIV-G2 elicited the highest Th1 antibody IgG2a before RSV challenge compared to all other groups. These mice also elicited the highest IgG and IgA antibody titers, lower lung viral loads, and lower histopathology scores after RSV challenge (56).

1.6 Nucleic acid vaccines

Another strategy to develop an effective RSV vaccine involves immunizing with plasmid DNA or mRNA encoding RSV antigens. One such study used a bacterial host to deliver a DNA vaccine to induce a specific immune response. C57BL/6J mice were immunized with either a DNA vaccine of truncated RSV G, consisting of the central conserved region amino acids 130 to 230 with the CTL epitope of RSV M replacing the CX3C motif and a histidine tag, by orally infecting the mice with *Salmonella* Typhimurium containing the plasmid or by an intramuscular injection of purified truncated G produced in *Escherichia coli* (57). Both vaccines induced anti-G antibodies and also reduced expression of pro-inflammatory cytokines in the lung and trachea along with histamine concentration and immune cell infiltration into the lungs (57). These results suggest that a DNA vaccine delivered through *Salmonella* can reduce RSV induced pathology in C57BL/6J mice. To our knowledge, no mRNA vaccines encoding RSV G have been evaluated, however recently an mRNA vaccine encoding RSV F has entered phase III clinical trials (Moderna).

1.7 Virus-like particles vaccines

One RSV vaccine developmental strategy involves using virus-like particles (VLPs), which are similar to live viruses in that the antigens are presented on the surface of a lipid membrane particle, however VLPs do not contain a genome and thus cannot replicate (58). Strategies have involved using RSV F VLPs, RSV G VLPs, or a combination of RSV F and G VLPs to elicit protective immunity against RSV infection. One study used the RSV G sequence alone or RSV G fused to a

partial repeat, RSV G central conserved region amino acids 150 to 260, that contains known T and B cell epitopes (58). Both RSV G VLP-immunized mice had an increased population of memory B cells compared to mice that were mock immunized. Eosinophil infiltration, mucin production, and lung viral loads were decreased in VLP-immunized mice compared to FI-RSV immunized mice (58) which suggests that RSV G VLPs are protective in mice. However, a separate study found that mice immunized with VLPs expressing RSV F or RSV G or immunized with both VLPs had similar lung viral loads compared to mice immunized with FI-RSV (59). Additionally, mice immunized with VLP F or both VLPs elicited higher IgG titers compared to all other groups. Mice immunized with both VLPs also had the highest levels of the Th1 cytokines, IFNγ and IL-2, and mice immunized with FI-RSV had the lowest levels. Furthermore, mice immunized with FI-RSV or VLP G had the highest eosinophil infiltration into the lungs and the highest mucus production compared to all other groups (59). The differences observed in these two studies (Kim et al., and Lee et al.,) could be explained by the route of immunization. Kim et al., immunized mice intranasally and Lee et al., immunized mice intramuscularly which can lead to different immune responses. The studies also used different strains of RSV A2 to challenge immunized mice which can also lead to different responses because BALB/c mice are not as permissive to RSV infection compared to other animal models.

Furthermore, one study used two platforms of VLPs: RSV M + P or M + M2-1 expressing RSV F and G, RSV F and a G peptide, or truncated RSV F with full length

G. These VLPs were used to immunize BALB/c mice (60). Mice immunized with M + P VLPs expressing RSV F and G or RSV F and a G peptide (MFGpP) and challenged with RSV elicited the highest neutralizing antibody titers compared to all other groups. Additionally, mice immunized with MFGpP and challenged with RSV had lower lung viral titers and lower histopathology scores compared to all other groups (60).

Additional studies involve using VLPs containing RSV G and pre-fusion F protein or post-fusion F protein (61). Pregnant cotton rats were immunized with VLPs to determine whether their pups would be protected against RSV (61). Pups born from mothers infected or not with RSV before VLP vaccination had higher levels of maternal antibodies against RSV compared to pups that were born to mothers that were mock immunized (61). Pups born to mothers that were immunized with VLPs, had decreased viral loads compared to mock vaccinated after RSV challenge (61). Lung pathology, IL-6, and IFN-γ production were also decreased in pups born to mothers that were VLP immunized indicating immunizing pregnant cotton rats can induce a protective response in RSV challenged pups (61).

A study testing the efficacy and immunogenicity of a VLP containing RSV F and RSV G demonstrated that the VLP elicited RSV F specific IgG antibodies and virus neutralizing antibodies in immunized rats (62). Additionally, this RSV FG VLP did not lead to enhanced disease and decreased lung viral loads after RSV challenge (62).

These studies suggest that VLPs containing both immunogenic proteins can be protective in mice and cotton rats. Most of these studies showed that VLPs containing both RSV F and RSV G led to neutralizing antibodies, decreased lung viral loads, and decreased pathology scores in mice and cotton rats. However, Kim et al., and Lee et al., provide contradicting evidence on whether VLPs expressing RSV G alone are protective in mice. Additionally, VLPs expressing both RSV F and RSV G elicited antibodies mostly against RSV F in rats.

1.8 Virus vector vaccines

Virus vectors containing RSV F or RSV G have been included in the developmental strategies for an effective RSV vaccine with varying degrees of success. Animal models vaccinated with vaccinia virus expressing RSV G have been shown to develop vaccine enhanced disease upon RSV infection (34, 42).

Parainfluenza virus 5 (PIV5) that does not cause human disease has been explored as a vector carrying RSV F (PIV5/F) or RSV G (PIV5/G) (63). Both vaccine candidates were found to elicit protein specific antibodies in cotton rats and to protect against RSV infection (63). In African green monkeys, PIV5/F and PIV5/G provided protection against RSV infection and elicited serum and mucosal antibodies (63). Furthermore, a chimeric bovine/ human parainfluenza virus type 3 (rB/HPIV3) expressing wild-type G (WT G), membrane bound G (mG), secreted G (sG), or G without a CX3C motif was used to immunize hamsters. Hamsters immunized with rB/HPIV3 expressing WT G or mG elicited higher levels of RSV A2 neutralizing antibodies in the presence of complement compared to hamsters immunized with

rB/HPIV3 expressing sG or G without CX3C. Additionally, lower lung viral loads were detected in hamsters immunized with rB/HPIV3 expressing WT G or mG, and the antibodies elicited from hamsters immunized with rB/HPIV3 expressing WT G blocked RSV attachment to human airway epithelial cells (64). These studies show that parainfluenza as a vaccine vector for RSV G can be protective in several RSV disease models.

Recombinant vesicular stomatitis virus (rVSV) is another virus vector that has been explored to develop an RSV vaccine. Cotton rats that were intranasally immunized with a combination of rVSV expressing RSV G or RSV F and challenged with RSV had reduced lung viral titers with an immunization dose as low as 10^3 pfu and had reduced viral loads in the upper respiratory tract with immunization doses from 10^6-10^7 pfu (65). A separate study using rVSV co-expressed RSV F and RSV G (rVSV-G-2A-F). Cotton rats immunized with rVSV-G-2A-F and challenged with RSV had reduced lung viral loads in the lungs and nose and elicited high neutralizing antibody titers thorough intranasal and subcutaneous immunizations (66).

Measles AIK-C vector (MVAIK) has been used to develop an RSV vaccine. Cotton rats immunized with a chimeric measles virus expressing the ectodomains of RSV F and RSV G (MV/RSV) elicited neutralizing antibodies when immunized intramuscularly (i.m.) compared to intranasal (i.n.) immunization (67). MV/RSV i.m. immunized cotton rats challenged with RSV had lower lung viral titers and histopathology scores compared to all other groups and to i.n. immunization (67).

All these studies show that various virus vector vaccines are being explored to create an RSV vaccine, and that the immunization route of such vaccine is important to consider to induce an appropriate immune response. Markers to consider for using virus vectors are safety- ensuring that the vector will not undergo recombination with the host genome, cytotoxicity, and pre-existing immunity to the viral vector (68).

1.9 Nanoparticle vaccines

Nanoparticle vaccines such as the layer-by-layer nanoparticle (LbL-NP) vaccine containing RSV G's CX3C motif is an additional strategy being explored (69). This particular study also investigated the immunogenicity and efficacy of nanoparticle vaccines containing a mutated CX3C motif (i.e. CX2C, CX4C, and CX5C). Sera of mice immunized with the LbL-NP containing the CX3C inhibited RSV G's interaction with CX3CR1 more efficiently than did any of the LbL-NPs containing a mutated CX3C (69). Additionally, LbL-NP CX3C elicited protective antibodies, reduced lung viral loads, and leukocyte infiltration in the lungs of immunized mice (69). This study demonstrates the importance of the CX3C motif in RSV G's central conserved domain to induce an immune response that protects against RSV disease in mice.

Another study involved using a hepatitis B virus core nanoparticles fused to an RSV G central conserved region peptide (amino acids 144 to 204) with (HBcΔ-tG/M282-90) or without (HBcΔ-tG) RSV M2 peptide to immunize mice because a previous study demonstrated that it can induce CD8+ T cells that are needed for viral clearance (70). Mice immunized with HBcΔ-tG/M282-90 had a higher ratio of

IgG2a/IgG1 and Th1 cytokines indicative of a Th1 response compared to mice immunized with HBcΔ-tG that induced a Th2 response (70). Immunization with HBcΔ-tG/M282-90 decreased viral titers and lung histopathology (70). These results suggest that immunization of nanoparticles displaying RSV G central conserved region alone induced markers of VED whereas inclusion of the RSV M2 peptide led to a Th1 response and decreased Th2 response and reduced lung pathology. A separate study used Hepatitis B virus core particles with the central conserved domain of RSV G combined with a plasmid encoding IL-35 (HBc-tG + pIL-35) to immunize mice. Mice immunized with HBc-tG + pIL-35 and challenged with RSV had higher levels of Th1 cytokines IFN-γ and IL-2 and lower levels of Th2 cytokines IL-4 and IL-5. These mice also had lower lung viral loads compared to PBS immunized mice, and lower histopathology scores (71). Another study used Hepatitis B virus core as a carrier to express two RSV F epitopes, the CTL domain of RSV M2, and a truncated RSV G (aa 169-198) to immunize mice (tHBc/Fe1e2/M282-90/tG) (72). Mice immunized with tHBc/Fe1e2/M282-90/tG had a higher neutralizing antibody titer compared to all other groups except UV-RSV (UV inactivated RSV) immunized mice. Mice immunized with tHBc/Fe1e2/M282-90/tG or UV-RSV also had the highest IgG2a antibody levels, however also had the highest IgG1 antibody levels. tHBc/Fe1e2/M282-90/tG immunized mice had decreased lung viral loads, however also had decreased T regulatory cells, IL-10, and higher histopathology scores compared to other groups (72). While tHBc/Fe1e2/M282-90/tG elicited some protection in immunized mice, it also induced some markers of VED.

A separate study used polyanhydride nanoparticles encapsulating RSV F and RSV G to immunize neonatal calves with Bovine RSV (BRSV). BRSV induces similar symptoms of infection in calves as human RSV does in infants. This study showed that calves immunized with the nanoparticle encapsulating RSV F and G elicited higher levels of neutralizing antibodies, had lower overall lung viral loads, and lower histopathology scores compared to calves immunized with empty nanoparticles or unvaccinated calves (73). This study shows that nanoparticles can be an effective and safe vaccine delivery platform.

1.10 Recombinant RSV G protein vaccines with an adjuvant

One of the most common RSV G vaccine strategies involves the use of recombinant RSV G protein or peptides in combination with an adjuvant to induce an immune response. A subunit vaccine, BBG2Na, which was tested in clinical trials involved fusing the C-terminus of RSV A2 G central conserved region (amino acids 130 to 230) to the albumin binding domain of *Streptococcal* protein G (74, 75). BBG2Na was found to be immunogenic and increase virus neutralizing antibodies in healthy adults, however it induced a type III hypersensitivity response in phase III of clinical trials (74, 75). It was suggested that the hypersensitivity response observed in clinical trials was due to the BB portion of the vaccine, so G2Na in the absence of BB was tested in mice and rats to determine whether it could protect against RSV disease (75). G2Na elicited antibodies against RSV A and B in immunized rodents (75). Additionally, the protective immunity elicited in rats persisted for 148 days

suggesting that this vaccine could protect throughout the duration of a typical RSV season (75).

Only one other recombinant RSV G vaccine has been studied in both animal models and human clinical trials (described in section 1.12). One study immunized mice with recombinant nonglycosylated G, produced in *E. coli*, consisting of amino acids 67 to 298 and an immunosuppressant cyclosporine (CSA) (41). Mice immunized with G + CSA had decreased lung viral loads and maintained body weight (41). To determine whether T regulatory cells could be induced by G + CSA, T regulatory cells of transgenic mice were measured in the spleen after RSV challenge (41). Mice that were immunized with G + CSA had the highest levels of T regulatory cells compared to control mice or mice immunized with G alone, CSA alone, or FI-RSV. A separate study immunized five-day old mice with G + CSA, G alone, CSA alone, or FI-RSV to determine whether G + CSA can prevent vaccine enhanced disease in infants (76). This study showed that infant mice immunized with G + CSA challenged with RSV had decreased lung viral loads, histopathology scores, body weight loss, and no mucus production compared to all other groups. Additionally, infant mice immunized with G + CSA challenged with RSV had higher anti-G antibody titers and higher RSV neutralizing antibody titers compared to all other groups. These mice and mice immunized with G alone induced T regulatory cells in the spleen and lymph nodes, however only mice immunized with G + CSA had these cells producing IL-10, an anti-inflammatory cytokine (76). These results suggest that the recombinant G vaccine with cyclosporine can decrease pathology and vaccine

enhanced disease in mice. This G + CSA vaccine is currently in phase II clinical trials.

In a different approach, recombinant unglycosylated G protein vaccine, produced in *E. coli*, consisting of the RSV G ectodomain (amino acids 67 to 298), was compared to glycosylated G protein vaccine, produced in mammalian cells (38, 40). Both were used with the adjuvant Emulsigen to immunize mice and cotton rats (38, 40). Nonglycosylated E*. coli* produced RSV G (REG) + Emulsigen immunized rats had the highest levels of RSV neutralizing antibodies against RSV-A2 and cross neutralization of RSV-B1 (38). Mice immunized with glycocylated, mammalian produced RSV G + Emulsigen (RMG) did not induce RSV-A2 or B1 antibodies (40). Additionally, REG + Emulsigen immunized mice and rats had lower viral loads in the lung tissue compared to all other immunized groups including mice immunized with RMG + Emulsigen (38, 40). Mice and rats immunized with REG + Emulsigen had similar histopathology scores to rats that were mock challenged, and had decreased levels of IFN-γ, IL-4, and MCP-1 cytokines, however mice and rats immunized with RMG + Emulsigen had higher histopathology scores and increased levels of these cytokines (38, 40). These results suggest that recombinant unglycosylated RSV G produced in *E.coli* with Emulsigen can protect mice and cotton rats from RSV disease.

An additional strategy to develop a subunit RSV G vaccine involves fusing RSV A's G protein with RSV B's G protein (central conserved region amino acids 131 to 230) and administering it with Cholera toxin as an adjuvant (77). This fusion vaccine

elicited G-specific IgG antibodies and mucosal IgA antibodies in immunized mice and protected against RSV A, however only minimally protected against RSV B infection. Vaccine enhanced disease was observed in immunized mice depending on the route of immunization and the strain of challenge virus. Mice immunized sublingually and challenged with RSV A had higher eosinophil infiltration into the lungs and higher body weight loss compared to mice immunized intranasally (77). Another study that used Cholera toxin as an adjuvant determined that the CD4+ T cell epitope on RSV A's G protein is associated with eosinophilia, which is a characteristic of vaccine enhanced disease. An RSV G fragment consisting of amino acids 131 to 230 with a mutated CD4+ T cell epitope (aa 183 to 195) fused to the CD4+ T cell epitope of RSV F (aa 51 to 66) protected against RSV A and B infection in immunized mice (78). This study suggests that a mutated RSV G can protect against RSV disease in mice.

Additionally, mice immunized with an RSV G fragment consisting of amino acids 131 to 230 with Cholera toxin as an adjuvant, elicited RSV G-specific IgG antibodies and IgA antibodies (79). RSV G-specific IgG antibodies and IgA antibodies were elicited even in the absence of Cholera toxin as the adjuvant (79). The vaccine candidate also induced the chemotaxis of monocyte-like cells in an *in vitro* chemotaxis assay (79). This study suggests that RSV G amino acids 131 to 230 are immunogenic and elicit protective antibodies.

A different study intramuscularly immunized BALB/c mice with *E.coli* produced RSV G aa 131-230 using baculovirus expressing RSV M2 as the adjuvant.

Immunized mice had reduced lung viral loads after RSV challenge compared to control mice. Immunized mice also had reduced eosinophil infiltration into the lungs and reduced alveolar macrophages in the lungs, however had increased neutrophils. Furthermore, immunized mice had similar body weight loss to control mice (80). This study shows that baculovirus expressing RSV M2 as an adjuvant can lead to some protection in mice, however, still leads to symptoms of vaccine enhanced disease.

CpG oligodeoxynucleotides, which are a TLR9 agonist, have also been used as an adjuvant in RSV G vaccine candidates to induce a Th1 response in immunized mice. BALB/c mice were immunized either intranasally or intraperitoneally with recombinant G1F/M2 (RSV G aa 125-225, cytotoxic T lymphocyte epitope of RSV M2 aa 81-92) with and without CpG as the adjuvant. Mice immunized with G1F/M2 + CpG and challenged with RSV were found to have higher levels of the Th1 cytokine IFN-γ and higher levels of the Th1 response antibody IgG2a compared to all other groups. These mice also had a lower pulmonary pathology score compared to all other groups and lower lung viral loads compared to negative control phosphate buffered saline (PBS) immunized mice (81).

As described in Chapter two and Appendix A2 of this thesis, we contributed to a study that used monophosphoryl lipid A (MPLA) as an adjuvant in combination with recombinant wild-type RSV G, RSV G with a single point mutation at serine 177 (S177Q, S177R), or with an alanine insertion at position 186 (within the CX3C motif to create CX4C) (82). BALB/c mice immunized with RSV G S177Q + MPLA elicited higher levels of Th1 antibodies IgG2a compared to all other groups before

and after RSV challenge (82). These mice also had reduced BAL cell influx into the lungs compared to all other groups suggesting that the mutation within RSV G can provide some protection against VED.

Overall, these studies show that recombinant RSV G as a vaccine immunogen with certain adjuvants can be protective in mice and cotton rats by inducing neutralizing antibodies, Th1 cytokines, or T regulatory cells, and decreasing lung viral loads, weight loss, histopathology scores, and mucus production. However, the studies above showed that RSV G alone as an immunogen led to VED and had low immunogenicity. Either dramatic changes to RSV G (i.e. no glycosylation) or adjuvants were required to eliminate markers of VED and increase the immunogenicity of RSV G. Notably, these studies did not show that RSV G maintained the conformational epitopes required to bind neutralizing antibodies, as many of these studies were done before the structure of RSV G was solved, which suggests that the immunogens that were used could have a disrupted structure.

1.11 Recombinant RSV G protein vaccines without an adjuvant

RSV G vaccines have been explored without the use of an adjuvant. For example, RSV G polypeptides expressed in *E. coli* (aa 148 to 198 encompassing the central conserved domain) or synthetic peptides consisting of amino acids 171 to 201, 171 to 183, and 181 to 192 with isoleucine deleted in the CX3C motif were conjugated to keyhole limpet hemocyanin and investigated for their ability to induce antibodies that block RSV G interaction with CX3CR1 and decrease disease in mice (83). Antibodies from mice immunized with polypeptides and peptides encompassing

the cysteine noose had the highest RSV G binding inhibition (83). Additionally, the antibodies inhibited leukocyte chemotaxis *in vitro* and immunized mice had decreased weight loss and lung viral loads and histopathology scores following RSV infection (83). These results suggest that vaccine candidates that encompass the central conserved domain can induce protective antibodies that inhibit CX3CR1 interactions to decrease disease severity.

Another vaccine strategy involved an RSV G peptide of amino acids 163 to 190, which contains the binding site to an anti-RSV G antibody (131-2G), conjugated to keyhole limpet hemocyanin (84). Mice immunized with RSV G peptide had decreased pulmonary cell infiltration, eosinophilia, IL-4 levels, and weight loss (all are markers of vaccine enhanced disease) compared to FI-RSV immunized mice (84). These results suggest that a recombinant RSV G peptide can protect against RSV disease in mice.

A different study intranasally immunized BALB/c mice with a recombinant fusion protein produced in *E. coli*, encompassing aa 243-296 of RSV F fused to aa 132-230 of RSV G and Gb1 at the C-terminus (FG-Gb1). This study showed that the Gb1 ligand targeted the fusion protein to M cells, which could pass the fusion protein to underlying dendritic and macrophage cells. Mice immunized with FG-Gb1 had higher viral clearance, less body weight loss, and elicited higher levels of neutralizing antibodies compared to mice immunized with FG alone after RSV challenge which shows that intranasal immunization with an immunogen containing RSV G can also lead to a protective immune response (85).

A separate recombinant fusion protein, SBP from Hepatitis B, that shares similar domains to Fc from IgG fused to RSV F (aa 243-296) and G (aa 131-230) (SBP-FG) was used to immunize mice (86). SBP was used to stimulate the delivery and uptake of the fusion protein to dendritic cells to induce a Th1 immune response. Immunized mice were shown to elicit higher levels of RSV neutralizing antibodies and IgG2a (Th1 antibodies) compared to IgG1 (Th2 antibodies). SBP-FG immunized mice also induced higher levels of Th1 cytokines IFN-γ and IL-2 compared to PBS and FI-RSV immunized mice and lower levels of Th2 cytokines IL-4 and IL-5 compared to FI-RSV immunized mice. Additionally, SBP-FG immunization reduced lung viral loads, mouse weight loss, and eosinophilia (86). This study shows the importance of a Th1 response to protect against RSV infection.

Furthermore, RSV G vaccine candidates produced in *E. coli* involving antigenic sites outside the central conserved domain consisting of amino acids 67 to 298 with the central conserved domain (aa 172 to 186) deleted and replaced with a $(Gly_4Ser)_2$ linker, amino acids 67 to 163, or aa 187 to 298 elicited RSV G-specific antibodies in immunized rabbits and mice (87). This vaccine candidate decreased pathology scores, viral loads, and Th2 to Th1 cytokine ratio in immunized animals (87). This study demonstrates the existence of antigenic sites outside of RSV G's central conserved domain and suggests that they should be considered when developing an RSV vaccine.

Overall, these studies highlight the potential of peptides or fragments of RSV G as immunogens. While there are some antigenic sites outside of the CCD of RSV

G, most recombinant RSV G vaccine developmental strategies involve mutating the CX3C motif within the CCD, mutating the CD4+ T cell epitope, or fusing the RSV G protein to another protein to elicit a specific immune response. The mutations to the CX3C motif or the CD4+ T cell epitope on RSV G can potentially disrupt the structure of RSV G. We have shown that adding an alanine into the CX3C motif to create a CX4C RSV G protein disrupted the epitopes required to bind to high affinity neutralizing antibodies (88). Furthermore, fusion proteins can potentially elicit antibodies against the protein that is not RSV G, which can lead to low titers against RSV G and to non-neutralizing antibodies being elicited.

Even though these studies show that recombinant RSV G as a vaccine immunogen without the use of an adjuvant can be protective in animal models when RSV G is mutated or fused to another protein, studies that do not take the structure of RSV G into consideration when designing an immunogen can potentially lead to the production of non-neutralizing antibodies in immunized animals, which can lead to VED. Additionally, the immunogenicity of the recombinant proteins should be considered because wild-type RSV G alone induces a low abundance of neutralizing antibodies. Studies that involve using RSV G amino acids outside the central conserved domain should test for cross neutralization of different RSV strains because the mucin like domains of RSV G contain many O-linked glycosylation sites that vary.

1.12 Clinical trials

While most of the vaccine antigen candidates and prophylaxis candidates have focused on RSV F, one recombinant vector vaccine candidate, a modified vaccinia Ankara (MVA)-BN (Bavarian Nordic) includes RSV G from RSV A and B, RSV F, N, and M2 (89, 90). This vaccine candidate was tested for safety and immunogenicity in healthy older (over 65 years) adults. After six months, an antibody response was still measured. MVA-BN-RSV has also been tested in a phase I clinical trial of young adults (20-49 years) and again in older adults (50-62 years) for safety and reaction to the injection, and humoral and cell immunity (91). This study found that MVA-BN-RSV was safe and tolerable and induced a T cell response in these adults (91). This vaccine candidate moved on to a phase II clinical trials in older adults (92). MVA-BN-RSV was found to elicit neutralizing antibodies and a Th1 immune response in older adults.

There is currently one RSV G subunit vaccine in phase II clinical trials. This subunit vaccine uses cyclosporine as an adjuvant and is from Advaccine Biotechnology. It is being tested in the elderly and pediatric populations (preclinical data is described in section 1.10) (12).

1.13 Concluding remarks

RSV causes severe lower respiratory tract infections in infants, elderly, and immunocompromised individuals. The first vaccine candidate, formalin inactivated RSV, led to enhanced disease upon RSV infection and resulted in two deaths. Most of the current vaccine developmental strategies currently in clinical trials are focused on

the fusion glycoprotein RSV F, however some preclinical studies are now focusing on the attachment glycoprotein RSV G.

There are currently many vaccine developmental strategies to develop an RSV vaccine utilizing RSV G as the vaccine antigen. These strategies include: virus-like particles, nucleic acid vaccines, recombinant RSV G vaccines, virus vector vaccines, nanoparticle vaccines, and live attenuated RSV vaccines. Additionally, anti-RSV G antibodies are also being explored as a prophylaxis or treatment.

RSV G structural studies have identified RSV G antigenic sites, which may provide direction to developing an effective and protective RSV vaccine.

1.14 References

1. Shi T, Balsells E, Wastnedge E, Singleton R, Rasmussen ZA, Zar HJ, Rath BA, Madhi SA, Campbell S, Vaccari LC, Bulkow LR, Thomas ED, Barnett W, Hoppe C, Campbell H, Nair H. 2015. Risk factors for respiratory syncytial virus associated with acute lower respiratory infection in children under five years: Systematic review and meta–analysis. J Glob Health 5.
2. Scheltema NM, Gentile A, Lucion F, Nokes DJ, Munywoki PK, Madhi SA, Groome MJ, Cohen C, Moyes J, Thorburn K, Thamthitiwat S, Oshitani H, Lupisan SP, Gordon A, Sánchez JF, O'Brien KL, Gessner BD, Sutanto A, Mejias A, Ramilo O, Khuri-Bulos N, Halasa N, de-Paris F, Pires MR, Spaeder MC, Paes BA, Simões EAF, Leung TF, da Costa Oliveira MT, de Freitas Lázaro Emediato CC, Bassat Q, Butt W, Chi H, Aamir UB, Ali A, Lucero MG,

Fasce RA, Lopez O, Rath BA, Polack FP, Papenburg J, Roglić S, Ito H, Goka EA, Grobbee DE, Nair H, Bont LJ, James Nokes D, Munywoki PK, Madhi SA, Groome MJ, Cohen C, Moyes J, Thorburn K, Thamthitiwat S, Oshitani H, Lupisan SP, Gordon A, Sánchez JF, O KL, Khuri-Bulos N, Halasa N, de-Paris F, Rosane Pires M, Spaeder MC, Paes BA, F Simões EA, Leung TF, Tereza da Costa Oliveira M, Cecília de Freitas Lázaro Emediato C, Bassat Q, Butt W, Chi H, Bashir Aamir U, Ali A, Lucero MG, Fasce RA, Lopez O, Rath BA, Polack FP, Papenburg J, Roglić S, Ito H, Goka EA, Grobbee DE, Nair H, Bont LJ. 2017. Global respiratory syncytial virus-associated mortality in young children (RSV GOLD): a retrospective case seriesThe Lancet Global Health.

3. Hall CB, Weinberg GA, Iwane MK, Blumkin AK, Edwards KM, Staat MA, Auinger P, Griffin MR, Poehling KA, Erdman D, Grijalva CG, Zhu Y, Szilagyi P. 2009. The Burden of Respiratory Syncytial Virus Infection in Young Children. Pediatr Biostat https://doi.org/10.1056/NEJMoa0804877.

4. Li Y, Wang X, Blau DM, Caballero MT, Feikin DR, Gill CJ, Madhi SA, Omer SB, F Simões EA, Campbell H, Bermejo Pariente A, Bardach D, Bassat Q, Casalegno J-S, Chakhunashvili G, Crawford N, Danilenko D, Anh Ha Do L, Echavarria M, Gentile A, Gordon A, Heikkinen T, Sue Huang Q, Jullien S, Krishnan A, Luis Lopez E, Markić J, Mira-Iglesias A, Moore HC, Moyes J, Mwananyanda L, James Nokes D, Noordeen F, Obodai E, Palani N, Romero C, Salimi V, Satav A, Seo E, Shchomak Z, Singleton R, Stolyarov K, Stoszek SK, von Gottberg A, Wurzel D, Yoshida L-M, Fu Yung C, Zar HJ. 2022.

Global, regional, and national disease burden estimates of acute lower respiratory infections due to respiratory syncytial virus in children younger than 5 years in 2019: a systematic analysis. www.thelancet.com 399.

5. Branche AR, Ann Falsey BR. 2015. Respiratory Syncytial Virus Infection in Older Adults: An Under-Recognized Problem. Drugs Aging https://doi.org/10.1007/s40266-015-0258-9.

6. Satakel M, Coligan2 JE, Elango3 N, Norrby4 E, Venkatesan5 S. 1985. Respiratory syncytial virus envelope glycoprotein (G) has a novel structure. Nucleic Acids Res 13:7795–7812.

7. Mclellan JS, Ray WC, Peeples ME. 2013. Structure and Function of RSV Surface Glycoproteins https://doi.org/10.1007/978-3-642-38919-1_4.

8. Tripp RA, Power UF, Openshaw PJM, Kauvar LM. 2017. Respiratory Syncytial Virus: Targeting the G Protein Provides a New Approach for an Old Problem. J Virol 92:e01302-17.

9. Graham BS. 2017. Vaccine development for respiratory syncytial virus This review comes from a themed issue on Preventive and therapeutic vaccines Epidemiology and vaccine target populations. Curr Opin Virol 23:107–112.

10. Jorquera PA, Tripp RA. 2017. Expert Review of Respiratory Medicine Respiratory syncytial virus: prospects for new and emerging therapeutics Respiratory syncytial virus: prospects for new and emerging therapeutics https://doi.org/10.1080/17476348.2017.1338567.

11. Higgins D, Trujillo C, Keech C. 2016. Advances in RSV vaccine research and

development – A global agenda. Vaccine 34:2870–2875.

12. RSV Vaccine and mAb Snapshot | PATH.

13. Olchanski N, Hansen RN, Pope E, D 'cruz B, Fergie J, Goldstein M, Krilov LR, Mclaurin KK, Nabrit-Stephens B, Oster G, Schaecher K, Shaya FT, Neumann PJ, Sullivan SD. 2018. Palivizumab Prophylaxis for Respiratory Syncytial Virus: Examining the Evidence Around Value. Open Forum Infect Dis https://doi.org/10.1093/ofid/ofy031.

14. Perk Y, Özdil M. 2018. Cite this article as: Perk Y, Özdil M. Respiratory syncytial virüs infections in neonates and infants. Turk Pediatr Ars 53:63–70.

15. Rezaee F, Linfield DT, Harford TJ, Piedimonte G. 2017. Ongoing developments in RSV prophylaxis: a clinician's analysis. Curr Opin Virol.

16. Simoes EAF, Bont L, Manzoni P, Fauroux B, Paes B, Figueras-Aloy J, Checchia PA, Carbonell-Estrany X. 2018. Past, Present and Future Approaches to the Prevention and Treatment of Respiratory Syncytial Virus Infection in Children. Infect Dis Ther 7.

17. Resch B. 2017. Product review on the monoclonal antibody palivizumab for prevention of respiratory syncytial virus infection https://doi.org/10.1080/21645515.2017.1337614.

18. Fedechkin SO, George NL, Wolff JT, Kauvar LM, Dubois RM. 2018. Structures of respiratory syncytial virus G antigen bound to broadly neutralizing antibodies. Sci Immunol 3:1–8.

19. Chirkova T, Lin S, P Oomens AG, Gaston KA, Boyoglu-Barnum S, Meng J,

Stobart CC, Cotton CU, Hartert T V, Moore ML, Ziady AG, Anderson LJ, Larry Anderson CJ. 2015. CX3CR1 is an important surface molecule for respiratory syncytial virus infection in human airway epithelial cells. J Gen Virol https://doi.org/10.1099/vir.0.000218.

20. Jeong K-I, Piepenhagen PA, Kishko M, Dinapoli JM, Groppo RP, Zhang L, Almond J, Kleanthous H, Delagrave S, Parrington M. 2015. CX3CR1 Is Expressed in Differentiated Human Ciliated Airway Cells and Co-Localizes with Respiratory Syncytial Virus on Cilia in a G Protein-Dependent Manner. PLoS One https://doi.org/10.1371/journal.pone.0130517.

21. Johnson SM, Mcnally BA, Ioannidis I, Flano E, Teng MN, Oomens AG, Walsh EE, Peeples ME. 2015. Respiratory Syncytial Virus Uses CX3CR1 as a Receptor on Primary Human Airway Epithelial Cultures. PLoS Pathog 11.

22. Hijano DR, Kalergis AM, Kauvar LM, Tripp RA, Polack FP, Cormier SA. 2019. Role of Type I Interferon (IFN) in the Respiratory Syncytial Virus (RSV) Immune Response and Disease Severity. Front Immunol | www.frontiersin.org 1:566.

23. Tripp RA, Jones LP, Haynes LM, Zheng HQ, Murphy PM, Anderson LJ. 2001. CX3C chemokine mimicry by respiratory syncytial virus G glycoprotein. Nat Immunol 2:732–738.

24. Harcourt J, Alvarez R, Jones LP, Henderson C, Anderson LJ, Tripp RA. 2006. Respiratory Syncytial Virus G Protein and G Protein CX3C Motif Adversely Affect CX3CR1 T Cell Responses. J Immunol 176:1600–1608.

25. Arnold R, Kfnig B, Werchau H, Kfnig W. 2004. Respiratory syncytial virus deficient in soluble G protein induced an increased proinflammatory response in human lung epithelial cells. Virology https://doi.org/10.1016/j.virol.2004.10.004.

26. Haynes LM, Jones LP, Barskey A, Anderson LJ, Tripp RA. 2003. Enhanced disease and pulmonary eosinophilia associated with formalin-inactivated respiratory syncytial virus vaccination are linked to G glycoprotein CX3C-CX3CR1 interaction and expression of substance P. J Virol 77:9831–9844.

27. Collarini EJ, Lee FE-H, Foord O, Park M, Sperinde G, Wu H, Harriman WD, Carroll SF, Ellsworth SL, Anderson LJ, Tripp RA, Walsh EE, Keyt BA, Kauvar LM. 2009. Potent High-Affinity Antibodies for Treatment and Prophylaxis of Respiratory Syncytial Virus Derived from B Cells of Infected Patients. J Immunol 183:6338–6345.

28. Han J, Takeda K, Wang M, Zeng W, Jia Y, Shiraishi Y, Okamoto M, Dakhama A, Gelfand EW. 2014. Effects of Anti-G and Anti-F Antibodies on Airway Function after Respiratory Syncytial Virus Infection. Am J Respir Cell Mol Biol 51.

29. Caidi H, Miao C, Thornburg NJ, Tripp RA, Anderson LJ, Haynes LM. 2018. Anti-respiratory syncytial virus (RSV) G monoclonal antibodies reduce lung inflammation and viral lung titers when delivered therapeutically in a BALB/c mouse model. Antivir Res 154:149–157.

30. Capella C, Chaiwatpongsakorn S, Gorrell E, Risch ZA, Ye F, Mertz SE,

Johnson SM, Moore-Clingenpeel M, Ramilo O, Mejias A, Peeples ME. 2017. Prefusion F, Postfusion F, G Antibodies, and Disease Severity in Infants and Young Children With Acute Respiratory Syncytial Virus Infection. J Infect Dis ® 1398:1398–406.

31. Shaw CA, Ciarlet M, Cooper BW, Dionigi L, Keith P, O 'brien KB, Rafie-Kolpin M, Dormitzer PR, O'Brien KB, Rafie-Kolpin M, Dormitzer PR. 2013. The path to an RSV vaccine. Curr Opin Virol 3:332–342.
32. Chanock RM, Jensen K, Parrott RH. 1969. Respiratory Syncytial Virus Disease in Infants 89:422–434.
33. Villafana T, Falloon J, Griffin MP, Zhu Q, Esser MT. 2017. Expert Review of Vaccines Passive and active immunization against respiratory syncytial virus for the young and old Passive and active immunization against respiratory syncytial virus for the young and old https://doi.org/10.1080/14760584.2017.1333425.
34. Johnson TR, Graham BS. 1999. Secreted Respiratory Syncytial Virus G Glycoprotein Induces Interleukin-5 (IL-5), IL-13, and Eosinophilia by an IL-4-Independent Mechanism. J Virol 73:8485–8495.
35. Johnson TR, Teng MN, Collins PL, Graham BS. 2004. Respiratory Syncytial Virus (RSV) G Glycoprotein Is Not Necessary for Vaccine-Enhanced Disease Induced by Immunization with Formalin-Inactivated RSV. J Virol 78:6024–6032.
36. Knudson CJ, Hartwig SM, Meyerholz DK, Varga SM. 2015. RSV Vaccine-

Enhanced Disease Is Orchestrated by the Combined Actions of Distinct CD4 T Cell Subsets. PLOS Pathog https://doi.org/10.1371/journal.ppat.1004757.

37. Acosta PL, Caballero MT, Polack FP. 2016. Brief History and Characterization of Enhanced Respiratory Syncytial Virus Disease https://doi.org/10.1128/CVI.00609-15.

38. Fuentes S, Klenow L, Golding H, Khurana S. 2017. Preclinical evaluation of bacterially produced RSV-G protein vaccine: Strong protection against RSV challenge in cotton rat model. Sci Rep 7:1–13.

39. Tripp RA. 2004. Pathogenesis of Respiratory Syncytial Virus InfectionVIRAL IMMUNOLOGY.

40. Fuentes S, Coyle EM, Golding H, Khurana S. 2015. Nonglycosylated G-Protein Vaccine Protects against Homologous and Heterologous Respiratory Syncytial Virus (RSV) Challenge, while Glycosylated G Enhances RSV Lung Pathology and Cytokine Levels. J Virol 89:8193–8205.

41. Li C, Zhou X, Zhong Y, Li C, Dong A, He Z, Zhang S, Wang B. 2016. A Recombinant G Protein Plus Cyclosporine A–Based Respiratory Syncytial Virus Vaccine Elicits Humoral and Regulatory T Cell Responses against Infection without Vaccine-Enhanced Disease. J Immunol.

42. Johnson TR, Johnson JE, Roberts SR, Wertz GW, Parker RA, Graham BS. 1998. Priming with Secreted Glycoprotein G of Respiratory Syncytial Virus (RSV) Augments Interleukin-5 Production and Tissue Eosinophilia after RSV ChallengeJOURNAL OF VIROLOGY.

43. Johnson TR, Varga SM, Braciale TJ, Graham BS. 2004. Vβ14 + T Cells Mediate the Vaccine-Enhanced Disease Induced by Immunization with Respiratory Syncytial Virus (RSV) G Glycoprotein but Not with Formalin-Inactivated RSV . J Virol 78:8753–8760.

44. Jorquera PA, Anderson L, Tripp RA. 2015. Expert Review of Vaccines Understanding respiratory syncytial virus (RSV) vaccine development and aspects of disease pathogenesis Understanding respiratory syncytial virus (RSV) vaccine development and aspects of disease pathogenesis https://doi.org/10.1586/14760584.2016.1115353doi.org/10.1586/14760584.2016.1115353.

45. Jones HG, Ritschel T, Pascual G, Brakenhoff JPJ, Keogh E, Furmanova-Hollenstein P, Lanckacker E, Wadia JS, Gilman MSA, Williamson RA, Roymans D, Van 't Wout AB, Langedijk JP, Mclellan JS. 2018. Structural basis for recognition of the central conserved region of RSV G by neutralizing human antibodies. PLOS Pathog https://doi.org/10.1371/journal.ppat.1006935.

46. Radu GU, Caidi H, Miao † Congrong, Tripp RA, Anderson LJ, Haynes LM. 2010. Prophylactic Treatment with a G Glycoprotein Monoclonal Antibody Reduces Pulmonary Inflammation in Respiratory Syncytial Virus (RSV)-Challenged Naïve and Formalin-Inactivated RSV-Immunized BALB/c Mice. J Virol 84:9632–9636.

47. Caidi H, Harcourt JL, Tripp RA, Anderson LJ, Haynes LM, Varga SM. 2012. Combination Therapy Using Monoclonal Antibodies against Respiratory

Syncytial Virus (RSV) G Glycoprotein Protects from RSV Disease in BALB/c Mice. PLoS One https://doi.org/10.1371/journal.pone.0051485.

48. Haynes LM, Caidi H, Radu GU, Miao C, Harcourt JL, Tripp RA, Anderson LJ. 2009. Therapeutic Monoclonal Antibody Treatment Targeting Respiratory Syncytial Virus (RSV) G Protein Mediates Viral Clearance and Reduces the Pathogenesis of RSV Infection in BALB/c Mice. J Infect Dis 200:439–486.

49. Miao C, Radu GU, Caidi H, Tripp RA, Anderson LJ, Haynes LM. 2009. Treatment with respiratory syncytial virus G glycoprotein monoclonal antibody or F(ab9) 2 components mediates reduced pulmonary inflammation in mice. J Gen Virol https://doi.org/10.1099/vir.0.009308-0.

50. Boyoglu-Barnum S, Gaston KA, Todd SO, Boyoglu C, Chirkova T, Barnum TR, Jorquera P, Haynes LM, Tripp RA, Moore ML, Anderson LJ. 2013. A Respiratory Syncytial Virus (RSV) Anti-G Protein F(ab=) 2 Monoclonal Antibody Suppresses Mucous Production and Breathing Effort in RSV rA2-line19F-Infected BALB/c Mice. J Virol https://doi.org/10.1128/JVI.01164-13.

51. Boyoglu-Barnum S, Chirkova T, Todd SO, Barnum TR, Gaston KA, Jorquera P, Haynes LM, Tripp RA, Moore ML, Anderson LJ. 2014. Prophylaxis with a Respiratory Syncytial Virus (RSV) Anti-G Protein Monoclonal Antibody Shifts the Adaptive Immune Response to RSV rA2-line19F Infection from Th2 to Th1 in BALB/c Mice. J Virol https://doi.org/10.1128/JVI.01503-14.

52. Boyoglu-Barnum S, Todd SO, Chirkova T, Barnum TR, Gaston KA, Haynes LM, Tripp RA, Moore ML, Anderson LJ. 2015. An anti-G protein monoclonal

antibody treats RSV disease more effectively than an anti-F monoclonal antibody in BALB/c mice HHS Public Access. Virology 483:117–125.

53. Lee H-J, Lee J-Y, Park M-H, Kim J-Y, Chang J. 2017. Monoclonal Antibody against G Glycoprotein Increases Respiratory Syncytial Virus Clearance In Vivo and Prevents Vaccine- Enhanced Diseases. PLoS One https://doi.org/10.1371/journal.pone.0169139.

54. Hammitt LL, Dagan R, Yuan Y, Baca Cots M, Bosheva M, Madhi SA, Muller WJ, Zar HJ, Brooks D, Grenham A, Wählby Hamrén U, Mankad VS, Ren P, Takas T, Abram ME, Leach A, Griffin MP, Villafana T. 2022. Nirsevimab for Prevention of RSV in Healthy Late-Preterm and Term Infants. N Engl J Med 386:837–846.

55. Boyoglu-Barnum S, Todd SO, Meng J, Barnum TR, Chirkova T, Haynes LM, Jadhao SJ, Tripp RA, Oomens AG, Moore ML, Anderson LJ. 2017. Mutating the CX3C Motif in the G Protein Should Make a Live Respiratory Syncytial Virus Vaccine Safer and More Effective. J Virol https://doi.org/10.1128/JVI.02059-16.

56. Jung Y-J, Lee Y-N, Kim K-H, Lee Y, Jeeva S, Park BR, Kang S-M. 2020. Recombinant Live Attenuated Influenza Virus Expressing Conserved G-Protein Domain in a Chimeric Hemagglutinin Molecule Induces G-Specific Antibodies and Confers Protection against Respiratory Syncytial Virus. Vaccines https://doi.org/10.3390/vaccines8040716.

57. Tian P, Xu D, Huang Z, Meng F, Fu J, Wei H, Chen T. 2018. Evaluation of

truncated G protein delivered by live attenuated Salmonella as a vaccine against respiratory syncytial virus. Microb Pthogenes 115:299–303.

58. Kim A-R, Lee D-HD-H, Lee S-H, Rubino I, Choi H-JH-J, Quan F-S. 2018. Protection induced by virus-like particle vaccine containing tandem repeat gene of respiratory syncytial virus G protein. PLoS One 13:1–14.

59. Lee S, Quan F-S, Kwon Y, Sakamoto K, Kang S-M, Compans RW, Moore ML. 2014. Additive Protection Induced by Mixed Virus-like Particles Presenting Respiratory Syncytial Virus Fusion or Attachment Glycoproteins. Antivir Res 111:129–135.

60. Ha B, Yang JE, Chen X, Jadhao SJ, Wright ER, Anderson LJ. 2020. Two RSV Platforms for G, F, or G+F Proteins VLPs. Viruses https://doi.org/10.3390/v12090906.

61. Blanco JCG, Pletneva LM, Mcginnes-Cullen L, Otoa RO, Patel MC, Fernando LR, Boukhvalova MS, Morrison TG. 2018. Efficacy of a respiratory syncytial virus vaccine candidate in a maternal immunization model. Nat Commun https://doi.org/10.1038/s41467-018-04216-6.

62. Hwang HS, Kim K-H, Lee Y, Lee Y-T, Ko E-J, Park S, Lee JS, Lee B, Kwon Y-M, Moore ML, Kang S-M. 2017. Virus-like particle vaccines containing F or F and G proteins confer protection against respiratory syncytial virus without pulmonary inflammation in cotton rats. Hum Vaccin Immunother 13:1031–1039.

63. Wang D, Phan S, Distefano DJ, Citron MP, Callahan CL, Indrawati L, Dubey

SA, Heidecker GJ, Govindarajan D, Liang X, He B, Espeseth AS. 2017. A Single-Dose Recombinant Parainfluenza Virus 5-Vectored Vaccine Expressing Respiratory Syncytial Virus (RSV) F or G Protein Protected Cotton Rats and African Green Monkeys from RSV Challenge. J Virol https://doi.org/10.1128/JVI.

64. Liang B, Kabatova B, Kabat J, Dorward DW, Liu X, Surman S, Liu X, Park Moseman A, Buchholz UJ, Collins PL, Munir S, Liang CB, Terence Dermody ES. 2019. Effects of Alterations to the CX3C Motif and Secreted Form of Human Respiratory Syncytial Virus (RSV) G Protein on Immune Responses to a Parainfluenza Virus Vector Expressing the RSV G Protein Downloaded fromjvi.asm.org 1 Journal of Virology.

65. Binjawadagi B, Ma Y, Binjawadagi R, Brakel K, Harder O, Peeples M, Li J, Niewiesk S. 2021. Mucosal Delivery of Recombinant Vesicular Stomatitis Virus Vectors Expressing Envelope Proteins of Respiratory Syncytial Virus Induces Protective Immunity in Cotton Rats https://doi.org/10.1128/JVI.

66. Brakel KA, Binjawadagi B, French-Kim K, Watts M, Harder O, Ma Y, Li J, Niewiesk S. 2021. Coexpression of respiratory syncytial virus (RSV) fusion (F) protein and attachment glycoprotein (G) in a vesicular stomatitis virus (VSV) vector system provides synergistic effects against RSV infection in a cotton rat model https://doi.org/10.1016/j.vaccine.2021.10.042.

67. Sawada A, Ito T, Yamaji Y, Nakayama T, Henry O. 2021. Chimeric Measles Virus (MV/RSV), Having Ectodomains of Respiratory Syncytial Virus (RSV)

F and G Proteins Instead of Measles Envelope Proteins, Induced Protective Antibodies against RSV https://doi.org/10.3390/vaccines9020156.

68. Ura T, Okuda K, Shimada M. 2014. Developments in Viral Vector-Based Vaccines 2:624–641.

69. Jorquera PA, Oakley KE, Powell TJ, Palath N, Boyd JG, Tripp RA. 2015. Layer-By-Layer Nanoparticle Vaccines Carrying the G Protein CX3C Motif Protect against RSV Infection and Disease. Vaccines 3:829–849.

70. Qiao L, Zhang Y, Chai F, Tan Y, Huo C, Pan Z. 2016. Chimeric virus-like particles containing a conserved region of the G protein in combination with a single peptide of the M2 protein confer protection against respiratory syncytial virus infection. Antiviral Res 131:131–140.

71. Yang J, Ma C, Zhao Y, Fan A, Zou X, Pan Z, Yang CJ. 2020. Hepatitis B Virus Core Particles Containing a Conserved Region of the G Protein Combined with Interleukin-35 Protected Mice against Respiratory Syncytial Virus Infection without Vaccine-Enhanced Immunopathology 94:7–20.

72. Lei L, Qin H, Luo J, Tan Y, Yang J, Pan Z. 2021. Construction and immunological evaluation of hepatitis B virus core virus-like particles containing multiple antigenic peptides of respiratory syncytial virus. Virus Res 298:198410.

73. Mcgill JL, Kelly SM, Kumar P, Speckhart S, Haughney SL, Henningson J, Narasimhan B, Sacco RE. 2018. Efficacy of mucosal polyanhydride nanovaccine against respiratory syncytial virus infection in the neonatal calf

OPEN. Sci Rep https://doi.org/10.1038/s41598-018-21292-2.

74. Power UF, Nguyen TN, Rietveld E, De Swart RL, Groen J, Osterhaus ADME, De Groot R, Corvaia N, Beck A, Bouveret-Le-Cam N, Bonnefoy J-Y. 2001. Safety and Immunogenicity of a Novel Recombinant Subunit Respiratory Syncytial Virus Vaccine (BBG2Na) in Healthy Young Adults. J Infect Dis.

75. Nguyen TN, Power UF, Robert A, Haeuw J-F, Helffer K, Perez A, Asin M-A, Corvaia N, Libon C. 2012. The Respiratory Syncytial Virus G Protein Conserved Domain Induces a Persistent and Protective Antibody Response in Rodents. PLoS One 7.

76. Zhang S, Zhao G, Su C, Li C, Zhou X, Zhao W, Zhong Y, He Z, Peng H, Dong A, Wang B. 2020. Neonatal priming and infancy boosting with a novel respiratory syncytial virus vaccine induces protective immune responses without concomitant respiratory disease upon RSV challenge. Hum Vaccines Immunother 16:664–672.

77. Lee JY, Chang J. 2017. Universal vaccine against respiratory syncytial virus A and B subtypes. PLoS One 12:1–19.

78. Cheon IS, Shim B-SS, Park S-MM, Choi Y, Jang JE, Jung DI, Kim J-OO, Chang J, Yun C-HH, Song MK, Cheon S, Shim B-SS, Park S-MM, Choi Y, Jang JE, Jung DI, Kim J-OO, Chang J, Yun C-HH, Song K. 2014. Development of safe and effective RSV vaccine by modified CD4 epitope in g protein core fragment (GcF). PLoS One 9:1–10.

79. Kim S, Joo D-H, Lee J-B, Shim B-S, Cheon IS, Jang J-E, Song H-H, Kim K-

H, Song K, Chang J. 2012. Dual Role of Respiratory Syncytial Virus Glycoprotein Fragment as a Mucosal Immunogen and Chemotactic Adjuvant. PLoS One 7.

80. Jo Y-M, Kim J, Chang J. 2019. Vaccine containing G protein fragment and recombinant baculovirus expressing M2 protein induces protective immunity to respiratory syncytial virus. Clin Exp Vaccine Res 43–53.

81. Li N, Zhang L, Zheng B, Li W, Liu J, Zhang H, Zeng R. 2019. RSV recombinant candidate vaccine G1F/M2 with CpG as an adjuvant prevents vaccine-associated lung inflammation, which may be associated with the appropriate types of immune memory in spleens and lungs https://doi.org/10.1080/21645515.2019.1596710.

82. Bergeron HC, Murray J, Nuñez Castrejon AM, Dubois RM, Tripp RA, Mccormick C. 2021. Respiratory Syncytial Virus (RSV) G Protein Vaccines With Central Conserved Domain Mutations Induce CX3C-CX3CR1 Blocking Antibodies. Viruses 13.

83. Zhang W, Choi Y, Haynes LM, Harcourt JL, Anderson LJ, Jones LP, Tripp RA. 2010. Vaccination To Induce Antibodies Blocking the CX3C-CX3CR1 Interaction of Respiratory Syncytial Virus G Protein Reduces Pulmonary Inflammation and Virus Replication in Mice. J Virol 84:1148–1157.

84. Rey GU, Miao C, Caidi H, Trivedi SU, Harcourt JL, Tripp RA, Anderson LJ, Haynes LM. 2013. Decrease in Formalin-Inactivated Respiratory Syncytial Virus (FI-RSV) Enhanced Disease with RSV G Glycoprotein Peptide

Immunization in BALB/c Mice https://doi.org/10.1371/journal.pone.0083075.

85. Khan IU, Huang J, Li X, Xie J, Zhu N. 2018. Nasal immunization with RSV F and G protein fragments conjugated to an M cell-targeting ligand induces an enhanced immune response and protection against RSV infection https://doi.org/10.1016/j.antiviral.2018.10.001.

86. Khan IU, Ahmad F, Zhang S, Lu P, Wang J, Xie J, Zhu N. 2018. Respiratory syncytial virus F and G protein core fragments fused to HBsAg-binding protein (SBP) induce a Th1-dominant immune response without vaccine-enhanced disease. Int Immunol 31:199–209.

87. Lee J, Klenow L, Coyle EM, Golding H, Khurana S. 2018. Protective antigenic sites in respiratory syncytial virus G attachment protein outside the central conserved and cysteine noose domains. PLoS One https://doi.org/10.1371/journal.ppat.1007262.

88. Nuñez Castrejon AM, O'Rourke SM, Kauvar LM, DuBois RM. 2022. Structure-Based Design and Antigenic Validation of Respiratory Syncytial Virus G Immunogens. J Virol 96.

89. G Blanco JC, Boukhvalova MS, Morrison TG, Vogel SN. 2018. A Multifaceted Approach to RSV Vaccination. Hum Vaccin Immunother 0.

90. Bont LJ, Nunes C, Mejias A, Falsey AR, Kragten-Tabatabaie L, Baraldi E, Papadopoulos NG, Polack FP, Stein RT, Mazur NI, Higgins D, Nunes MC, Melero JA, Langedijk AC, Horsley N, Buchholz UJ, Openshaw PJ, Mclellan JS, Englund JA, Mejias A, Karron RA, Simões EA, Knezevic I, Ramilo O,

Piedra PA, Chu HY, Falsey AR, Nair H, Kragten-Tabatabaie L, Greenough A, Baraldi E, Papadopoulos NG, Vekemans J, Polack FP, Powell M, Satav A, Walsh EE, Stein RT, Graham BS, Bont LJ. 2018. The respiratory syncytial virus vaccine landscape: lessons from the graveyard and promising candidates. Lancet Infect Dis https://doi.org/10.1016/S1473-3099(18)30292-5.

91. Samy N, Reichhardt D, Schmidt D, Chen LM, Silbernagl G, Vidojkovic S, Meyer TP, Jordan E, Adams T, Weidenthaler H, Stroukova D, De Carli S, Chaplin P. 2020. Safety and immunogenicity of novel modified vaccinia Ankara-vectored RSV vaccine: A randomized phase I clinical trial https://doi.org/10.1016/j.vaccine.2020.01.055.

92. Jordan E, Lawrence SJ, Meyer TPH, Schmidt D, Schultz S, Mueller J, Stroukova D, Koenen B, Gruenert R, Silbernagl G, Vidojkovic S, Chen LM, Weidenthaler H, Samy N, Chaplin P. 2020. Broad Antibody and Cellular Immune Response From a Phase 2 Clinical Trial With a Novel Multivalent Poxvirus-Based Respiratory Syncytial Virus Vaccine. J Infect Dis ® 223:1062–72.

93. Hendricks DA, Baradaran K, Mclntosh K, Patterson ~' JL. 1987. Appearance of a Soluble Form of the G Protein of Respiratory Syncytial Virus in Fluids of Infected Cells. J gen Virol 68:1705–1714.

94. Hendricks,' DA, Mcintosh K, Patterson2' JL. 1988. Further Characterization of the Soluble Form of the G Glycoprotein of Respiratory Syncytial Virus. J Virol 62:2228–2233.

95. Roberts,' Drew Lichtenstein SR, Ball,' And LA, Wertz' GW. 1994. The Membrane-Associated and Secreted Forms of the Respiratory Syncytial Virus Attachment Glycoprotein G Are Synthesized from Alternative Initiation Codons. J Virol 68:4538–4546.

96. Barr FE, Pedigo H, Johnson TR, Shepherd VL. 2000. Surfactant Protein-A Enhances Uptake of Respiratory Syncytial Virus by Monocytes and U937 MacrophagesAm. J. Respir. Cell Mol. Biol.

97. Hickling TP, Malhotra R, Bright H, Mcdowell W, Blair ED, Sim RB. 2000. Lung Surfactant Protein A Provides a Route of Entry for Respiratory Syncytial Virus into Host CellsVIRAL IMMUNOLOGY.

98. Hickling TP, Bright H, Wing K, Gower D, Martin SL, Sim RB, Malhotra R. 1999. A recombinant trimeric surfactant protein D carbohydrate recognition domain inhibits respiratory syncytial virus infection in vitro and in vivo. Eur J Immunol 29:3478–3484.

99. Levine AM, Elliott J, Whitsett JA, Srikiatkhachorn A, Crouch E, Desilva N, Korfhagen T. 2004. Surfactant Protein-D Enhances Phagocytosis and Pulmonary Clearance of Respiratory Syncytial Virus. Am J Respir Cell Mol Biol 31:193–199.

100. Ehl S, Bischoff R, Ostler T, Vallbracht S, Schulte-Mönting J, Poltorak A, Freudenberg M. 2004. The role of Toll-like receptor 4 versus interleukin-12 in immunity to respiratory syncytial virus. Eur J Immunol 34:1146–1153.

101. Lizundia R, Sauter K-S, Taylor G, Werling D. 2008. Host species-specific

usage of the TLR4–LPS receptor complex. Innate Immun https://doi.org/10.1177/1753425908095957.

102. Marchant D, Singhera GK, Utokaparch S, Hackett TL, Boyd JH, Luo Z, Si X, Dorscheid DR, Mcmanus BM, Hegele RG. 2010. Toll-Like Receptor 4-Mediated Activation of p38 Mitogen-Activated Protein Kinase Is a Determinant of Respiratory Virus Entry and Tropism. J Virol 84:11359–11373.

103. Marr N, Turvey SE. 2012. Role of human TLR4 in respiratory syncytial virus-induced NF-iB activation, viral entry and replication. Innate Immun https://doi.org/10.1177/1753425912444479.

104. Malhotra R, Ward M, Bright H, Priest R, Foster MR, Hurle M, Blair E, Bird M. 2003. Isolation and characterisation of potential respiratory syncytial virus receptor(s) on epithelial cells. Microbes Infect.

105. Arnold R, König W. 2005. Respiratory Syncytial Virus Infection of Human Lung Endothelial Cells Enhances Selectively Intercellular Adhesion Molecule-1 Expression. J Immunol 174:7359–7367.

106. Liu X, Qin X, Xiang Y, Liu H, Gao G, Qin L, Liu C, Qu X. 2013. Progressive Changes in Inflammatory and Matrix Adherence of Bronchial Epithelial Cells with Persistent Respiratory Syncytial Virus (RSV) Infection (Progressive Changes in RSV Infection). Int J Mol Sci 14:18024–18040.

107. Behera AK, Matsuse H, Kumar M, Kong X, Lockey RF, Mohapatra SS. 2001. Blocking Intercellular Adhesion Molecule-1 on Human Epithelial Cells Decreases Respiratory Syncytial Virus Infection. Biochem Biophys Res

Commun 280.

108. Lingemann M, Mccarty T, Liu X, Buchholz Id UJ, Surman S, Martin SE, Collins PL, Munir Id S. 2019. The alpha-1 subunit of the Na + ,K +-ATPase (ATP1A1) is required for macropinocytic entry of respiratory syncytial virus (RSV) in human respiratory epithelial cells. PLOS Pathog https://doi.org/10.1371/journal.ppat.1007963.

109. Wellemans V, Benhassou HA, Fuselier E, Bellesort F, Dury S, Lebargy F, Dormoy V, Fichel C, Naour R Le, Gounni AS, Lamkhioued B. 2021. Role of CCR3 in respiratory syncytial virus infection of airway epithelial cells. iScience 24.

110. Fong AM, Alam SM, Imai T, Haribabu B, Patel DD. 2002. CX 3 CR1 Tyrosine Sulfation Enhances Fractalkine-induced Cell Adhesion*. J Biol Chem 277.

111. Johnson PR, Spriggs MK, Olmsted RA, Collins PL. 1987. The G glycoprotein of human respiratory syncytial viruses of subgroups A and B: Extensive sequence divergence between antigenically related proteins (viral attachment protein/O-linked glycosylation/protein structure). Biochemistry 84:5625–5629.

112. Green G, Johnson SM, Costello H, Brakel K, Harder O, Oomens AG, Peeples ME, Moulton HM, Niewiesk S. 2021. CX3CR1 Is a Receptor for Human Respiratory Syncytial Virus in Cotton Rats. J Virol 95.

113. Johnson CH, Miao C, Blanchard EG, Caidi H, Radu GU, Hartcourt JL, Haynes LiM. 2012. Effect of Chemokine Receptor CX3CR1 Deficiency in a Murine

Model of Respiratory Syncytial Virus Infection. Comp Med 62:14–20.

114. Das S, Raundhal M, Chen J, Oriss TB, Huff R, Williams J V, Ray A, Ray P. 2017. Respiratory syncytial virus infection of newborn CX3CR1-deficient mice induces a pathogenic pulmonary innate immune response. JCI insight https://doi.org/10.1172/jci.insight.94605.

115. Cepika AM, Gagro A, Bace A, Tjesic-Drinkovic D, Kelecic J, Baricic-Voskresensky T, Matic M, Drazenovic V, Marinic I, Mlinaric-Galinovic G, Tjesic-Drinkovic D, Vrtar Z, Rabatic S. 2008. Expression of chemokine receptor CX3CR1 in infants with respiratory syncytial virus bronchiolitis. Pediatr Allergy Immunol 19:148–156.

116. Zhivaki D, Bastien Lemoine S, Lim A, Zhang X, Tissiè P, Lo R, Correspondence M. 2017. Respiratory Syncytial Virus Infects Regulatory B Cells in Human Neonates via Chemokine Receptor CX3CR1 and Promotes Lung Disease Severity. Immunity https://doi.org/10.1016/j.immuni.2017.01.010.

117. Anderson CS, Chu C-Y, Wang Q, Mereness JA, Ren Y, Donlon K, Bhattacharya S, Misra RS, Walsh EE, Pryhuber GS, Mariani TJ. 2019. CX3CR1 as a respiratory syncytial virus receptor in pediatric human lung. Pediatr Res https://doi.org/10.1038/s41390-019-0677-0.

118. Anderson CS, Chirkova T, Slaunwhite CG, Qiu X, Walsh EE, Anderson LJ, Mariani TJ. 2021. CX3CR1 Engagement by Respiratory Syncytial Virus Leads to Induction of Nucleolin and Dysregulation of Cilium-Related Genes. J Virol

95.

119. Fedechkin SO, George NL, Castrejon AMN, Dillen JR, Kauvar LM, Dubois RM. 2020. Conformational Flexibility in Respiratory Syncytial Virus G Neutralizing Epitopes. J Virol 94.

A version of this paper was published in Journal of Virology.

Chapter 2:

Structure-based design and antigenic validation of respiratory syncytial virus G immunogens

2.1 Abstract

Respiratory syncytial virus (RSV) is a leading cause of severe lower respiratory tract disease of children, the elderly, and immunocompromised individuals. Currently, there are no FDA-approved RSV vaccines. The RSV G glycoprotein is used for viral attachment to host cells and impairment of host immunity by interacting with the human chemokine receptor CX3CR1. Antibodies that disrupt this interaction are protective against infection and disease. Nevertheless, development of an RSV G vaccine antigen has been hindered by its low immunogenicity and safety concerns. A previous study described three engineered RSV G proteins containing single-point mutations that induce higher levels of IgG antibodies and have improved safety profiles compared to wild-type RSV G (H. C. Bergeron, J. Murray, A. M. Nuñez Castrejon, et al., Viruses 13:352, 2021, https://doi.org/10.3390/v13020352).

However, it is unclear if the mutations affect RSV G protein folding and display of its conformational epitopes. In this study, we show that the RSV G S177Q protein retains high-affinity binding to protective human and mouse monoclonal antibodies and has equal reactivity as wild-type RSV G protein to human reference immunoglobulin to RSV. Additionally, we determined the high-resolution crystal structure of RSV G S177Q protein in complex with the anti-RSV G antibody 3G12, further validating its antigenic structure. These studies show for the first time that an engineered RSV G protein with increased immunogenicity and safety retains conformational epitopes to high-affinity protective antibodies, supporting its further development as an RSV vaccine immunogen.

2.2 Importance

Respiratory syncytial virus (RSV) causes severe lower respiratory diseases of children, the elderly, and immunocompromised populations. There currently are no FDA-approved RSV vaccines. Most vaccine development efforts have focused on the RSV F protein, and the field has generally overlooked the receptor-binding antigen RSV G due to its poor immunogenicity and safety concerns. However, single-point mutant RSV G proteins have been previously identified that have increased immunogenicity and safety. In this study, we investigate the antibody reactivities of three known RSV G mutant proteins. We show that one mutant RSV G protein retains high-affinity binding to protective monoclonal antibodies, is equally recognized by anti-RSV antibodies in human sera, and forms the same three-

dimensional structure as the wild-type RSV G protein. Our study validates the structure-guided design of the RSV G protein as an RSV vaccine antigen.

2.3 Introduction

Respiratory syncytial virus (RSV) is the leading cause of severe lower respiratory disease in children and infants, causing approximately 33 million cases and 118,000 deaths globally every year (1–3). RSV is also a major contributor of respiratory disease in the elderly and immunocompromised populations, causing approximately 10,000 deaths annually (4–8). The only FDA-approved prophylaxis is the monoclonal antibody (MAb) palivizumab (Synagis), which reduces hospitalizations due to RSV infection but does not prevent infection (9–11). There currently is no FDA-approved vaccine available to protect against RSV infection.

RSV contains two immunogenic envelope glycoproteins that elicit neutralizing antibodies: RSV F and RSV G (12). The membrane fusion glycoprotein, RSV F, exists in a prefusion form (RSV pre-F) that undergoes a conformational change to post-F in order to cause membrane fusion (12). RSV F is the target of most serum neutralizing antibodies, and thus it has been the focus of most monoclonal antibody and vaccine developmental strategies (13, 14). However, RSV F has known variability and antibody escape potential, and escape from an anti-F monoclonal antibody suptavumab was responsible for its failure in phase 3 trials (15, 16).

The attachment glycoprotein, RSV G, has important roles in RSV infection and in impairment of host immunity. RSV G on the virus surface promotes virus attachment to human airway epithelial cells by interacting with the human chemokine

receptor CX3CR1 (17–20). RSV G impairs host immunity through diverse mechanisms. RSV G dampens the type I antiviral interferon (IFN) responses in airway epithelial cells and dendritic cells, limiting host innate defenses against RSV infection (21). Furthermore, RSV G protein induces a Th2-biased cytokine response in CD41 T cells (22, 23) and downregulates Th1-mediated immune responses, at least in part by modulating neonatal regulatory B cells (24). Notably, RSV G is produced as both a membrane-bound form, for incorporation into new virion particles, as well as a secreted form (RSV sG) due to a conserved second start codon at Met 48 (25–27). RSV sG has been shown to compete with CX3CL1 for binding to CX3CR1, modulating signaling and trafficking to the lungs by CX3CR11 killer T cells and NK cells, which are needed for clearance of RSV-infected cells (20, 28–30). RSV sG has also been shown to modulate the responses of Fc-expressing immune cells, limiting their ability to clear RSV-antibody complexes and RSV-infected cells (31).

Despite RSV G's role in infection and disease, it has been mostly overlooked as a vaccine target due to its overall sequence variability, highly glycosylated mucin-like domains, and safety concerns (described below) (12, 32, 33). In addition, RSV G is less immunogenic than RSV F, with RSV G eliciting approximately 2 to 10% of human serum neutralizing antibodies (34, 35). RSV G does, however, contain a nonglycosylated region that is nearly invariant across strains, termed the central conserved domain (CCD), which interacts with CX3CR1 and is the target of broadly neutralizing antibodies (36–44). Structural studies have revealed that the RSV G CCD contains conformational epitopes where these protective antibodies bind (45–47).

Anti-RSV G antibodies that target the CCD have been shown to be protective in vivo in mouse and cotton rat models of RSV infection. The anti-RSV G mouse monoclonal antibodies (MAbs) 131-2G, 5A6, and 3A5 and the human MAbs 3D3 and 3G12 reduce lung viral loads and weight loss in mouse models (36–44, 48). Anti-RSV G MAbs also reduce disease symptoms, including pulmonary inflammation, airway resistance, and mucus production in mouse models (36–38, 40–42, 44, 48). Notably, the bivalent antigen binding fragment [F(ab9)2] of 131-2G reduces pulmonary cell infiltration, mucin production, weight loss, and airway dysfunction without reducing lung viral titers in mice, revealing that anti-RSV G antibody protection from disease symptoms is not due solely to reduced viral loads (36, 41). Moreover, F(ab9)2 131-2G shifted the antibody response toward a Th1 response, with higher IgG2a antibody titers in immunized mice, and lowered the percentage of interleukin-4 (IL-4)-positive T cells (48). In cotton rats, anti-RSV G antibody CB017.5 reduced viral loads, inflammation, and pathology in both treatment and prophylactic models (47).

Anti-RSV G antibodies that target the CCD are also protective in human models in vitro. MAbs 131-2G, CB002.5, and CB017.5, as well as others, directly neutralize RSV infection in primary human airway and bronchial epithelial cells (17, 19, 47, 49). One study developed an in vitro model of RSV infection. Peripheral blood mononuclear cells (PBMCs) were cocultured in the top chamber of a permeable membrane Transwell insert with RSV-infected human airway epithelial cells in the bottom chamber (50). The addition of F(ab9)2 131-2G to this in vitro system

decreased virus replication and increased the levels of alpha interferon (IFN-a) and tumor necrosis factor alpha (TNF-a) produced by plasmacytoid dendritic cells and monocytes within PBMCs (50). A separate study demonstrated anti-RSV G MAbs can induce the destruction of RSV-infected Hep-2 cells by PBMCs and phagocytosis by human blood neutrophils (49). Finally, in a study in human infants and young children, lower clinical disease severity upon natural RSV infection was correlated with higher maternal immunoglobulin G antibodies against RSV G and RSV pre-F ($P = 0.028$ and 0.038, respectively), despite the .30-fold lower abundance of antibodies against RSV G compared to RSV pre-F (35).

Despite the abundance of evidence that anti-RSV G antibodies are protective in vivo, poor immunogenicity and safety concerns have hindered the development of RSV G as a vaccine antigen. In a 1960s' clinical trial of formalin-inactivated RSV (FI-RSV), vaccine recipients experienced enhanced respiratory disease (ERD) upon natural RSV infection (51–55). Subsequent studies have identified several factors that may have contributed to ERD, including lung eosinophilia, a Th2-biased immune response, and low-avidity antibody responses leading to immune complex deposition in the lungs (56). RSV G as a vaccine antigen—either as a recombinant protein or vaccinia virus expressing RSV G—recapitulates some aspects of ERD in the mouse model: mainly eosinophilia and increased Th2 cytokines/chemokines following RSV challenge (51–55). Furthermore, immunization with sG increases the levels of the Th2 cytokines IL-5, which activates eosinophils, and IL-13 produced in the lungs of immunized mice (54, 57). However, subsequent studies revealed that the immune

responses from FI-RSV and RSV G antigen alone are distinct (23, 58), and there are contradictions in the literature as to whether immunization with FI-RSV from RSV lacking the G protein reduces ERD following RSV challenge (30, 59). Nevertheless, the ability of RSV G antigen to prime for eosinophilia and a Th2-biased response has hindered its development as a vaccine antigen.

One strategy to improve the safety and immunogenicity of the RSV G antigen has involved mutagenesis to inactivate the detrimental activities tied to the CCD. In one approach, mutagenesis of the CX3C motif to CX4C (insertion of an alanine before cysteine 186) was used to develop a live attenuated RSV vaccine (RSV CX4C). Evaluation of RSV CX4C in an in vitro model of RSV infection of human airway epithelial (HAE) cells incubated with human PMBCs revealed that RSV CX4C induced higher levels of type I and III interferons compared to wild-type (WT) RSV (50). Additionally, RSV CX4C is less effective at infecting HAE cells, which may decrease its pathogenicity (18, 60). Evaluation of RSV CX4C compared to wild-type RSV in vivo showed reduced lung inflammatory cell infiltration, mucus production, and airway resistance upon RSV challenge in mice (18, 50, 60, 61). Furthermore, RSV CX4C induced higher serum neutralizing antibody titers compared to wild-type RSV (61). Cotton rats, which are more permissible to RSV disease than mice, infected with RSV CX4C had less interstitial inflammation and alveolitis compared to rats infected with wild-type RSV (60).

In another approach, single-point mutagenesis of a different CCD residue, serine 177, which is conserved as a small amino acid glycine or serine, was compared

to the CX4C mutant in an RSV G subunit vaccine (62). In this study, mice immunized with recombinant RSV G proteins containing wild-type or CX4C, S177Q, or S177R mutant sequences were evaluated for antibody responses and markers of disease. RSV G S177Q and S177R proteins induced higher levels of anti-RSV IgG antibodies in immunized mice before and after RSV challenge compared to mice immunized with RSV G wild-type or CX4C proteins, as assessed by enzyme-linked immunosorbent assay (ELISA). Moreover, elicited antibodies were shown to block RSV G-CX3CR1 interaction, which is a known protective functional activity of anti-RSV G antibodies (described above). Additionally, mice immunized with RSV G S177Q protein had reduced bronchoalveolar lavage cell influx into the lungs.

Despite the promise of RSV G engineering to improve immunogenicity and overcome safety concerns, it has been unclear if the mutations affect antigen folding and display of RSV G conformational epitopes. This is important because structural distortion of RSV G protein could prevent binding of high-affinity antibodies and reduce vaccine efficacy. In this study, we compare RSV G wild-type and CX4C, S177Q, and S177R mutant proteins for their binding affinities to anti-RSV G MAbs 3G12, 3D3, 2D10, and 131-2G. Additionally, we compare RSV G wild-type and mutant proteins for binding to human reference immunoglobulin to RSV. Finally, we present the structure of antibody 3G12 bound to RSV G CCD S177Q to evaluate at the atomic level the mutant CCD folding and display of the 3G12 conformational epitope. These studies validate the structure and antigenicity of the RSV G S177Q mutant and support its further development as an RSV vaccine immunogen.

2.4 Results

2.4.1 Design of RSV G^{ecto} WT and mutant proteins

Recombinant RSV G ectodomain (G^{ecto}) wild-type (WT) and mutant (CX4C, S177Q, and S177R) proteins (residues 64 to 298) were designed, expressed, and secreted in mammalian cells and purified from the cell medium as described previously (62). Briefly, RSV G^{ecto} CX4C was engineered by insertion of an alanine into the CX3C motif before cysteine 186 (50) (Fig. 1A). RSV G^{ecto} S177 mutants were designed by investigating all known structures of the RSV G CCD bound to human antibodies 3G12, 3D3, 2D10, CB002.5, and CB017.5 to identify CCD amino acid side chains that do not contribute to the conformational epitopes (45–47) (Fig. 1A and B). Serine 177, which is conserved as a small amino acid glycine or serine, was mutated to a larger amino acid, glutamine, or arginine (S177Q and S177R, respectively), to potentially sterically disrupt interactions with CX3CR1 (Fig. 1C). Analysis of purified RSV G proteins confirmed purity (Fig. 1D). However, it is unclear from these studies if the mutant RSV G proteins fold correctly or display known conformational epitopes.

2.4.2 RSV G^{ecto} S177 mutant proteins retain high-affinity binding to anti-RSV G MAbs

To determine whether recombinant RSV G^{ecto} mutant proteins retain conformational epitopes for anti-RSV G MAbs, binding analyses were conducted using Octet biolayer interferometry. Anti-human or anti-mouse IgG Fc biosensors were loaded with anti-RSV G human MAbs (3G12, 2D10, and 3D3) or mouse MAb 131-2G, respectively. Biosensors were submerged into 1:2 serial dilutions of RSV G^{ecto} WT or mutant proteins to measure on-rates and then submerged into buffer to measure off-rates (Table 1). The binding constant (equilibrium dissociation constant [KD]) for each antibody-antigen interaction was then calculated (Table 1). RSV G^{ecto} WT protein bound to MAbs 3D3, 3G12, and 131-2G with a low-picomolar, high-picomolar, and low-nanomolar KD, respectively, consistent with previous binding

studies (39, 46, 49) (Table 1). We also determined for the first time that RSV G^{ecto} WT protein binds to MAb 2D10 with a low-picomolar KD, similar to the known highest-affinity anti-RSV G Mab, 3D3. RSV G^{ecto} S177Q and S177R mutant proteins had the same or modestly reduced affinity for all four MAbs compared to RSV G^{ecto} WT protein. In the cases of reduced binding, affinities were still maintained at high-picomolar or low-nanomolar KDs. Together, these data indicate that the S177Q or S177R mutations do not disturb the epitopes required to bind diverse anti-RSV G MAbs with high affinity. In contrast, RSV G^{ecto} CX4C protein had reduced binding affinities for all four anti- RSV G MAbs (Table 1). While binding affinity was only modestly reduced for MAb 131-2G, affinities for MAbs 3D3 and 3G12 were reduced by approximately 100-fold, and affinity to MAb 2D10 was reduced by approximately 10,000-fold. These data reveal that epitopes of the RSV G^{ecto} CX4C mutant protein are significantly disrupted by the mutation and have reduced affinities for diverse anti-RSV G MAbs.

2.4.3 Human reference immune globulin to RSV equally recognizes RSV G^{ecto} WT and S177Q mutant proteins

To determine whether RSV G^{ecto} WT and mutant proteins could be recognized by anti-RSV antibodies in human sera, enzyme-linked immunosorbent assays (ELISAs) were conducted using human reference immune globulin to RSV (human anti-RSV Ig), which has been shown to contain RSV neutralizing antibodies (63, 64). ELISA plates were coated with recombinant RSV G^{ecto} WT and mutant proteins, and reactivity to serially diluted human anti-RSV Ig was evaluated.

ELISA signals and area under the curve (AUC) calculations are shown in Fig. 2. RSV G^{ecto} WT and S177Q mutant proteins had indistinguishable reactivities, suggesting that the immunodominant epitopes in human anti-RSV Ig are not significantly affected by the S177Q mutation. In contrast, RSV G^{ecto} S177R and CX4C mutant proteins had reduced reactivities compared to RSV G^{ecto} WT. RSV G^{ecto} CX4C had the lowest reactivity of the three RSV G^{ecto} mutant proteins, consistent with MAb binding studies; however, it had some detectable reactivity over the "no-antigen" control ($P = 0.01$ to 0.05). The data indicate that the RSV G^{ecto} S177Q mutant protein displays immunodominant epitopes for human anti-RSV Ig.

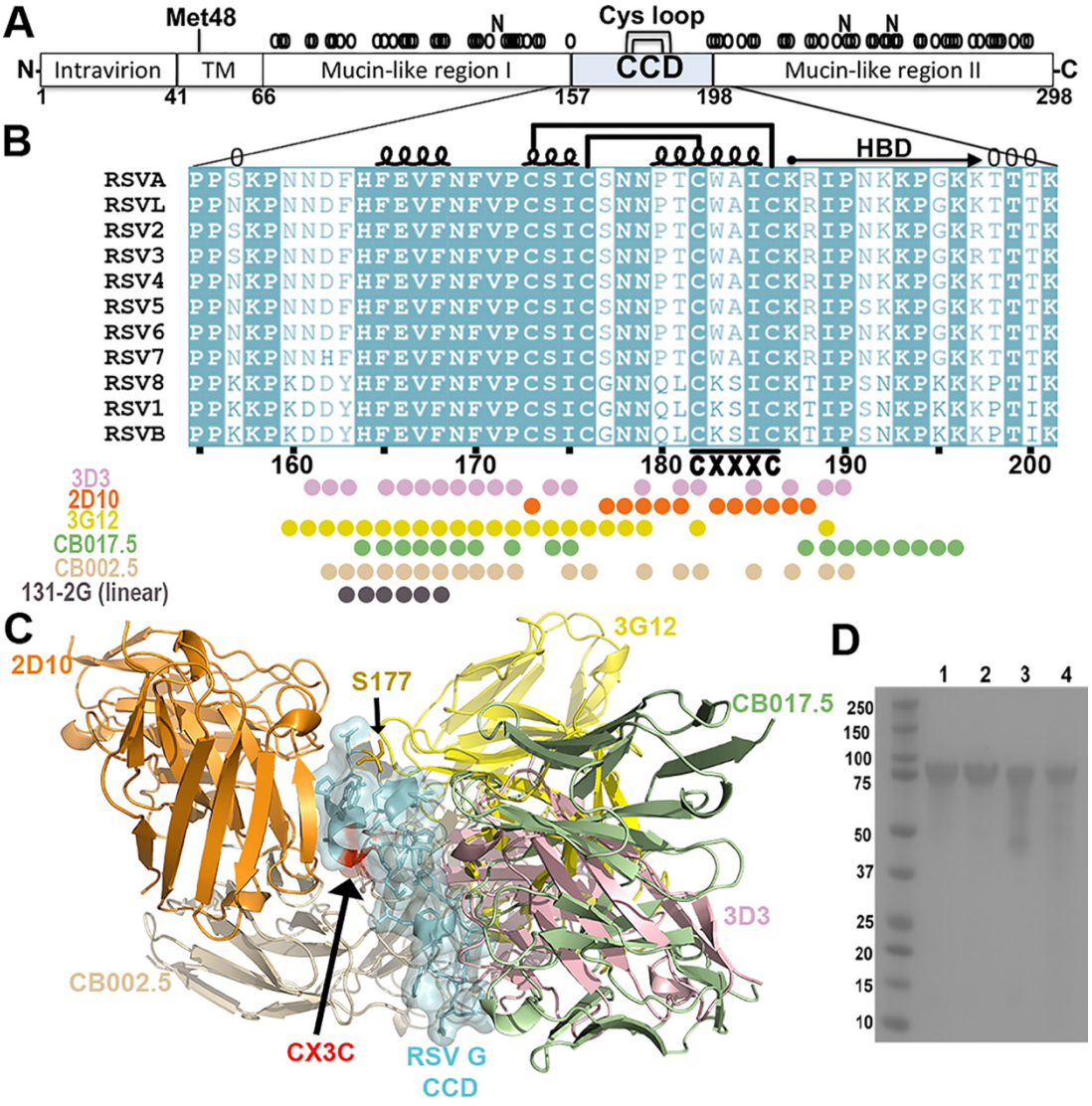

Figure 1: Anti-RSV G monoclonal antibody interactions with the RSV G central conserved domain (CCD).

(A) A schematic of RSV G protein of RSV strain A2 showing the transmembrane domain (TM), the alternate initiation site at methionine 48 that initiates the production of soluble RSV G protein, mucin-like regions I and II with predicted O- and N-linked glycans ("0" and "N," respectively) above, the CCD (amino acids [aa] 157 to 198), and the 4-cysteine loop (Cys loop) within the CCD. (B) Sequence alignment of the RSV G CCD from indicated strains. Conserved amino acids are highlighted in cyan. Secondary structure and disulfide bonds are represented

by loops and brackets, respectively. The heparin binding domain (HBD) is labeled. The CX3C motif is shown at amino acids 182 to 186. Conformational epitope amino acids for anti-RSV G monoclonal antibodies 3D3 (pink), 2D10 (orange), 3G12 (yellow), CB017.5 (green), and CB002.5 (wheat) and the linear epitope amino acids for 131-2G (gray) are indicated. It is unknown if antibody 131-2G has a larger or conformational epitope. (C) RSV G CCD (side view) shown in cyan, with S177 highlighted in gold and the CX3C motif highlighted in red. Variable domains of monoclonal antibodies 2D10 (orange; PDB code 5WN9), 3G12 (yellow; PDB code 6UVO), CB017.5 (green; PDB code 6BLH), 3D3 (pink; PDB code 5WNA), and CB002.5 (wheat; PDB code 6BLI) when bound to overlaid RSV G CCD structures are displayed. (D) Coomassie-stained SDS-PAGE gel of RSV Gecto WT and mutant proteins at ;90 kDa. Lane 1, WT; lane 2, S177Q mutant; lane 3, S177R mutant; lane 4, CX4C mutant.

Table 1 Binding affinity constant (KD), on-rates (k_a), off-rates (k_d), R^2, and χ^2 of RSV G^{ecto} WT and mutant proteins to anti-RSV G mAbs

Sample	**mAb**	**K_D (pM)**	**k_a ($x10^5$ $M^{-1}s^{-1}$)**	**k_d ($x10^{-5}$ s^{-1})**	**R^2**	**χ^2**
RSV G ^{ecto} WT	3G12	260	2.52	6.55	0.9992	0.4802
		262	1.98	5.19	0.9993	0.4809
RSV G ^{ecto} S177Q	3G12	2280	2.32	52.8	0.9974	0.6908
		1880	2.38	44.7	0.9975	0.5193
RSV G ^{ecto} S177R	3G12	4340	1.34	58.1	0.9949	1.4869
		4600	1.46	67.2	0.9965	0.8916
RSV G ^{ecto} CX4C	3G12	27700	0.399	110	0.9751	0.5311
		28000	0.367	103	0.9681	0.6455
RSV G ^{ecto} WT	2D10	<1	3.70	<0.01	0.998	0.8776
		<1	3.83	<0.01	0.9975	1.0426
RSV G ^{ecto} S177Q	2D10	605	3.71	22.5	0.9985	0.5392
		485	3.1	15	0.9959	1.4183
RSV G ^{ecto} S177R	2D10	<1	3.18	<0.01	0.9983	0.6609
		<1	2.53	<0.01	0.9962	1.1652
RSV G ^{ecto} CX4C	2D10	65100	0.249	162	0.9848	0.6959
		93300	0.213	199	0.9839	0.5709
RSV G ^{ecto} WT	3D3	<1	4.26	<0.01	0.9988	0.5743

		<1	4.31	<0.01	0.9983	0.5431
RSV G ^{ecto} S177Q	3D3	538	3.69	19.9	0.9974	0.4947
		264	4.14	10.9	0.9982	0.2435
RSV G ^{ecto} S177R	3D3	422	2.47	10.4	0.9972	0.6466
		570	2.65	15.1	0.9972	0.6919
RSV G ^{ecto} CX4C	3D3	6080	0.531	32.3	0.9946	0.6276
		6230	0.479	29.8	0.9893	0.7662
RSV G ^{ecto} WT	131-2G	1900	2.87	54.4	0.9891	0.1445
		3200	2.89	92.4	0.9609	0.4062
RSV G ^{ecto} S177Q	131-2G	3480	3.38	118	0.9928	0.102
		6540	2.3	151	0.9875	0.1745
RSV G ^{ecto} S177R	131-2G	8600	0.481	41.4	0.9933	0.1485
		2360	2.48	58.6	0.9853	0.4089
RSV G ^{ecto} CX4C	131-2G	13200	0.477	62.8	0.9591	0.2116
		19600	0.496	97	0.9813	0.1074

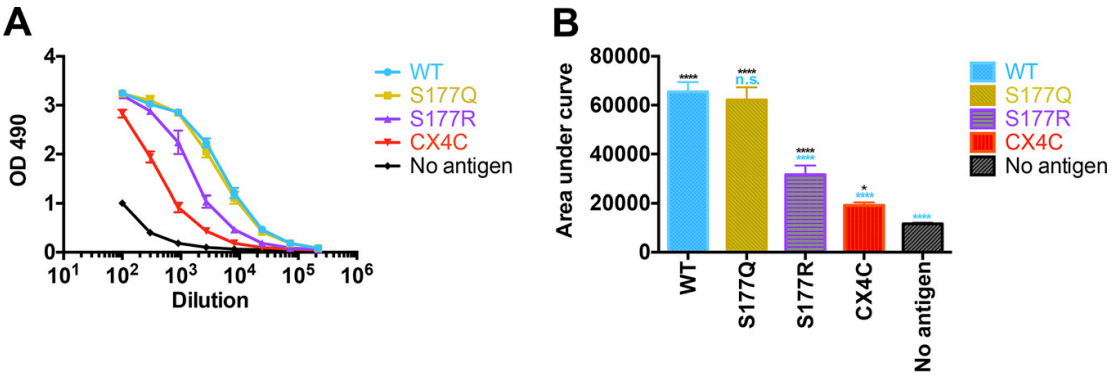

Figure 2: Human reference immunoglobulin to RSV binding to RSV G^{ecto} WT and mutant proteins.

(A) Dilution series ELISA to evaluate the human reference IgG reactivity to recombinant RSV G^{ecto} WT and mutant proteins. Samples were evaluated in biological quadruplicates, and error bars represent 1 standard deviation (SD) from the mean. A curve is shown for RSV G^{ecto} WT (cyan) and S177Q (gold), S177R (purple), and CX4C (red) mutant proteins, as well as a negative control with no antigen (black). (B) The area under the curve for each sample was calculated in Prism. Error bars represent the mean and SD. Data were analyzed by a one-way analysis of

variance (ANOVA): n.s., not significant (P≥0.05); *, P = 0.01 to 0.05; ****, P , 0.0001.

2.4.4 Fab 3G12-RSV G CCD S177Q structure

To further show at the atomic level that the S177Q mutation does not disrupt CCD folding and display of conformational epitopes, we used X-ray crystallography to solve the structure of RSV G CCD S177Q bound to 3G12 antibody (Fig. 3 and Table 2). Recombinant RSV G CCD residues 157 to 197 containing the S177Q mutation were copurified with the fragments of antigen binding (Fab) 3G12. The complex was crystallized, and the structure was solved to 3.1-Å resolution. The structure reveals that the 3G12 conformational epitope is displayed by the RSV G CCD containing the S177Q mutant, consistent with MAb 3G12 binding studies showing high-affinity binding. The electron density maps show extended density for the mutant glutamine side chain compared to the density of the wild-type serine side chain at RSV G residue 177 (Fig. 3A). Comparison of the RSV G CCD wild-type and S177Q mutant structures shows that they are nearly identical, with a root mean square deviation (RMSD) of 0.16 Å, and their contacts with antibody 3G12 are largely conserved (Fig. 3B). Notably, although residue 177 is in the middle of a loop constrained by the four cysteines in two disulfide bonds, the S177Q mutation does not prevent the formation of these disulfide bonds, which are important for the display of all known conformational epitopes. Indeed, structural comparison of RSV G CCD S177Q with wild-type RSV G CCDs bound to different antibodies reveals that the central disulfide-bonded regions of the CCDs (residues 169 to 187) are nearly identical (Fig.

3C). Overall, this structure reveals that the RSV G CCD containing the S177Q mutation is structurally intact and displays conformational epitopes.

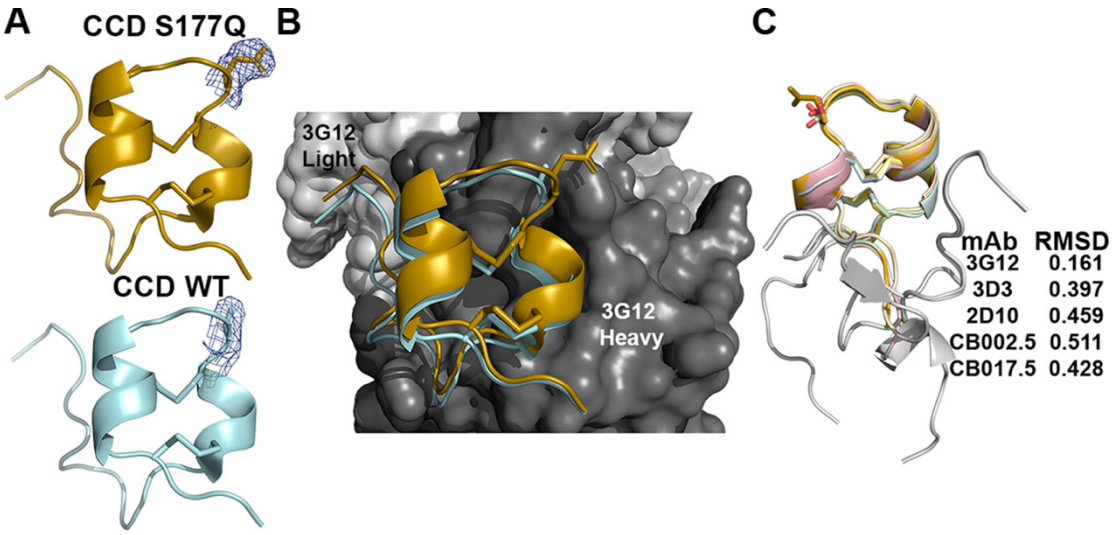

Figure 3: Crystal structure of Fab 3G12 in complex with RSV G CCD S177Q at a 3.1-Å resolution.

(A) Comparison of RSV G CCD WT (cyan; PDB code 6UVO) and S177Q (gold; PDB code 7T8W) when bound to Fab 3G12. Electron density maps, contoured at 1.0 sigma within 1.8 Å of amino acid 177, are shown. (B) Overlay of the structures of RSV G CCD WT (cyan) and RSV G CCD S177Q (gold) bound to Fab 3G12. (C) Overlay of RSV G CCD WT bound to anti-RSV G antibodies 3G12 (yellow; PDB code 6UVO), 3D3 (pink; PDB code 5WNA), and 2D10 (orange; PDB code 5WN9) and CB002.5 (wheat; PDB code 6BLI), CB017.5 (green; PDB code 6BLH), and RSV G CCD S177Q bound to 3G12 Fab (gold; PDB code 7T8W). Flexible amino acids are shown in gray. RMSD values were determined using PyMOL.

Table 2 Data collection and refinement statistics for Fab 3G12 – RSV G CCD S177Q complex

PDB code	7T8W
Data collection	
Space group	P 31 2 1
Cell dimensions	
a, b, c (Å)	139.39, 139.39, 98.05
α, β, γ (°)	90, 90, 120
Resolution (Å)	98.05-3.10 (3.31-3.10)
R_{sym} or R_{merge}	0.705 (3.614)
I/σI	5.8 (1.8)
Completeness (%)	100 (100)
Redundancy	19.1 (18.7)
$CC_{1/2}$	0.974 (0.567)
Refinement	
Number of reflections	20274 (1983)
Resolution (Å)	76.106-3.1 (3.211-3.1)
R_{work}/R_{free}	0.2369/0.2500
Number of atoms	
Protein	3598
Ligands	0
Water	0
B factors	
Protein	53.35
Ligands	0
Water	0
RMSD	
Bond lengths (Å)	0.014
Bond angles (°)	2.03
Ramachandran statistics	
Favored (%)	96.13
Allowed (%)	3.87
Outliers (%)	0

Data from one crystal were used for each structure determination. Values in parentheses are for the highest-resolution shell.

2.5 Discussion

The value of a structure-based approach for the improvement of vaccine antigens has become widely appreciated (65). Here, we investigated human antibody reactivities to three RSV G mutant proteins (CX4C, S177Q, and S177R), which were previously shown to have increased immunogenicity and safety in vivo compared to wild-type RSV G protein (62). The CX4C mutation had been designed to disrupt the CX3C motif, which is associated with detrimental RSV G activities. However, the CX4C mutation had been designed before antibody-RSV G complex structures and conformational epitopes had been elucidated. The S177 mutations had been designed with these structures in mind to minimize disruption of conformational epitopes.

Affinity binding studies for MAbs against the RSV G S177 mutant proteins reveal that their conformational epitopes are largely intact (Table 1). MAb binding affinity constants remained in the picomolar or low-nanomolar range. Interestingly, in all cases of reduced binding, such as the 17-fold reduction in binding of MAb 3G12 to RSV G S177R protein, analyses of binding kinetics reveal that the on-rates were the same as for binding to wild-type RSV G, but the off-rates were slightly faster (Table 1). As the S177 side chain is only 3.5 to 4.0 Å away from MAb 3G12 CDR3 residues (Fig. 3B), it is likely that the size or charge of the S177R mutation caused some repulsion and affected off-rates. On the other hand, the S177 side chain is .10 Å away from MAb 3D3 residues, yet S177 mutations modestly reduced MAb 3D3 binding. This suggests that CCD mutations may affect MAb binding by mechanisms other than direct repulsion—perhaps by restricting CCD flexibility and entropy.

In contrast to studies with RSV G S177 mutant proteins, MAb binding affinity studies with the RSV G CX4C mutant protein reveal that its conformational epitopes are significantly disrupted (Table 1). Binding of MAb 2D10 to RSV G CX4C protein was severely reduced (10,000-fold), which is not surprising given that the CX3C motif forms; 40% of the 2D10 epitope. On the other hand, binding to MAb 3G12 was reduced by approximately 100-fold, despite the CX3C motif forming only 0.01% of the 3G12 epitope, suggesting that the CX4C mutation induces global changes to the CCD structure beyond just the CX3C motif. Consistent with this, a 6-fold reduction in binding to MAb 131-2G was observed, despite the CX4C mutation being 17 amino acids downstream of the 131-2G linear epitope (Fig. 1B), suggesting that the CX4C mutation broadly distorts the CCD structure and/or MAb 131-2G may have a conformational epitope. Notably, analyses of binding kinetics reveal that both on-rates and off-rates are significantly affected by the CX4C mutation (Table 1).

We further evaluated the RSV G mutant proteins in ELISA studies with human reference immune globulin to RSV. Consistent with MAb binding studies, ELISA studies reveal that the RSV G CX4C mutant protein has significantly reduced binding to human anti-RSV antibodies compared to wild-type RSV G. Interestingly, we observed a difference between the two RSV G S177 mutant proteins: whereas the RSV G S177R protein has reduced binding compared to wild-type RSV G, the RSV G S177Q protein has equal binding to human anti-RSV antibodies compared to wild-type RSV G. We note that a generally understood distinction between binding affinity studies with human MAbs and ELISAs with human anti-RSV antibodies is that MAb

studies evaluate individual epitopes, whereas ELISAs with human serum antibodies are biased in favor of immunodominant epitopes. These data suggest that the S177Q mutation has little or no effect on the immunodominant epitopes of RSV G protein.

Finally, we validated the structure of RSV G S177Q protein by solving the high-resolution structure of its CCD bound to antibody 3G12. The structure confirms the structural integrity of CCD with the S177Q mutation and is consistent with human MAb and human anti-RSV antibody binding studies.

Altogether, these studies validate for the first time that RSV G immunogens can be engineered for increased immunogenicity and safety while retaining conformational epitopes to high-affinity protective antibodies. In particular, our studies, in combination with those of Bergeron et al. (62), identify the RSV G S177Q mutant protein as a promising RSV vaccine immunogen. The RSV G S177Q mutant protein could be studied further as a subunit vaccine or integrated into other candidate RSV vaccine platforms, including subunit, virus-like particles, live attenuated RSV, virus-vectored, and mRNA vaccines (14). We note that several RSV vaccine candidates targeting the RSV pre-F antigen are currently in phase 3 clinical trials, with some preliminary efficacy data from phase 2 clinical trials suggesting approximately 70% efficacy against symptomatic RSV infection, an improvement over previous RSV vaccine candidates targeting RSV post-F but with potential for additional improvement. Mutational escape from the MAbs against the F protein has already proven to be clinically significant, and widespread use of F protein vaccines or MAbs given prophylactically runs the risk of generating escape mutants. Notably,

none of these candidates includes an RSV G immunogen, meaning that they will not elicit the broadly protective anti-RSV G antibodies that block RSV engagement of the human CX3CR1 receptor, which is key for infection of human airway epithelial cells and for RSV dampening of host immune responses. Thus, addition of engineered RSV G immunogens to RSV pre-F vaccine candidates may increase both efficacy and universality while reducing escape potential.

2.6 Materials and Methods

2.6.1 Expression and purification of wild-type and mutant RSV G^{ecto} proteins.

A synthetic gene encoding RSV (strain A2) G protein ectodomain (RSV G^{ecto}) amino acids 64 to 298 (UniProtKB entry P03423), in frame with an N-terminal tissue plasminogen activator (TPA) or CD5 signal sequence and tandem C-terminal 6 histidine and Twin-Strep purification tags, was cloned into cytomegalovirus (CMV) promoter-driven expression plasmids pCF or a derivative of pcDNA3.1 (66). Mutations in the RSV G gene were introduced by Phusion site-directed mutagenesis and verified by Sanger sequencing. The CX4C mutant contains an additional alanine within the CX3C motif before the second cysteine (C^{186}) to encode CWAIAC (CX4C) instead of the wild-type sequence CWAIC (CX3C). Serine 177 was mutated to glutamine or arginine for mutants S177Q and S177R, respectively. Recombinant RSV G^{ecto} proteins were expressed by transient transfection in CHO-S cells using electroporation (Maxcyte STX) and purified from the media by StrepTrap affinity chromatography. All proteins were concentrated to 1 mg/ml and dialyzed into

phosphate buffered saline (PBS). Purity was verified by SDS-polyacrylamide gel electrophoresis (Figure 1D).

2.6.2 Anti-RSV G mAbs 3D3, 2D10, 3G12, and 131-2G

Synthetic genes encoding the heavy chain or light chain variable regions of human mAb 2D10 were cloned by Gibson assembly into the pCMVR VRC01 antibody vectors for light and heavy chains obtained from the AIDS Reagent Program, in place of the variable regions of antibody VRC01, a human anti-HIV antibody (IgG1) targeting the gp120 protein (67). The plasmids were verified by DNA sequencing. Recombinant mAb 2D10 was expressed by transient transfection in CHO-S cells and purified from the media by immobilized protein A affinity chromatography. Purity was verified by SDS-polyacrylamide gel electrophoresis. Recombinant mAbs 3D3 and 3G12 were produced as described previously and obtained from Trellis Bioscience (27). Mouse mAb 131-2G was purchased from EMD Millipore (MAB858-2).

2.6.3 Binding affinity analyses

An Octet RED384 biolayer interferometry instrument was used to determine binding affinities of wild-type and mutant RSV G^{ecto} proteins to anti-RSV G mAbs. Anti-human IgG Fc capture AHC biosensors (for mAbs 3D3, 2D10, and 3G12) or anti-mouse IgG Fc capture AMC biosensors (for mAb 131-2G) were submerged in Octet buffer (PBS pH 7.4, 0.05% Tween-20, 1% BSA) for 60 s. The sensors were loaded for 120 s with 1 μg/mL of human or mouse anti-RSV G mAb and then submerged into Octet buffer for 120 s. Association of mAbs with wild-type and mutant RSV

G^{ecto} was measured for 300 s and dissociation in Octet buffer was measured for 600 s. RSV G^{ecto} proteins started at 40 nM and were two-fold serially diluted to 0.63 nM to measure binding to anti-RSV G mAbs. Higher starting concentrations were required to be able to fit curves for RSV G^{ecto} CX4C protein. A global association 1:1 model was used to fit at least three curves to determine the on- and off-rates to calculate the dissociation constant (K_D). All binding assays were performed in duplicate.

2.6.4 ELISA with anti-RSV human immune globulin

Flat bottom, high binding Costar 3590 ELISA plates were coated with wild-type and mutant RSV G^{ecto} proteins at 1 μg/mL in PBS at 4ºC overnight. The plates were washed three times with wash buffer (PBS pH 7.4, 0.1% Tween-20). Plates were blocked overnight at 4ºC with blocking buffer (PBS pH 7.4, 5% dry milk, 1% BSA). The blocking buffer was decanted and Human Reference Immune Globulin to Respiratory Syncytial Virus, CBER RSV Lot 1 (BEI Resources NR-21973) was added starting at 1:100 dilution in blocking buffer and serially diluted three-fold for 1 hour at 37ºC. The plates were washed three times with wash buffer. Goat anti-Human IgG Fc secondary antibody conjugated to horseradish peroxidase (HRP) (Invitrogen A18817) was added at a 1:3000 dilution for 1 hour at 37ºC. The plates were washed two times with wash buffer. Plates were developed for 10 minutes with phosphate citrate buffer, 12.5 μL of 30% hydrogen peroxide, and two o-phenylenediamine dihydrochloride (OPD) tablets. The reaction was stopped with 2N sulfuric acid and the plates were measured at OD_{490} using a Molecular Devices Spectramax plate reader. Human anti-RSV G mAb 3G12 was used as a positive control starting at 1

μg/mL and serially diluted three-fold. No antigen was used as a negative control. Curves were graphed in Graphpad Prism and are the average of four replicates.

2.6.5 Expression and purification of RSV G CCD S177Q.

A synthetic gene encoding RSV (strain A2) G CCD amino acids 157 to 197 (UnitProtKB entry P03423) was cloned into pRSFDuet-1 with an N-terminal methionine and a C-terminal 6x histidine tag. The S177Q mutation was introduced by Phusion site-directed mutagenesis and verified by Sanger sequencing. Recombinant RSV G CCD S177Q was expressed in T7Express *E. coli* overnight at 18ºC. Cells were lysed by ultrasonication in wash buffer (20 mM Tris pH 8, 25 mM imidazole, 150 mM NaCl) with 0.1 mM $MgCl_2$, protease inhibitors, and benzonase. RSV G CCD S177Q was purified from clarified *E. coli* lysates by affinity chromatography using a HisTrap FF crude column and washed with wash buffer containing 6 M Urea. Protein was eluted in wash buffer containing 500 mM imidazole.

2.6.6 Fab preparation of 3G12

The Fab fragments of human anti-RSV G mAb 3G12 were produced using the Pierce Fab Preparation Kit (Thermo Scientific 44985). Briefly, mAb 3G12 was incubated with immobilized papain in PBS for five hours at 37ºC. Fc fragments were removed using immobilized Protein A. Fab purity was verified by SDS-polyacrylamide gel electrophoresis.

2.6.7 Purification of Fab 3G12 - RSV G CCD S177Q complex structure

To generate the Fab 3G12 - RSV G CCD S177Q complex, Fab 3G12 was incubated with a four-molar excess of RSV G CCD S177Q on ice for 30 minutes. A Superdex

75 size exclusion chromatography column was used to purify the complex and eluted in 10 mM Tris-HCl pH 8 and 150 mM NaCl. The complex was concentrated to 8.26 mg/mL. Crystals were grown by hanging drop vapor diffusion in a well solution of 1.8 M ammonium sulfate and 100 mM sodium acetate trihydrate pH 4.4 at room temperature. Crystals were transferred to a cryoprotectant solution of 2 M ammonium sulfate, 100 mM sodium acetate trihydrate pH 4.4, 25% glycerol and 18% of a 1:1:1 ratio of 100% ethylene glycol, dimethylsulfoxide, and glycerol (EDG), and flash frozen in liquid N_2. Diffraction data were collected at the Advanced Light Source on beamline 5.0.1. Data were processed using DIALS and scaled using Aimless (within CCP4). Phaser was used for molecular replacement, and Phenix Refinement and Coot were used for structure refinement.

2.7 Data availability

Coordinates and structure factors for the Fab 3G12 - RSV G CCD S177Q complex structure have been deposited in the Protein Data Bank under accession code 7T8W. All other data has been made available in the manuscript.

2.8 Acknowledgements

We thank Dr. John Dzimianski for his assistance in diffraction data processing. The following reagent was obtained through BEI Resources, NIAID, NIH: Human Reference Immune Globulin to Respiratory Syncytial Virus, CBER RSV Lot 1, NR-21973. R.M.D. is supported by the National Institute of Allergy and Infectious Diseases (NIAID) grant R56AI141537. L.M.K. acknowledges partial support from NIAID grant 5R44AI122360. A.M.N.C. was supported by a Cota Robles Fellowship.

Funding for the purchase of the Octet RED384 instrument was supported by the NIH S10 shared instrumentation grant 1S10OD027012-01. The Berkeley Center for Structural Biology is supported in part by the National Institutes of Health, National Institute of General Medical Sciences, and the Howard Hughes Medical Institute. The Advanced Light Source is supported by the Director, Office of Science, Office of Basic Energy Sciences, of the U.S. Department of Energy under Contract No. DE-AC02-05CH11231. The Pilatus detector on beamline 5.0.1 was funded under NIH grant S10OD021832. The ALS-ENABLE beamlines are supported in part by the National Institutes of Health, National Institute of General Medical Sciences, grant P30 GM124169.

2.9 References

1. Shi T, Mcallister DA, O 'brien KL, Simoes EAF, Madhi SA, Gessner BD, Polack FP, Balsells E, Acacio S, Aguayo C, Alassani I, Ali A, Antonio M, Awasthi S, Awori JO, Azziz-Baumgartner E, Baggett HC, Baillie VL, Balmaseda A, Barahona A, Basnet S, Bassat Q, Basualdo W, Bigogo G, Bont L, Breiman RF, Brooks WA, Broor S, Bruce N, Bruden D, Buchy P, Campbell S, Carosone-Link P, Chadha M, Chipeta J, Chou M, Clara W, Cohen C, De Cuellar E, Dang D-A, Dash-Yandag B, Deloria-Knoll M, Dherani M, Eap T, Ebruke BE, Echavarria M, Cecília De Freitas C, Emediato L, Fasce RA, Feikin DR, Feng L, Gentile A, Gordon A, Goswami D, Goyet S, Groome M, Halasa N, Hirve S, Homaira N, Howie SRC, Jara J, Jroundi I, Kartasasmita CB, Khuri-Bulos N, Kotloff KL, Krishnan A, Libster R, Lopez O, Lucero MG,

Lucion F, Lupisan SP, Marcone DN, Mccracken JP, Mejia M, Moisi JC, Montgomery JM, Moore DP, Moraleda C, Moyes J, Munywoki P, Mutyara K, Nicol MP, Nokes DJ, Nymadawa P, Tereza M, Oliveira DC, Oshitani H, Pandey N, Paranhos-Baccalà G, Phillips Md LN, Picot VS, Rahman M, Rakoto-Andrianarivelo M, Rasmussen ZA, Rath BA, Robinson A, Romero C, Russomando G, Salimi V, Sawatwong P, Scheltema N, Schweiger B, Anthony J, Scott G, Seidenberg P, Shen K, Singleton R, Sotomayor V, Strand TA, Sutanto A, Sylla M, Tapia MD, Thamthitiwat S, Thomas ED, Tokarz R, Turner C, Venter M, Waicharoen S, Wang J, Watthanaworawit W, Yoshida L-M, Yu H, Zar HJ, Campbell H, Nair H. 2017. Global, regional, and national disease burden estimates of acute lower respiratory infections due to respiratory syncytial virus in young children in 2015: a systematic review and modelling study for RSV Global Epidemiology Network. Artic 946 www.thelancet.com https://doi.org/10.1016/S0140-6736(17)30938-8.

2. Shi T, Balsells E, Wastnedge E, Singleton R, Rasmussen ZA, Zar HJ, Rath BA, Madhi SA, Campbell S, Vaccari LC, Bulkow LR, Thomas ED, Barnett W, Hoppe C, Campbell H, Nair H. 2015. Risk factors for respiratory syncytial virus associated with acute lower respiratory infection in children under five years: Systematic review and meta–analysis. J Glob Health 5.

3. Lozano R, Naghavi M, Lim SS, Ahn MPH SY, Alvarado MB, Andrews MPH KG, Atkinson CB, Bolliger IA, Chou DB, Colson BA KE, Delossantos AB, Dharmaratne MBBS SD, Flaxman AD, Lozano R, Naghavi M, Foreman K,

Lim S, Shibuya K, Aboyans V, Abraham J, Adair T, Aggarwal R, Ahn SY, AlMazroa MA, Alvarado M, Ross Anderson H, Anderson LM, Andrews KG, Atkinson C, Baddour LM, Barker-Collo S, Bartels DH, Bell ML, Benjamin EJ, Bennett D, Bhalla K, Bikbov B, Bin Abdulhak A, Birbeck G, Blyth F, Bolliger I, ane Boufous S, Bucello C, Burch M, Burney P, Carapetis J, Chen H, Chou D, Chugh SS, Coff eng LE, Colan SD, Colquhoun S, Ellicott Colson K, Condon J, Connor MD, Cooper LT, Corriere M, Cortinovis M, Courville de Vaccaro K, Couser W, Cowie BC, Criqui MH, Cross M, Dabhadkar KC, Dahodwala N, De Leo D, Degenhardt L, Delossantos A, Denenberg J, Des Jarlais DC, Dharmaratne SD, Ray Dorsey E, Driscoll T, Duber H, Ebel B, Erwin PJ, Espindola P, Ezzati M, Feigin V, Flaxman AD, Forouzanfar MH, Gerry Fowkes FR, Franklin R, Fransen M, Freeman MK, Gabriel SE, Gakidou E, Gaspari F, Gillum RF, Gonzalez-Medina D, Halasa YA, Haring D, Harrison JE, Havmoeller R, Hay RJ, Hoen B, Hotez PJ, Hoy D, Jacobsen KH, James SL, Jasrasaria R, Jayaraman S, Johns N, Karthikeyan G, Kassebaum N, Keren A, Khoo J-P, Marie Knowlton L, Kobusingye O, Koranteng A, Krishnamurthi R, Lipnick M, Lipshultz SE, Lockett Ohno S, Mabweijano J, MacIntyre MF, Mallinger L, March L, Marks GB, Marks R, Matsumori A, Matzopoulos R, Mayosi BM, McAnulty JH, McDermott MM, McGrath J, Memish ZA, Mensah GA, Merriman TR, Michaud C, Miller M, Miller TR, Mock C, Olga Mocumbi A, Mokdad AA, Moran A, Mulholland K, Nathan Nair M, Naldi L, Venkat Narayan KM, Nasseri K, Norman P, Omer SB, Ortblad K, Osborne R, Ozgediz

D, Pahari B, Durai Pandian J, Panozo Rivero A, Perez Padilla R, Perez-Ruiz F, Perico N, Phillips D, Pierce K, Arden Pope III C, Porrini E, Pourmalek F, Raju M, Ranganathan D, Rehm JT, Rein DB, Remuzzi G, Rivara FP, Roberts T, Rodriguez De León F, Rosenfeld LC, Rushton L, Sacco RL, Salomon JA, Sampson U, Sanman E, Schwebel DC, Segui-Gomez M, Shepard DS, Singh D, Singleton J, Sliwa K, Smith E, Steer A, Taylor JA, Thomas B, Tleyjeh IM, rey Towbin JA, Truelsen T, Undurraga EA, Venketasubramanian N, Vijayakumar L, Vos T, Wagner GR, Wang M, Wang W, Watt K, Weinstock MA, Weintraub R, Wilkinson JD, Woolf AD, Wulf S, Yeh P-H, Yip P, Zabetian A, Zheng Z-J, Lopez AD, L Murray CJ. 2012. Global and regional mortality from 235 causes of death for 20 age groups in 1990 and 2010: a systematic analysis for the Global Burden of Disease Study 2010Lancet.

4. Branche AR, Ann Falsey BR. 2015. Respiratory Syncytial Virus Infection in Older Adults: An Under-Recognized Problem. Drugs Aging https://doi.org/10.1007/s40266-015-0258-9.

5. Falsey AR, Hennessey PA, Formica MA, Cox C, Walsh EE. 2005. Respiratory Syncytial Virus Infection in Elderly and High-Risk Adults.

6. Falsey AR, Walsh EE. 2005. Respiratory Syncytial Virus Infection in Elderly Adults. Drugs Aging 22:577–587.

7. Widmer K, Griffin MR, Zhu Y, Williams J V, Keipp Talbot H. 2014. Respiratory syncytial virus-and human metapneumovirus-associated emergency department and hospital burden in adults. Influ Other Respi Viruses

https://doi.org/10.1111/irv.12234.

8. Zhou H, Thompson WW, Viboud CG, Ringholz CM, Cheng P-Y, Steiner C, Abedi GR, Anderson LJ, Brammer L, Shay DK. 2012. Hospitalizations Associated With Influenza and Respiratory Syncytial Virus in the United States, 1993-2008. Clin Infect Dis https://doi.org/10.1093/cid/cis211.

9. Group* TIm-RS. 1998. Palivizumab, a Humanized Respiratory Syncytial Virus Monoclonal Antibody, Reduces Hospitalization From Respiratory Syncytial Virus Infection in High-risk Infants. Pediatrics 102:531–537.

10. Resch B. 2017. Product review on the monoclonal antibody palivizumab for prevention of respiratory syncytial virus infection https://doi.org/10.1080/21645515.2017.1337614.

11. Olchanski N, Hansen RN, Pope E, D 'cruz B, Fergie J, Goldstein M, Krilov LR, Mclaurin KK, Nabrit-Stephens B, Oster G, Schaecher K, Shaya FT, Neumann PJ, Sullivan SD. 2018. Palivizumab Prophylaxis for Respiratory Syncytial Virus: Examining the Evidence Around Value. Open Forum Infect Dis https://doi.org/10.1093/ofid/ofy031.

12. Mclellan JS, Ray WC, Peeples ME. 2013. Structure and Function of RSV Surface Glycoproteins https://doi.org/10.1007/978-3-642-38919-1_4.

13. Shan J, Britton PN, King CL, Booy R. 2021. The immunogenicity and safety of respiratory syncytial virus vaccines in development: A systematic review. Influ Other Respi Viruses 15:539–551.

14. RSV Vaccine and mAb Snapshot | PATH.

15. Simões EAF, Forleo-Neto E, Geba GP, Kamal M, Yang F, Cicirello H, Houghton MR, Rideman R, Zhao Q, Benvin SL, Hawes A, Fuller ED, Wloga E, Pizarro JMN, Munoz FM, Rush SA, Mclellan JS, Lipsich L, Stahl N, Yancopoulos GD, Weinreich DM, Kyratsous CA, Sivapalasingam S. 2020. Suptavumab for the Prevention of Medically Attended Respiratory Syncytial Virus Infection in Preterm Infants. Clin Infect Dis https://doi.org/10.1093/cid/ciaa951.

16. Tabor DE, Fernandes F, Langedijk AC, Wilkins D, Lebbink RJ, Tovchigrechko A, Ruzin A, Kragten-Tabatabaie L, Jin H, Esser MT, Bont LJ, Abram ME. 2021. Global molecular epidemiology of respiratory syncytial virus from the 2017-2018 INFORM-RSV study. J Clin Microbiol 59:1–13.

17. Johnson SM, Mcnally BA, Ioannidis I, Flano E, Teng MN, Oomens AG, Walsh EE, Peeples ME. 2015. Respiratory Syncytial Virus Uses CX3CR1 as a Receptor on Primary Human Airway Epithelial Cultures. PLoS Pathog 11.

18. Chirkova T, Lin S, P Oomens AG, Gaston KA, Boyoglu-Barnum S, Meng J, Stobart CC, Cotton CU, Hartert T V, Moore ML, Ziady AG, Anderson LJ, Larry Anderson CJ. 2015. CX3CR1 is an important surface molecule for respiratory syncytial virus infection in human airway epithelial cells. J Gen Virol https://doi.org/10.1099/vir.0.000218.

19. Jeong K-I, Piepenhagen PA, Kishko M, Dinapoli JM, Groppo RP, Zhang L, Almond J, Kleanthous H, Delagrave S, Parrington M. 2015. CX3CR1 Is Expressed in Differentiated Human Ciliated Airway Cells and Co-Localizes

with Respiratory Syncytial Virus on Cilia in a G Protein-Dependent Manner https://doi.org/10.1371/journal.pone.0130517.

20. Tripp RA, Jones LP, Haynes LM, Zheng HQ, Murphy PM, Anderson LJ. 2001. CX3C chemokine mimicry by respiratory syncytial virus G glycoprotein. Nat Immunol 2:732–738.

21. Hijano DR, Kalergis AM, Kauvar LM, Tripp RA, Polack FP, Cormier SA. 2019. Role of Type I Interferon (IFN) in the Respiratory Syncytial Virus (RSV) Immune Response and Disease Severity. Front Immunol | www.frontiersin.org 1:566.

22. Becker Y, Becker Y. 2006. Respiratory syncytial virus (RSV) evades the human adaptive immune system by skewing the Th1/Th2 cytokine balance toward increased levels of Th2 cytokines and IgE, markers of allergy— a review. Virus Genes 33:235–252.

23. Knudson CJ, Hartwig SM, Meyerholz DK, Varga SM. 2015. RSV Vaccine-Enhanced Disease Is Orchestrated by the Combined Actions of Distinct CD4 T Cell Subsets. PLOS Pathog https://doi.org/10.1371/journal.ppat.1004757.

24. Zhivaki D, Bastien Lemoine S, Lim A, Zhang X, Tissiè P, Lo R, Correspondence M. 2017. Respiratory Syncytial Virus Infects Regulatory B Cells in Human Neonates via Chemokine Receptor CX3CR1 and Promotes Lung Disease Severity https://doi.org/10.1016/j.immuni.2017.01.010.

25. Hendricks DA, Baradaran K, Mclntosh K, Patterson ~' JL. 1987. Appearance of a Soluble Form of the G Protein of Respiratory Syncytial Virus in Fluids of

Infected Cells. J gen Virol 68:1705–1714.

26. Hendricks,' DA, Mcintosh K, Patterson2' JL. 1988. Further Characterization of the Soluble Form of the G Glycoprotein of Respiratory Syncytial Virus. J Virol 62:2228–2233.

27. Roberts,' Drew Lichtenstein SR, Ball,' And LA, Wertz' GW. 1994. The Membrane-Associated and Secreted Forms of the Respiratory Syncytial Virus Attachment Glycoprotein G Are Synthesized from Alternative Initiation Codons. J Virol 68:4538–4546.

28. Arnold R, Kfnig B, Werchau H, Kfnig W. 2004. Respiratory syncytial virus deficient in soluble G protein induced an increased proinflammatory response in human lung epithelial cells. Virology https://doi.org/10.1016/j.virol.2004.10.004.

29. Harcourt J, Alvarez R, Jones LP, Henderson C, Anderson LJ, Tripp RA. 2006. Respiratory Syncytial Virus G Protein and G Protein CX3C Motif Adversely Affect CX3CR1 T Cell Responses. J Immunol 176:1600–1608.

30. Haynes LM, Jones LP, Barskey A, Anderson LJ, Tripp RA. 2003. Enhanced disease and pulmonary eosinophilia associated with formalin-inactivated respiratory syncytial virus vaccination are linked to G glycoprotein CX3C-CX3CR1 interaction and expression of substance P. J Virol 77:9831–9844.

31. Bukreyev A, Yang L, Fricke J, Cheng L, Ward JM, Murphy BR, Collins PL. 2008. The Secreted Form of Respiratory Syncytial Virus G Glycoprotein Helps the Virus Evade Antibody-Mediated Restriction of Replication by Acting as an

Antigen Decoy and through Effects on Fc Receptor-Bearing Leukocytes. J Virol 82:12191–12204.

32. Satakel M, Coligan2 JE, Elango3 N, Norrby4 E, Venkatesan5 S. 1985. Respiratory syncytial virus envelope glycoprotein (G) has a novel structure. Nucleic Acids Res 13:7795–7812.

33. Wertz GW, Collins PL, Huang Y, Gruber C, Levine S, Andrew Ball1' L. 1985. Nucleotide sequence of the G protein gene of human respiratory syncytial virus reveals an unusual type of viral membrane protein . Proc Natl Acad Sci USA 82:4075–4079.

34. Ngwuta JO, Chen M, Modjarrad K, Joyce MG, Kanekiyo M, Kumar A, Yassine HM, Moin SM, Killikelly AM, Chuang GY, Druz A, Georgiev IS, Rundlet EJ, Sastry M, Stewart-Jones GBE, Yang Y, Zhang B, Nason MC, Capella C, Peeples ME, Ledgerwood JE, McLellan JS, Kwong PD, Graham BS. 2015. Prefusion F-specific antibodies determine the magnitude of RSV neutralizing activity in human sera. Sci Transl Med 7.

35. Capella C, Chaiwatpongsakorn S, Gorrell E, Risch ZA, Ye F, Mertz SE, Johnson SM, Moore-Clingenpeel M, Ramilo O, Mejias A, Peeples ME. 2017. Prefusion F, Postfusion F, G Antibodies, and Disease Severity in Infants and Young Children With Acute Respiratory Syncytial Virus Infection. J Infect Dis ® 1398:1398–406.

36. Boyoglu-Barnum S, Gaston KA, Todd SO, Boyoglu C, Chirkova T, Barnum TR, Jorquera P, Haynes LM, Tripp RA, Moore ML, Anderson LJ. 2013. A

Respiratory Syncytial Virus (RSV) Anti-G Protein F(ab=) 2 Monoclonal Antibody Suppresses Mucous Production and Breathing Effort in RSV rA2-line19F-Infected BALB/c Mice https://doi.org/10.1128/JVI.01164-13.

37. Boyoglu-Barnum S, Todd SO, Chirkova T, Barnum TR, Gaston KA, Haynes LM, Tripp RA, Moore ML, Anderson LJ. 2015. An anti-G protein monoclonal antibody treats RSV disease more effectively than an anti-F monoclonal antibody in BALB/c mice HHS Public Access. Virology 483:117–125.

38. Caidi H, Harcourt JL, Tripp RA, Anderson LJ, Haynes LM, Varga SM. 2012. Combination Therapy Using Monoclonal Antibodies against Respiratory Syncytial Virus (RSV) G Glycoprotein Protects from RSV Disease in BALB/c Mice. PLoS One https://doi.org/10.1371/journal.pone.0051485.

39. Collarini EJ, Lee FE-H, Foord O, Park M, Sperinde G, Wu H, Harriman WD, Carroll SF, Ellsworth SL, Anderson LJ, Tripp RA, Walsh EE, Keyt BA, Kauvar LM. 2009. Potent High-Affinity Antibodies for Treatment and Prophylaxis of Respiratory Syncytial Virus Derived from B Cells of Infected Patients. J Immunol 183:6338–6345.

40. Haynes LM, Caidi H, Radu GU, Miao C, Harcourt JL, Tripp RA, Anderson LJ. 2009. Therapeutic Monoclonal Antibody Treatment Targeting Respiratory Syncytial Virus (RSV) G Protein Mediates Viral Clearance and Reduces the Pathogenesis of RSV Infection in BALB/c Mice. J Infect Dis 200:439–486.

41. Miao C, Radu GU, Caidi H, Tripp RA, Anderson LJ, Haynes LM. 2009. Treatment with respiratory syncytial virus G glycoprotein monoclonal antibody

or F(ab9) 2 components mediates reduced pulmonary inflammation in mice. J Gen Virol https://doi.org/10.1099/vir.0.009308-0.

42. Radu GU, Caidi H, Miao C, Tripp RA, Anderson LJ, Haynes LM. 2010. Prophylactic Treatment with a G Glycoprotein Monoclonal Antibody Reduces Pulmonary Inflammation in Respiratory Syncytial Virus (RSV)-Challenged Naïve and Formalin-Inactivated RSV-Immunized BALB/c Mice. J Virol 84:9632–9636.

43. Lee H-J, Lee J-Y, Park M-H, Kim J-Y, Chang J. 2017. Monoclonal Antibody against G Glycoprotein Increases Respiratory Syncytial Virus Clearance In Vivo and Prevents Vaccine- Enhanced Diseases. PLoS One https://doi.org/10.1371/journal.pone.0169139.

44. Han J, Takeda K, Wang M, Zeng W, Jia Y, Shiraishi Y, Okamoto M, Dakhama A, Gelfand EW. 2014. Effects of Anti-G and Anti-F Antibodies on Airway Function after Respiratory Syncytial Virus Infection. Am J Respir Cell Mol Biol 51.

45. Fedechkin SO, George NL, Wolff JT, Kauvar LM, Dubois RM. 2018. Structures of respiratory syncytial virus G antigen bound to broadly neutralizing antibodies. Sci Immunol 3:1–8.

46. Fedechkin SO, George NL, Castrejon AMN, Dillen JR, Kauvar LM, Dubois RM. 2020. Conformational Flexibility in Respiratory Syncytial Virus G Neutralizing Epitopes https://doi.org/10.1128/JVI.

47. Jones 1¤ HG, Ritschel T, Pascual G, Brakenhoff JPJ, Keogh E, Furmanova-

Hollenstein P, Lanckacker E, Wadia JS, Gilman MSA, Williamson RA, Roymans D, Van ’t Wout AB, Langedijk JP, Mclellan JS. 2018. Structural basis for recognition of the central conserved region of RSV G by neutralizing human antibodies https://doi.org/10.1371/journal.ppat.1006935.

48. Boyoglu-Barnum S, Chirkova T, Todd SO, Barnum TR, Gaston KA, Jorquera P, Haynes LM, Tripp RA, Moore ML, Anderson LJ. 2014. Prophylaxis with a Respiratory Syncytial Virus (RSV) Anti-G Protein Monoclonal Antibody Shifts the Adaptive Immune Response to RSV rA2-line19F Infection from Th2 to Th1 in BALB/c Mice. J Virol https://doi.org/10.1128/JVI.01503-14.

49. Cortjens B, Yasuda E, Yu X, Wagner K, Claassen YB, Bakker AQ, Van Woensel JBM, Beaumont T. 2017. Broadly Reactive Anti-Respiratory Syncytial Virus G Antibodies from Exposed Individuals Effectively Inhibit Infection of Primary Airway Epithelial Cells. J Virol.

50. Chirkova T, Boyoglu-Barnum S, Gaston KA, Malik FM, Trau SP, Oomens AGP, Anderson LJ. 2013. Respiratory Syncytial Virus G Protein CX3C Motif Impairs Human Airway Epithelial and Immune Cell Responses. J Virol https://doi.org/10.1128/JVI.01741-13.

51. Fuentes S, Coyle EM, Golding H, Khurana S. 2015. Nonglycosylated G-Protein Vaccine Protects against Homologous and Heterologous Respiratory Syncytial Virus (RSV) Challenge, while Glycosylated G Enhances RSV Lung Pathology and Cytokine Levels. J Virol 89:8193–8205.

52. Fuentes S, Klenow L, Golding H, Khurana S. 2017. Preclinical evaluation of

bacterially produced RSV-G protein vaccine: Strong protection against RSV challenge in cotton rat model. Sci Rep 7:1–13.

53. Li C, Zhou X, Zhong Y, Li C, Dong A, He Z, Zhang S, Wang B. 2016. Vaccine-Enhanced Disease Cell Responses against Infection without Vaccine Elicits Humoral and Regulatory T Based Respiratory Syncytial Virus − A A Recombinant G Protein Plus Cyclosporine A Recombinant G Protein Plus Cyclosporine A–Based Respiratory Syncyt. July 4.

54. Johnson TR, Johnson JE, Roberts SR, Wertz GW, Parker RA, Graham BS. 1998. Priming with Secreted Glycoprotein G of Respiratory Syncytial Virus (RSV) Augments Interleukin-5 Production and Tissue Eosinophilia after RSV ChallengeJOURNAL OF VIROLOGY.

55. Tripp RA. 2004. Pathogenesis of Respiratory Syncytial Virus InfectionVIRAL IMMUNOLOGY.

56. Acosta PL, Caballero MT, Polack FP. 2016. Brief History and Characterization of Enhanced Respiratory Syncytial Virus Disease https://doi.org/10.1128/CVI.00609-15.

57. Johnson TR, Graham BS. 1999. Secreted Respiratory Syncytial Virus G Glycoprotein Induces Interleukin-5 (IL-5), IL-13, and Eosinophilia by an IL-4-Independent Mechanism. J Virol 73:8485–8495.

58. Johnson TR, Varga SM, Braciale TJ, Graham BS. 2004. Vβ14 + T Cells Mediate the Vaccine-Enhanced Disease Induced by Immunization with Respiratory Syncytial Virus (RSV) G Glycoprotein but Not with Formalin-

Inactivated RSV . J Virol 78:8753–8760.

59. Johnson TR, Teng MN, Collins PL, Graham BS. 2004. Respiratory Syncytial Virus (RSV) G Glycoprotein Is Not Necessary for Vaccine-Enhanced Disease Induced by Immunization with Formalin-Inactivated RSV. J Virol 78:6024–6032.

60. Ha B, Chirkova T, Boukhvalova MS, Sun Y, Walsh EE, Anderson CS, Mariani TJ, Anderson LJ. 2019. Mutation of Respiratory Syncytial Virus G Protein's CX3C Motif Attenuates Infection in Cotton Rats and Primary Human Airway Epithelial Cells. Vaccines https://doi.org/10.3390/vaccines7030069.

61. Boyoglu-Barnum S, Todd SO, Meng J, Barnum TR, Chirkova T, Haynes LM, Jadhao SJ, Tripp RA, Oomens AG, Moore ML, Anderson LJ. 2017. Mutating the CX3C motif in the G protein should make a live respiratory syncytial virus vaccine safer and more effective. J Virol 91:1–17.

62. Bergeron HC, Murray J, Nuñez Castrejon AM, Dubois RM, Tripp RA, Mccormick C. 2021. Respiratory Syncytial Virus (RSV) G Protein Vaccines With Central Conserved Domain Mutations Induce CX3C-CX3CR1 Blocking Antibodies. Viruses 13.

63. Fuentes S, Crim RL, Beeler J, Teng MN, Golding H, Khurana S. 2013. Development of a simple, rapid, sensitive, high-throughput luciferase reporter based microneutralization test for measurement of virus neutralizing antibodies following respiratory syncytial virus vaccination and infection. Vaccine 31:3987–3994.

64. Kumari S, Crim RL, Kulkarni A, Audet SA, Mdluli T, Murata H, Beeler JA. 2014. Development of a luciferase immunoprecipitation system assay to detect IgG antibodies against human respiratory syncytial virus nucleoprotein. Clin Vaccine Immunol 21:383–390.

65. Graham BS, Gilman MSA, Mclellan JS. 2019. Structure-Based Vaccine Antigen Design. Annu Rev Med https://doi.org/10.1146/annurev-med-121217.

66. O'rourke SM, Byrne G, Tatsuno G, Wright M, Yu B, Mesa KA, Doran RC, Alexander D, Berman PW. 2018. Robotic selection for the rapid development of stable CHO cell lines for HIV vaccine production https://doi.org/10.1371/journal.pone.0197656.

67. Wu X, Yang ZY, Li Y, Hogerkorp CM, Schief WR, Seaman MS, Zhou T, Schmidt SD, Wu L, Xu L, Longo NS, McKee K, O'Dell S, Louder MK, Wycuff DL, Feng Y, Nason M, Doria-Rose N, Connors M, Kwong PD, Roederer M, Wyatt RT, Nabel GJ, Mascola JR. 2010. Rational design of envelope identifies broadly neutralizing human monoclonal antibodies to HIV-1. Science (80-) 329:856–861.

Chapter 3:

Unpublished work- Analyzing the interaction between RSV G and CX3CR1

3.1 Introduction

Respiratory syncytial virus (RSV) expresses its attachment glycoprotein (RSV G) as a transmembrane protein and as a soluble secreted protein due to a second start codon at Methionine 48 (93–95). Many receptors for RSV G have been reported including: CX3CR1, surfactant protein A (96, 97) and D (98, 99) , TLR4 (100–103), annexin II (104), ICAM-1 (105–107), ATP1A1 (108), and CCR3 (109). The most accepted RSV G receptor is CX3CR1 which is why Chapter 3 is dedicated to analyzing the interactions between RSV G and CX3CR1.

RSV G is thought to interact with the human chemokine receptor CX3CR1 for virus attachment to host cells and to modulate immune cell function. CX3CR1 is a seven transmembrane G protein coupled receptor with a Gαi. It is expressed in natural killer cells, monocytes, macrophages, dendritic cells, cytotoxic T cells, and airway epithelial cells. The only ligand of CX3CR1 is CX3CL1 (fractalkine), which in its membrane-bound form is used to attach rolling leukocytes which may depend on the tyrosine sulfation of CX3CR1 (110), and in its soluble form is used to induce chemotaxis of $CX3CR1^{+}$ leukocytes. Although CX3CL1 and RSV G both contain a CX3C motif, they do not share structural similarities (18, 45).

RSV G contains a CX3C motif (amino acids 182-186, Cysteine, three amino acids, Cysteine) within the central conserved domain (CCD, amino acids 157-198) (111). Several studies have investigated the possibility of CX3CR1 to be a receptor

for RSV infection due to the CX3C motif within RSV G. RSV G has been shown to bind HEK293 cells that were transfected with CX3CR1 (23), however when heparin was added to these cells, binding of RSV G was dramatically reduced suggesting that most of the binding of RSV G to HEK293 cells expressing CX3CR1 was due to RSV G's heparin binding domain (aa 187-197). This study also showed that there was a higher plaque reduction of Vero cells infected with RSV when heparin was added to cells compared to RSV G (23). RSV G was shown to induce chemotaxis of mouse leukocytes, however CX3CR1 expression was not measured, and an anti-CX3CR1 antibody did reduce this RSV G induced chemotaxis but did not fully block it, which suggests that the chemotaxis observed was activated through an additional receptor(s).

Other studies have also transfected CX3CR1 into different cell lines to measure RSV G binding CX3CR1. Only 25-30% of CHOK1 cells or CHOK1 cells lacking heparin sulfate proteoglycans (HSPGs) (CHOK1Δ HSPG) transfected with CX3CR1 expressed CX3CR1 (19). RSV internalization was higher in CHOK1Δ HSPG expressing CX3CR1 cells compared to CHOK1Δ HSPG not expressing CX3CR1, however RSV internalization was also higher in CHOK1 cells compared to CHOK1 cells expressing CX3CR1, suggesting a preference for HSPGs for virus entry when they are present on a cell (19). A separate study transfected CHOA745 cells that express little to no HSPGs with CX3CR1 (21). They found that only 10% of cells expressed CX3CR1, RSV infection increased in transfected cells, and that anti-CX3CR1 and anti-RSV G antibodies decreased this infection (21). Another study

transfected CHOpgsA-745 cells which have reduced expression of heparan sulfate proteoglycans with cotton rat CX3CR1 (112). This study found that transfected cells had increased RSV infection (112). While these studies show that CX3CR1 can increase RSV infection, the expression of CX3CR1 in these cell lines is poor or was not measured.

More relevant *in vitro* cell models that express CX3CR1 have also been investigated. Two studies conflicted on whether HSPGs are important for viral infection of human airway epithelial cells (HAEC), which are a more relevant cell model for RSV infection. Chirkova et al. (19) found that incubating HAEC with an antibody to block HSPGs reduced RSV infection, however Johnson et al. (21) found that adding soluble heparin sulfate to HAEC did not affect RSV infection. Both studies found that an anti-CX3CR1 antibody reduced RSV infection. Another study showed RSV co-localized with CX3CR1 in infected HAEC, specifically in the motile cilia (20). These studies show that CX3CR1 and HSPGs may both be important for RSV infection in HAEC.

The interaction of RSV G and CX3CR1 has been investigated using animal models. There is contradicting studies on whether mice lacking functional CX3CR1 have reduced lung viral loads. Johnson et al., (113) and Das et al. (114) found that there was no difference in lung viral loads in mice lacking CX3CR1 compared to control mice, however a separate study found that mice lacking CX3CR1 had reduced lung viral loads compared to control mice (21). Furthermore, another study found that cotton rats infected with RSV and pre-treated with PPMOS (peptide-conjugated

phosphorodiamidate morpholino oligomers) to inhibit translation of CX3CR1 mRNA had reduced lung and nose viral titers (112). This study also showed that incubating RSV with the anti-RSV G antibody 131-2G, but not with soluble heparan sulfate or soluble keratan sulfate, prior to infection reduced lung viral loads in cotton rats (112). These studies show that there is substantial evidence but not a complete consensus that CX3CR1 is an important receptor for RSV infection. Notably, infant mice lacking a functional CX3CR1 and infected with RSV were found to have more mucous producing goblet cells, higher mRNA levels of mucous producing genes, higher neutrophil infiltration of the lungs, and higher γδ T cells specifically IL-17$^+$ γδ T cells compared to wild-type mice (114). Treating CX3CR1 deficient mice with an IL-1β blocker reduced the numbers of IL-17$^+$ γδ T cells and treating with an IL-17 blocker reduced the inflammatory response discussed earlier (114). Furthermore, RSV G has been shown to reduce CX3CR1$^+$ T cell trafficking to the lungs (24). These studies show that while there is contradicting evidence on whether CX3CR1 is an important receptor for RSV infection, CX3CR1 appears to be important in RSV-induced inflammation and pathology.

The role of CX3CR1 in RSV infection in relation to RSV G has been investigated using human immune cells. One study showed that the expression of CX3CR1, perforin, and IFN-γ of white blood cells taken from infants with acute RSV infection and bronchiolitis were similar to that of their uninfected controls, however, white blood cells taken from infants in the convalescence phase had a lower expression of CX3CR1 and perforin (115). A different study found that neonatal

regulatory B cells (nBregs) are permissive to RSV infection (116). IgM expressed by nBregs recognizes RSV F, which can induce the expression of CX3CR1. RSV strains expressing RSV G were better able to infect nBregs compared to an RSV strain lacking RSV G. RSV infected nBregs secreted IL-10 when the RSV strain contained a functional RSV G (116). IL-10 is an anti-inflammatory cytokine that can inhibit the expression of Th1 cytokines, which are needed for RSV clearance. These two studies show that CX3CR1 expression on immune cells varies and may be associated with RSV infection.

Anderson et al., found that CX3CR1 was expressed at low levels in the upper respiratory tract and at even lower levels in the lower respiratory tract of human infants (117). This study showed that the *in vitro* model of pediatric lung epithelial cells (PHLE) expressed higher levels of CX3CR1 compared to Hep-2 cells. PHLEs that expressed CX3CR1 were more permissive to RSV infection compared to PHLEs that did not express CX3CR1, however CX3CR1 was not required for infection. An anti-CX3CR1 antibody and recombinant CX3CR1 reduced RSV infection of PHLEs (117).

Many studies have rationalized the interaction of RSV G with CX3CR1 due to the CX3C motif within the CCD of RSV G, similar to the CX3C motif in the human ligand CX3CL1. However, while CX3CL1 and RSV G both contain a CX3C motif, they do not share structural similarities (18, 45). Many studies have used an RSV strain containing an additional alanine within the CX3C motif to create a virus with a CX4C motif (aa 186 alanine) (19, 21, 112, 118), have mutated the CX3C motif (21,

23, 112) or deleted the CX3C motif (20) to disrupt the CX3C-CX3CR1 interaction. While differences are measured in cells and in animal models infected with RSV with a mutated or deleted CX3C motif and wild type RSV, it should be noted that RSV with a mutated/deleted CX3C does not infect or replicate as well as wild type RSV and differences observed may be due to differences in replication and not necessarily due to the disruption of RSV G-CX3CR1. Normal human bronchial epithelial cells (NHBE) incubated with soluble RSV G had decreased cilia related gene levels and increased nucleolin mRNA levels, however the increase in nucleolin mRNA levels was not significant even though NHBE infected with RSV CX4C had decreased nucleolin levels and increased cilia related gene levels (118). These data show that differences seen when using RSV CX4C may be due to the lack of a functional RSV G and not necessarily to RSV G's interaction with any receptor. Furthermore, our lab has shown that the cysteines within the CX3C motif create disulfide bonds with cysteines at amino acids 173 and 176 to create the cysteine loop, which is the only rigid structure observed in the central conserved domain (18, 119). Our lab has also shown that the insertion of the alanine in CX4C disrupts epitopes required for several high affinity neutralizing antibodies (88) suggesting that the alanine disrupts the cysteine loop structure.

Considering that there is contradicting evidence on the role CX3CR1 plays in RSV infection specifically in relation to RSV G, I chose to analyze the interaction RSV G has with CX3CR1 by various activity and binding assays using various cell lines and forms of RSV G which are described in Chapter 3 below.

3.2 Calcium Flux assay

3.2.1 Rationale

CX3CR1, a human chemokine receptor on epithelial and immune cells, is a G-protein coupled receptor (GPCR) that is involved in calcium flux pathway when it is activated. CX3CR1 has been thought to interact with RSV G *in vivo* for virus attachment. THP-1 cells are a monocyte-like cell line that expresses CX3CR1. I attempted to measure calcium influx of THP-1 cells by incubating the cells in a buffer containing calcium and activating CX3CR1 with RSV G 157-197 and RSV G^{ecto} to induce calcium influx. Activity was measured by detecting fluorescence using the ester form of a calcium indicator molecule Fluo-4 AM using a plate reader or FACS.

3.2.2 Material and methods

THP-1 cells were resuspended in 1X HBSS, 20 mM HEPES, 2.5 mM Probenecid, pH 7.4 (buffer). Cells were incubated with 5uM Fluo-4 AM (F14201 Thermofisher Scientific) in the dark for 30 minutes at room temperature. Cells were washed twice and resuspended in buffer and incubated for 30 minutes at room temperature in the dark. Cells were aliquoted out as follows: 90,000 cells per well in 200 uL in a 96-well black bottom, poly-L-lysine coated plate for plate reader measurement (Perkin Elmer EnVision Xcite) at 494 nm excitation and 506 nm emission, and 500,000 cells per sample in 500 uL in eppendorf tubes for FACS (FACS LSRII) measurement using the

FITC channel. For plate reader measurement, negative controls were “blank” (no ligand added), “HBSS” (buffer added), “PBS” (Phosphate buffered saline added), and fetal bovine serum (FBS) was the positive control. RSV G 157-197 was used at 1.33 uM and 0.13 uM, and RSV G ecto wild type (WT) was used at 0.97 uM. For FACS measurement, negative controls were “not loaded” (cells incubated with DMSO, 0.02% Pluronic F-127 instead of Fluo-4 AM), “loaded” (no ligand added), “PBS” (PBS added), and FBS was used as a positive control. RSV G^{ecto} WT was used at 1 uM.

3.2.3 Data: Calcium flux using plate reader

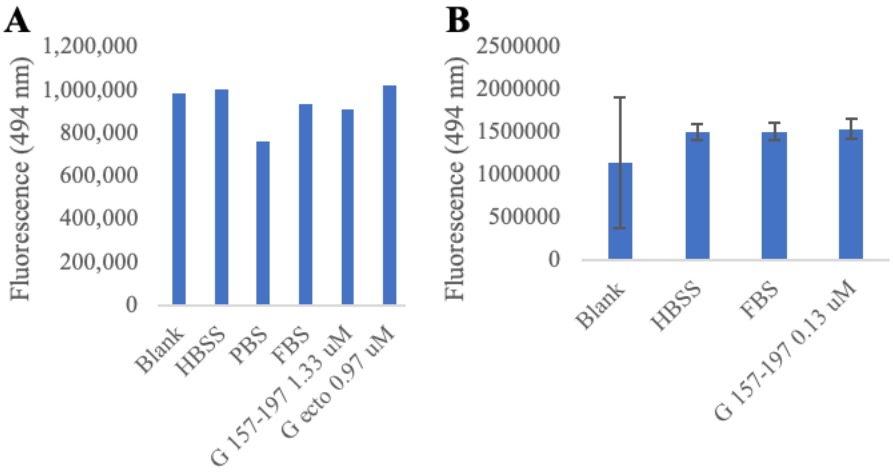

Figure 4: Fluorescence measurement of CX3CR1 activation on THP1 cells measured by Perkin Elmer EnVision Xcite at 494 nm.

A) Negative controls: Blank (no ligand), HBSS (1X HBSS, 20 mM HEPES, 2.5 mM Probenecid, pH 7.4), PBS (Phosphate buffered saline), and positive control: fetal bovine serum (FBS). RSV G 157-197 used at 1.33 uM and RSV G^{ecto} WT 0.97 uM. One replicate per sample. B) Same controls, RSV G 157-197 0.13 uM. Samples were done in triplicate and error bars represent SD.

3.2.4 Data: Calcium flux using FACS

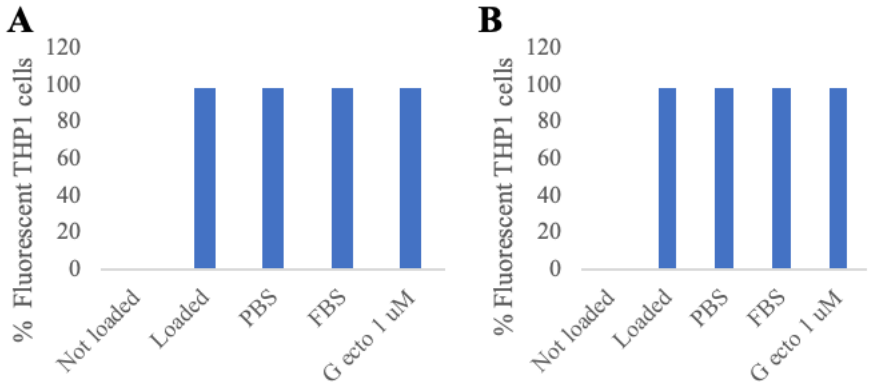

Figure 5: Fluorescence measurement of CX3CR1 activation on THP1 cells measured by FACS LSRII using the FITC channel.

A/B) Negative controls: Not loaded (cells incubated with DMSO, 0.02% Pluronic F-127 instead of Fluo-4 AM), Loaded (no ligand), PBS (Phosphate buffered saline), positive control: FBS (fetal bovine serum). RSV G^{ecto} was used at 1 uM. One replicate per sample.

3.2.5 Conclusion

RSV G 157-197 and RSV G^{ecto} were used to activate CX3CR1 and induce calcium influx into THP1 cells. Activation was measured by reading fluorescence of Fluo-4 AM that binds calcium ions in the cells. Measurements were taken using a plate reader and through FACS. CX3CR1 activation was not detected either way. Fluorescence was similar between negative and positive controls, and RSV G. The time it took to add the ligand and take the measurement was about 20 seconds, which was too slow suggesting peak calcium influx was missed every time. Future studies should consider a method where adding the ligand and having calcium flux measured takes a few milliseconds to less than 20 seconds.

3.3 Chemotaxis assay

3.3.1 Rationale

RSV G is a membrane bound glycoprotein on the surface of RSV. RSV G also exists in a secreted soluble form due to a second start codon. RSV G contains a heparin binding domain at amino acids (aa) 187-197 that interact with heparan sulfate proteoglycans on host cells. The secreted form of RSV G can modulate the immune response and compete with Fractalkine (CX3CL1) for binding to CX3CR1 and modulate chemotaxis of T and NK cells.

THP1 cells are monocyte-like (immune) cells that express CX3CR1. RSV G has been shown to induce chemotaxis of THP1 cells. I attempted to block RSV G induced chemotaxis of THP1 cells by two methods. The first method of blocking chemotaxis was by using anti-RSV G antibodies to prevent RSV G from interacting with CX3CR1. The second method of blocking chemotaxis was to create RSV G mutant proteins with a single-point mutation in the Central Conserved Domain (CCD, aa 157-197) to disrupt the interaction RSV G has with CX3CR1.

Refer to Chapter 2 section 2.6.1 for RSV G mutant protein details.

3.3.2 Chemotaxis counting with trypan blue and a hemocytometer 12 well or 96 well format

3.3.2.1. Materials and methods

THP1 cells were washed two times in RPMI 1640 1X (media) by centrifugation at 0.5 rcf for five minutes at room temperature. Cells were resuspended in media at 2,000,000 or 200,000 or 300,000 cells (for 100,000 or 200,000 cells) per sample in

250 uL or 75 uL for a 12 well or 96 well transwell respectively. Media and the chemoattractant were added to the bottom chamber of a transwell (420 uL or 235 uL per sample). Cells were added to the top chamber containing an 8 um pore membrane. Transwells were incubated for five hours, at 37C, 5% CO^2. A 10 uL aliquot was removed from the bottom chamber after the five hours and mixed with 10 uL of trypan blue to count cells using a hemocytometer. Alternatively, the volume of the bottom chamber was centrifuged after the five hours for two minutes, 2000 rcf at room temperature and cell pellets were resuspended in 20 uL of trypan blue for cell counting.

Phosphate buffered saline (PBS) was used as a negative control. Fetal bovine serum (FBS) was used as a positive control. RSV G 157-197 soluble and refolded, RSV G^{ecto} WT and mutants were tested at various concentrations.

For samples containing anti-RSV G monoclonal antibodies (mAbs) or fragment antigen binding (Fab), RSV G was incubated with these on ice for 20 minutes to 1 hour prior to adding to the bottom chamber. Anti-RSV G mAbs were obtained from Trellis BioScience. Fabs were prepared using the Pierce Fab Preparation Kit (ThermoFisher Scientific 44985). For samples with the polyclonal anti-CX3CR1 antibody (pAb, ThermoFisher Scientific PA5-19910), 2 uL of pAb were added to the top chamber with the cells and incubated for 30 minutes at room temperature prior to assembling and incubating the chambers. For samples containing heparin sodium salt from porcine (HS, Sigma Aldrich H3393-25KU), HS

was incubated with the sample on ice for 1 hour prior to adding to the bottom chamber.

3.3.2.2 Data

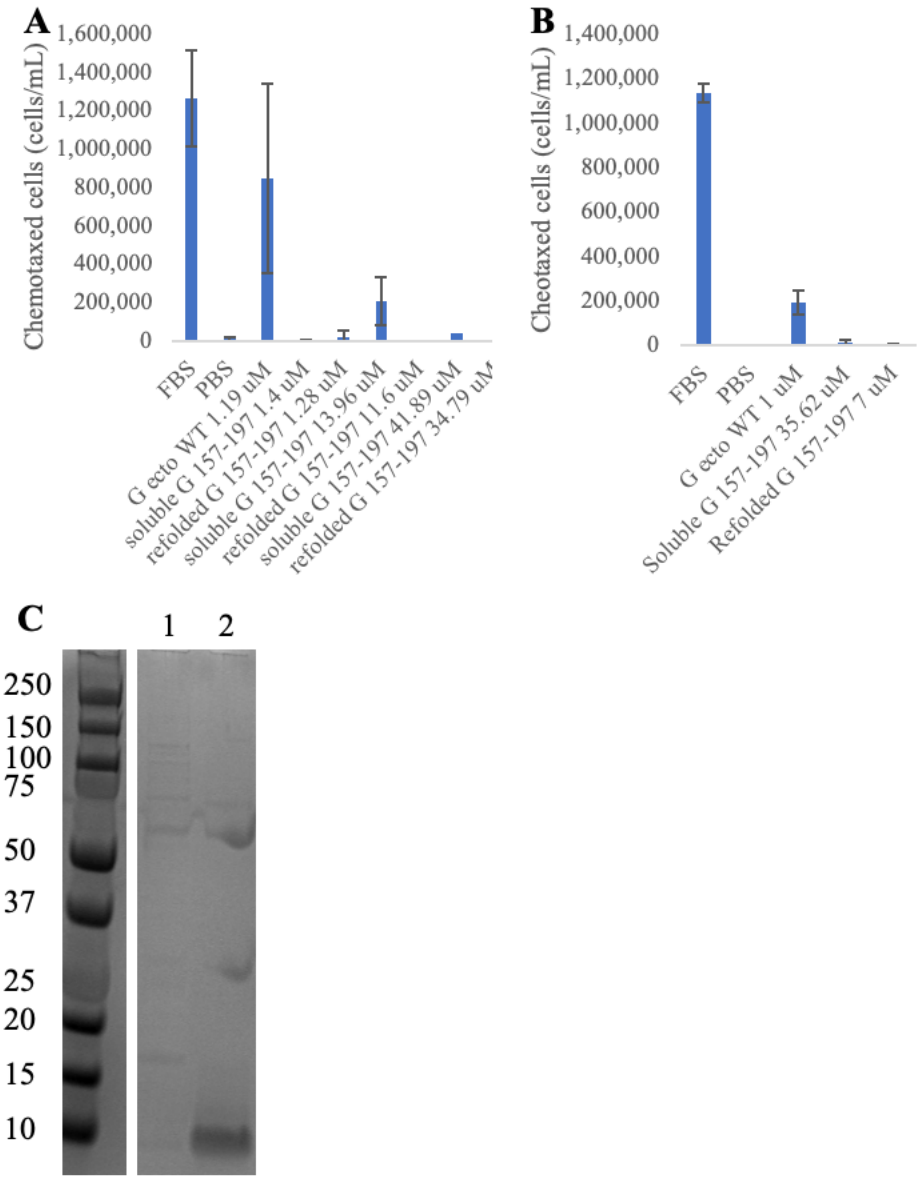

Figure 6: Soluble or refolded RSV G 157-197 do not induce chemotaxis of THP1 cells.

A/B) FBS and RSV G^{ecto} WT (1.19 and 1 uM) were used as positive controls and PBS was used as a negative control. RSV G 157-197 was used at various concentrations. Both forms of RSV G 157-197 were expressed in *E. coli* as a soluble form and refolded from the cell pellets. Cells of the bottom chamber were centrifuged and resuspended in trypan blue for cell counting. Samples were used in triplicates and error bars represent SD. C) Soluble RSV G 157-197 (lane 1, 5kD) contains *E. coli* contaminants, which may induce chemotaxis. Refolded RSV G 157-197 (lane 2, 5kD).

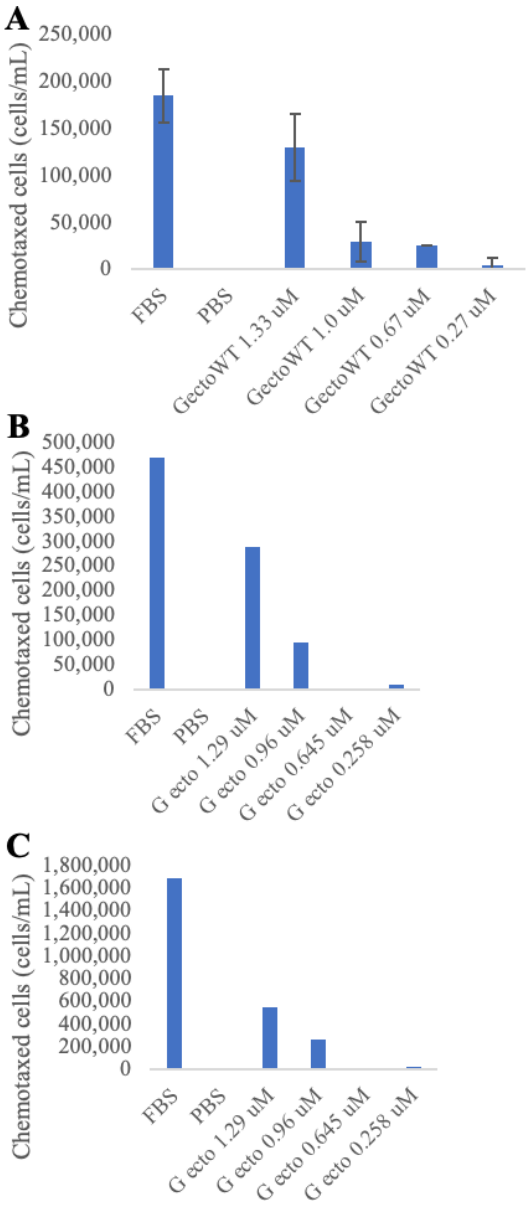

Figure 7: RSV G^{ecto} WT induced chemotaxis of THP1 cells in a concentration dependent manner.

THP1 cells were incubated in the top chamber of a 96 well transwell and FBS (positive control), PBS (negative control) were added to the bottom chamber. A) RSV G^{ecto} WT at 1.33 uM, 1.0 uM, 0.67 uM, or 0.27 uM was added to the bottom chamber. Cells of the bottom chamber were centrifuged and the pellet was resuspended in trypan blue for cell counting. Samples were done in duplicate and error bars represent SD. B/C) RSV G^{ecto} WT was used at 1.29, 0.96, 0.645, and 0.258 uM added to the bottom chamber. Cells of the bottom chamber were centrifuged and resuspended in trypan blue for cell counting. One replicate per sample.

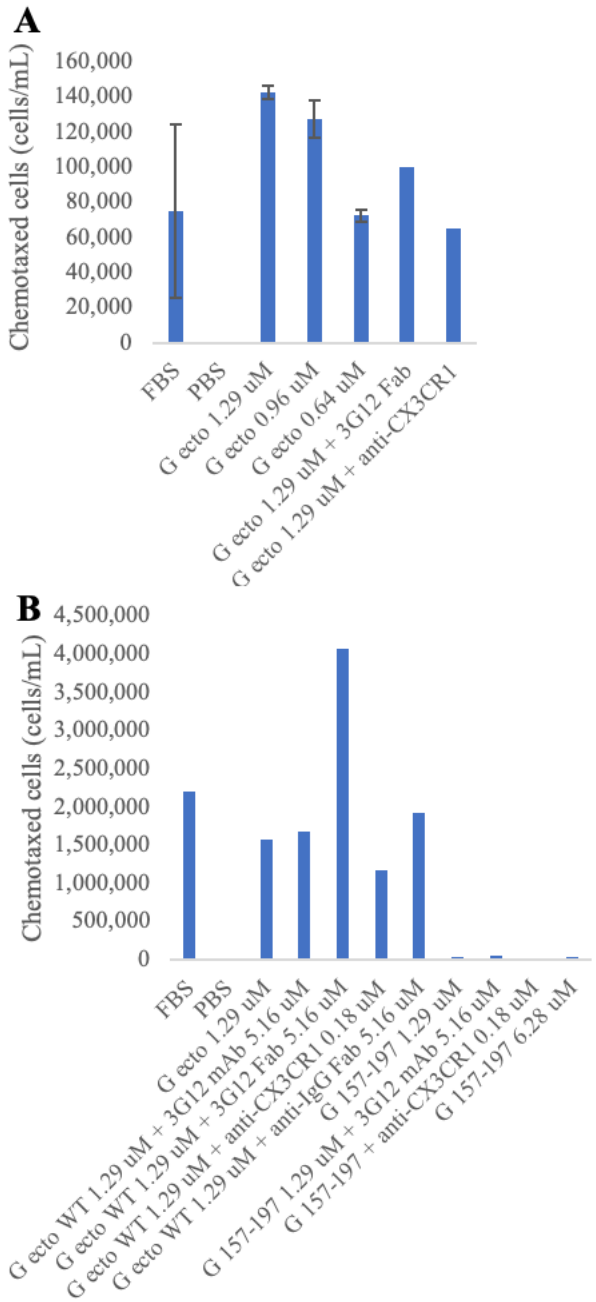

Figure 8: Anti-CX3CR1 polyclonal antibody slightly reduces RSV G^{ecto} WT induced chemotaxis of THP1 cells, however anti-RSV G 3G12 monoclonal antibody or fragment antigen binding region do not.

THP1 cells were incubated in the top chamber of a 96 well transwell. FBS was the positive control and PBS was the negative control. A) The anti-CX3CR1 polyclonal antibody (pAb) was incubated in the top chamber with the cells for 30 minutes. The anti-RSV G 3G12 fragment antigen binding region (Fab, 2.58 uM) was preincubated

with RSV G^{ecto} WT at 1.29 uM at room temperature for 20 minutes. RSV G^{ecto} WT at 1.29 uM. 0.96 uM, and 0.64 uM, and 1.29 uM with 3G12 Fab were added to the bottom chamber. Cells in the bottom chamber were centrifuged and re-suspended in trypan blue for cell counting. All samples except those with Fab or pAb were done in duplicate and error bars represent SD. B) RSV G^{ecto} and RSV G 157-197 were used at 1.29 uM and 6.28 uM. 3G12 monoclonal antibody (mAb) and Fab were used at 5.16 uM. An anti-IgG Fab was used as a control at 5.16 uM. The anti-CX3CR1 pAb was used at 0.18 uM and incubated with the cells for 36 minutes before transwell assembly. One replicate per sample. Cells in the bottom chamber were centrifuged and resuspended in trypan blue for cell counting.

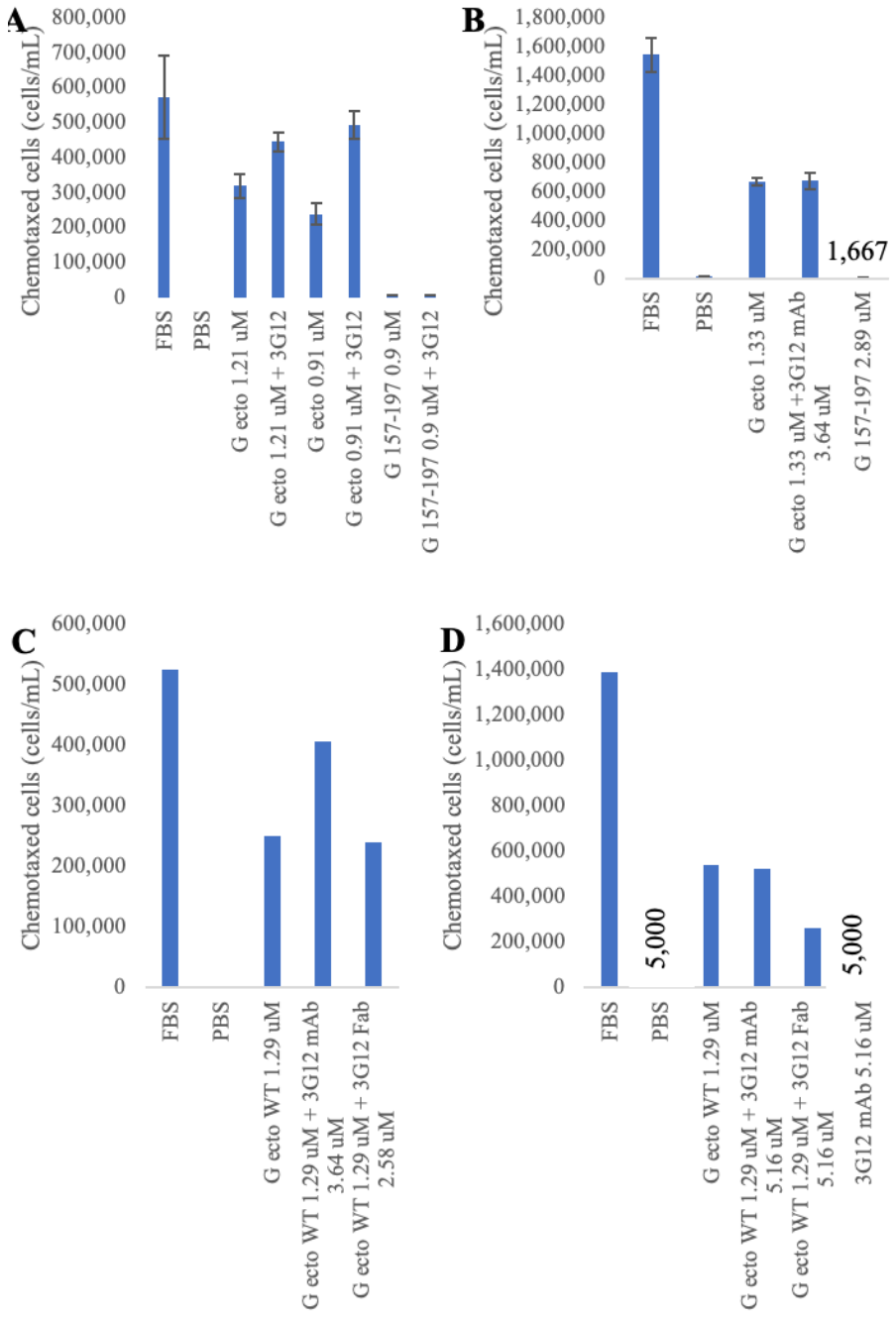

Figure 9: 3G12 mAb or Fab does not reduced RSV G^{ecto} WT induced chemotaxis of THP1 cells, and RSV G 157-197 does not induce chemotaxis of THP1 cells.

THP1 cells were incubated in the top chamber of a 96 well transwell and chemoattractants were added to the bottom chamber. FBS was used as a positive

control and PBS was used as a negative control. **A)** RSV G^{ecto} WT was used at 1.21 uM and 0.91 uM with and without 3G12 mAb at 3.64 uM and 2.73 uM respectively. RSV G 157-197 was used at 0.9 uM with and without 3.2 uM 3G12 mAb. All samples were done in triplicate and error bars represent SD. **B)** RSV G^{ecto} WT was used at 1.33 uM with and without 3.64 uM of 3G12 mAb, and RSV G 157-197 was used at 2.89 uM. All samples were done in triplicate and error bars represent SD. **C)** RSV G^{ecto} WT was used at 1.29 uM alone, with 3.64 uM of 3G12 mAb, or 2.58 uM 3G12 Fab. One replicate per sample. **D)** 3G12 mAb alone at 5.16 uM was used as a negative control. RSV G^{ecto} WT was used at 1.29 uM alone, with 5.16 uM of 3G12 mAb, or 5.16 uM 3G12 Fab. One replicate per sample. Cells were centrifuged after five hours of incubation and resuspended in trypan blue for cell counting.

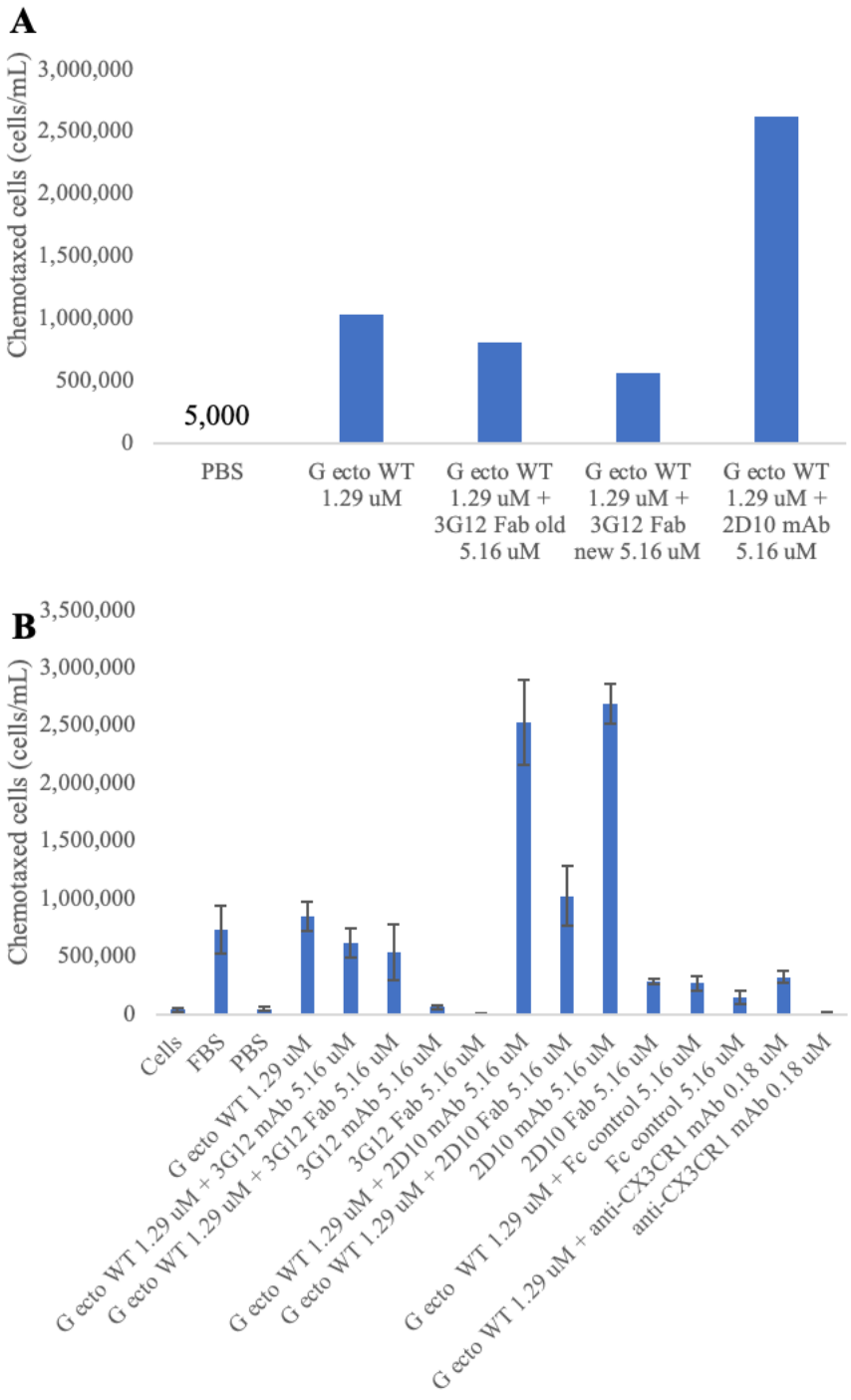

Figure 10: A newer prep of 3G12 Fab reduced RSV G^{ecto} WT induced chemotaxis of THP1 cells by half, however 2D10 mAb or Fab do not reduce chemotaxis.

THP1 cells were incubated in the top chamber of a 96 well transwell, and chemoattractants were incubated in the bottom chamber for five hours. A) PBS was used as a negative control. RSV G^{ecto} WT was used at 1.29 uM and 3G12 Fab (new prep and old prep) and 2D10 mAb were used at 5.16 uM. One replicate per sample. Cells of the bottom chamber were centrifuged and resuspended in trypan blue for cell counting. B) PBS and cells alone were used as negative controls. 3G12 mAb and Fab and 2D10 mAb and Fab alone were used as negative controls. An anti-human IgG Fab was used as a negative control and Fc control. FBS was used as a positive control. RSV G^{ecto} WT was used at 1.29 uM. All mAbs and Fabs were used at 5.16 uM, except anti-CX3CR1 pAb used as 0.18 uM. Samples were done in triplicate and error bars represent SD. Cells of the bottom chamber were centrifuged and resuspended in trypan blue for cell counting.

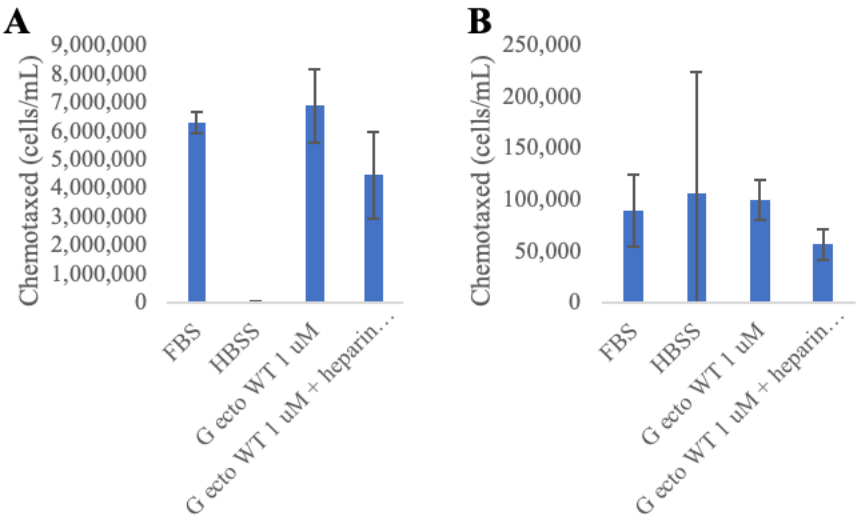

Figure 11: Heparin sodium salt from porcine reduces RSV G^{ecto} WT induced chemotaxis of THP1 cells.

FBS was used as a positive control and HBSS was used as a negative control. RSV G^{ecto} WT was used at 1 uM with and without 10 ug/ mL of heparin sodium salt from porcine. A) Cells of the bottom chamber were centrifuged and resuspended in trypan blue for cell counting. Samples were done in triplicate and error bars represent SD. B) A 10 uL aliquot was taken from the bottom chamber and added to 10 uL of trypan blue for cell counting. Samples were done in triplicate and error bars represent SD.

3.3.3 Chemotaxis using calcein dye

Calcein AM is cell permeable and is fluorescent when it is cleaved by intracellular esterases. I chose to add calcein dye to cells after chemotaxis to get a better

measurement of chemotaxed cells compared to counting cells using trypan blue and a hemocytometer. Counting with a hemocytometer gave too much variability and it was hard to see cell pellets when I centrifuged the cells to resuspend in trypan blue. Cell counting was automated using calcein dye and fluorescence was directly proportional to the number of chemotaxed cells.

3.3.3.1 Materials and methods

THP1 cells were washed three times with HBSS by centrifuging for five minutes at room temperature at 0.5 rcf. Cells were resuspended in HBSS with 2.5 mM probenecid for 2,000,000 cells per well in 250 uL per sample. Cells were incubated in the top chamber of a 12 well transwell with 8 um pore size. Chemoattractants were incubated in the bottom chamber in 430 uL per well. Transwells were incubated for five hours at 37C, 5% CO2. After incubation 500 uL of cells in the bottom chamber were added to new wells, and 1.25 mM calcein AM dye was added to the cells in the dark. Cells were incubated for 30 minutes at 37C, 5% CO2. To measure chemotaxis, 150 uL of dyed cells were added to a 96 well black plate for fluorescence reading using the Perkin Elmer EnVision Xcite at 485 nm excitation and 520 nm emission.

3.3.3.2 Data-12 well

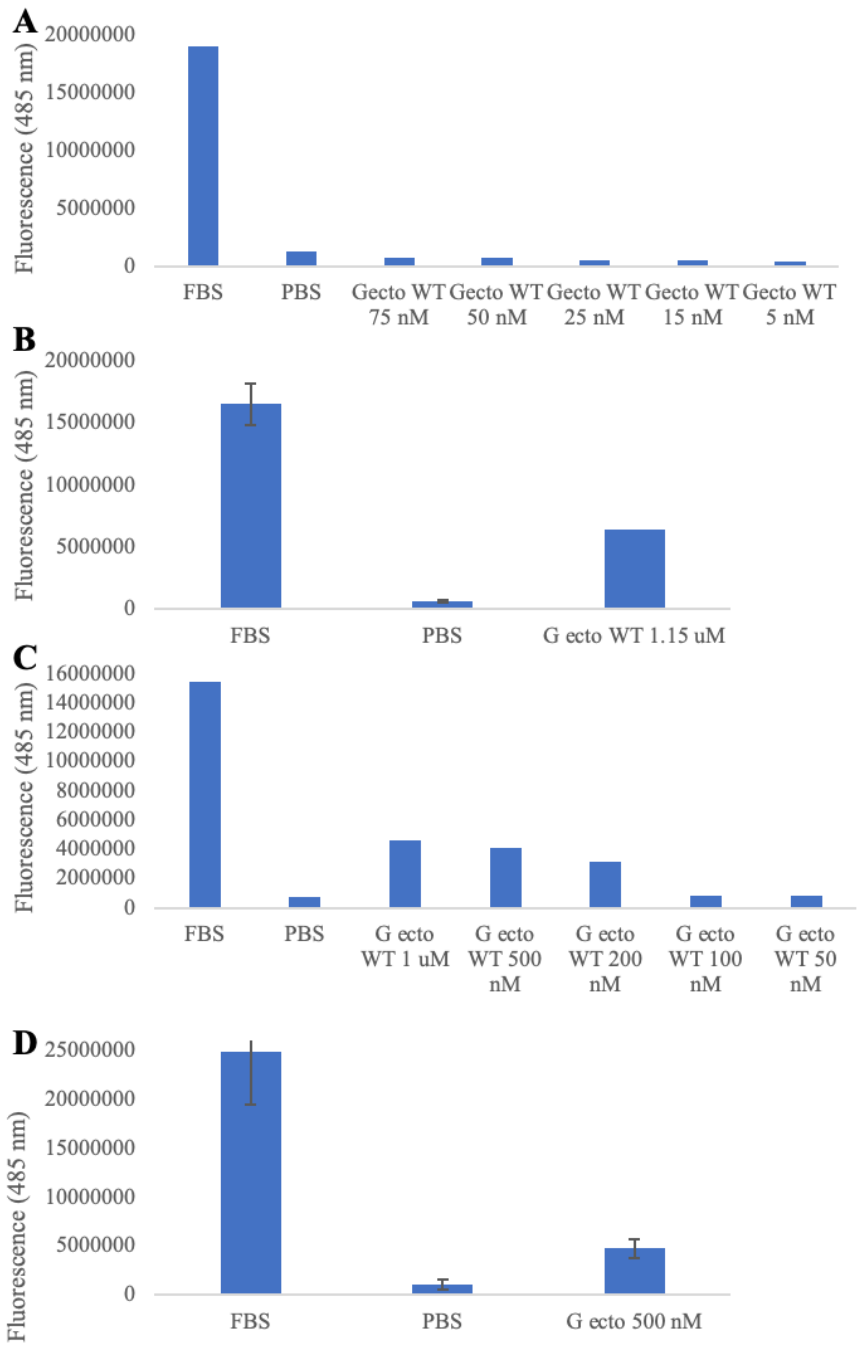

Figure 12: RSV G^{ecto} WT induced chemotaxis of THP1 cells is concentration dependent and requires higher concentrations.

THP1 cells were incubated in the top chamber of a 12 well transwell and chemoattractants were incubated in the bottom chamber. FBS was used as a positive

control and PBS was used as a negative control. A) RSV G ecto WT was used at 75, 50, 25, 15, and 5 nM concentrations. One replicate per sample. B) RSV G^{ecto} WT was used at 1.15 uM. Controls were done in triplicate and error bars represent SD. C) RSV G^{ecto} WT was used at 1 uM, 500, 200, 100, and 50 nM concentrations. D) RSV G^{ecto} WT was used at 500 nM. Samples were done in triplicate and error bars represent SD. Calcein dye was added to cells of the bottom chamber for fluorescence reading.

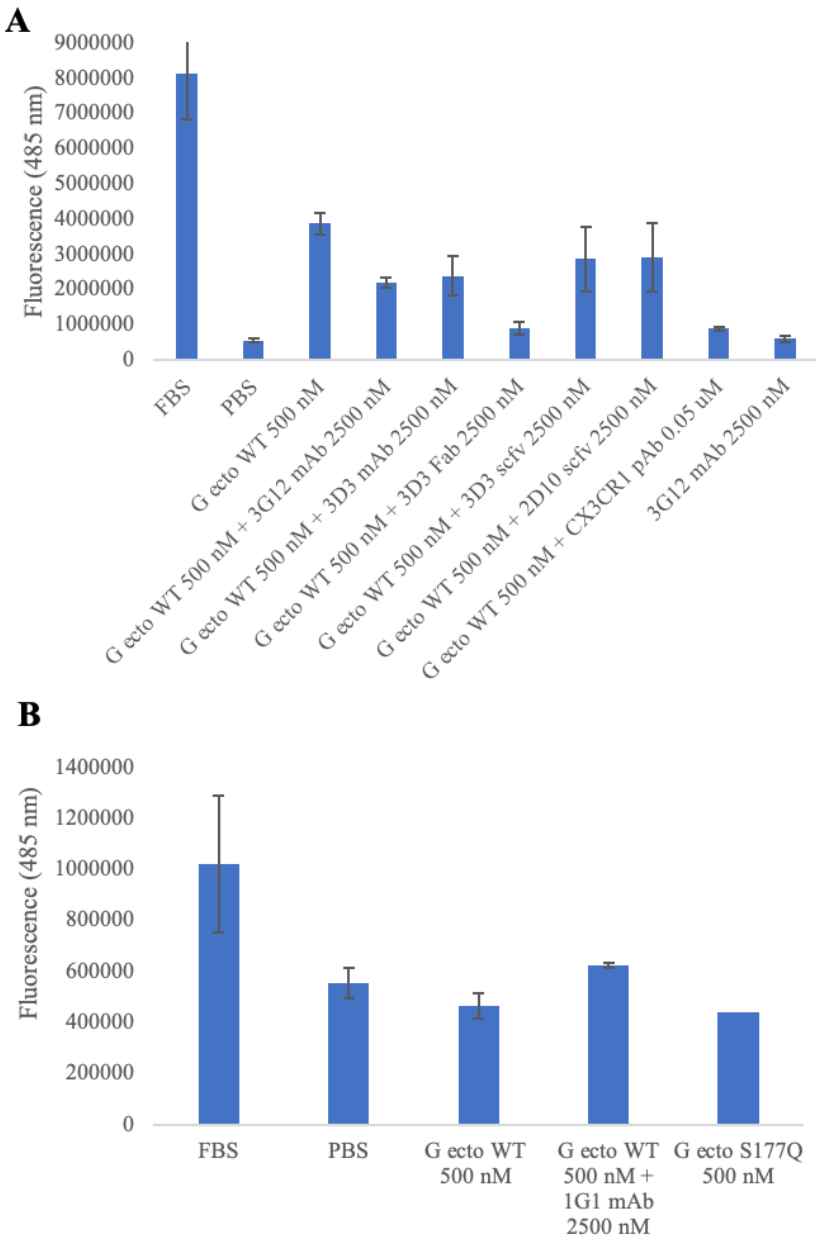

Figure 13: 3G12 and 3D3 mAb, 3D3 Fab, and anti-CX3CR1 pAb slightly reduce RSV G^{ecto} WT induced chemotaxis of THP1 cells, however 3D3 and 2D10 scFvs do not.

THP1 cells were incubated in the top chamber of a 12 well transwell and chemoattractants were added to the bottom chamber. FBS was used as a positive control and PBS was used as a negative control. A) 3G12 mAb alone at 2500 nM was used as an additional negative control. RSV G^{ecto} WT was used at 500 nM with and without antibodies. 3G12 and 3D3 mAb, 3D3 Fab, and 3D3 and 2D10 scFv were used at 2500 nM. The anti-CX3CR1 pAb was used at 0.05 uM and incubated with the cells in the top chamber before transwell assembly. Samples were done in triplicate and error bars represent SD. B) RSV G^{ecto} WT or S177Q were used at 500 nM. The anti-RSV G mAb, 1G1, was used at 2500 nM. Samples were done in triplicate and error bars represent SD. Calcein dye was added to cells in the bottom chamber for fluorescence reading.

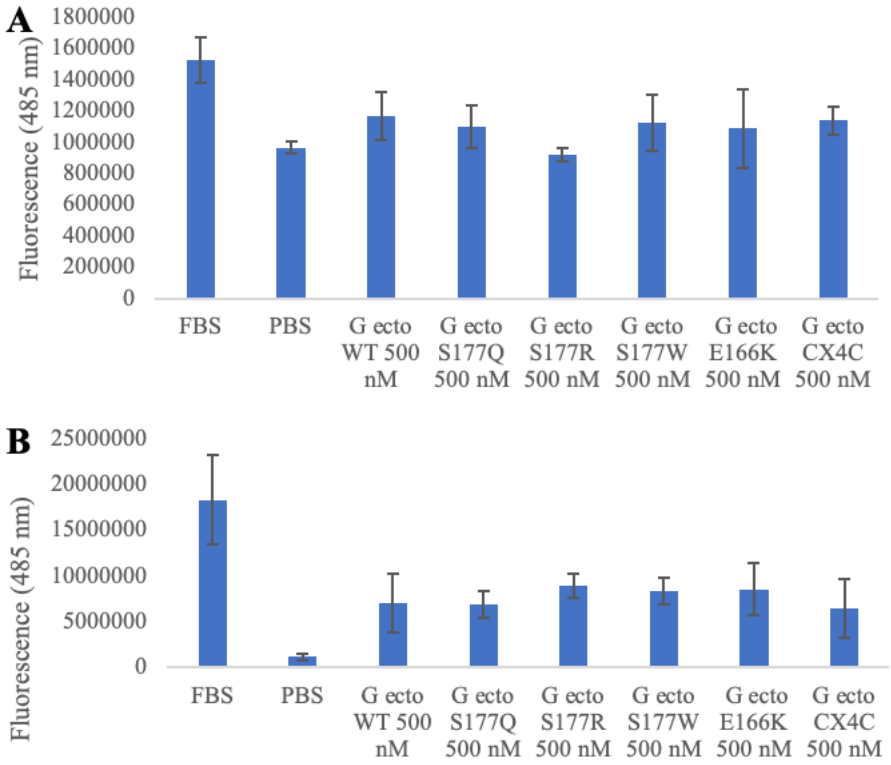

Figure 14: The E166K, CX4C, or S177 single point mutations do not reduce RSV G^{ecto} induced chemotaxis of THP1 cells.

A/B) FBS was used as a positive control and PBS was used as a negative control. RSV G^{ecto} WT, S177Q, S177R, S177W, E166K, and CX4C were used at 500 nM. Samples were done in triplicate and error bars represent SD. Calcein dye was added to the cells of the bottom chamber for fluorescence reading.

3.3.4 Chemotaxis counting with hoechst stain and molecular devices imagexpress

Counting chemotaxed THP1 cells using trypan blue and a hemocytometer led to too much variability and measuring fluorescence with calcein dye as a correlation for chemotaxed cells was not reproducible, which is why my next approach involved adding Hoechst stain to my chemotaxed cells. Hoechst stain is a cell permeable dye that binds DNA. The Molecular Devices ImageXpress imager can count nuclei using the DAPI channel and Hoechst stained cells. I added Hoechst stain to cells from the bottom chamber to count chemotaxed cells. The methods and results are below.

3.3.4.1 Materials and methods

THP1 cells were washed three times with 1X HBSS. Cells were resuspended in 1X HBSS for 100,000 cells in 75 uL per well of a 96 well transwell. Chemoattractants (samples) were added to the bottom chamber in a total of 235 uL in HBSS. Transwells were assembled and incubated for five hours at 37C, 5% CO2. An aliquot of 200 uL were removed from the bottom chamber after five hours of incubation and added to a 96 well black, clear bottom, tissue culture treated plate. Hoechst stain at 0.0016 mM were added to each well and incubated with 10 minutes at 37C, 5% CO2. Nuclei were counted using Molecular Devices ImageXpress.

3.3.4.2 Data

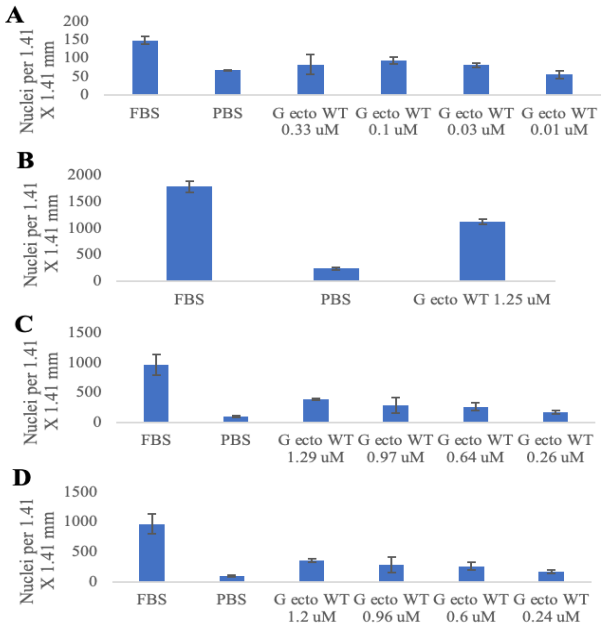

Figure 15: Using hoescht stain reduces variability of counting RSV G^{ecto} WT induced chemotaxed THP1 cells.

FBS was used as a positive control and PBS was used as a negative control. A) THP1 cells were incubated in a 12 well transwell. RSV G^{ecto} was used at 0.33, 0.1, 0.03 and 0.01 uM. Samples were done in duplicate and error bars represent SD. B-D) THP1 cells were incubated in a 96 well transwell. Samples were done in triplicate and error bars represent SD. B) RSV G^{ecto} WT was used at 1.25 uM. C) RSV G^{ecto} WT was used at 1.29, 0.97, 0.64, and 0.26 uM. D) RSV G^{ecto} WT was used at 1.2, 0.96, 0.6, and 0.24 uM.

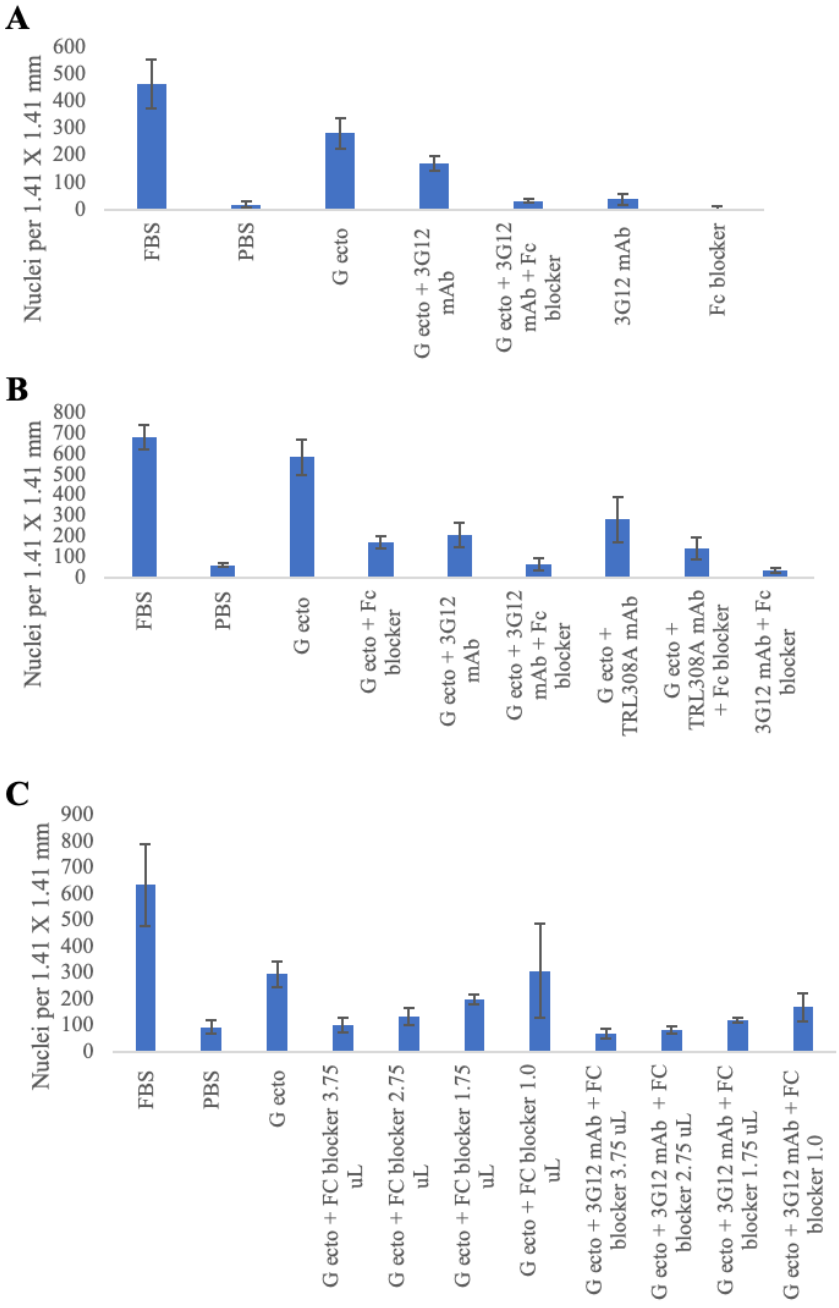

Figure 16: 3G12 Fab and mAb with and without Fc blocker reduce RSV G^{ecto} WT induced chemotaxis of THP1 cells as does Fc blocker alone.

THP1 cells were incubated in the top chamber of a 96 well transwell and chemoattractants were added to the bottom chamber. FBS was used as a positive control and PBS was used as a negative control. Fc blocker was added to the top chamber with cells for five minutes at room temperature before transwell assembly.

Samples were done in triplicate and error bars represent SD. A) 3G12 mAb alone was used at 5.16 uM as a negative control. Fc blocker alone was used as an additional negative control. RSV G^{ecto} WT was used at 1.29 uM.with and without 3G12 mAb and Fc blocker. B) Same samples as (A) with TRL308A (isotype control) as an additional negative control with and without Fc blocker. 3G12 mAb with Fc blocker alone was used as another negative control. RSV G^{ecto} WT was used at 1.29 uM in samples with Fc blocker in the top chamber. C) Same samples as (A) with varying volumes of Fc blocker added to the top chamber.

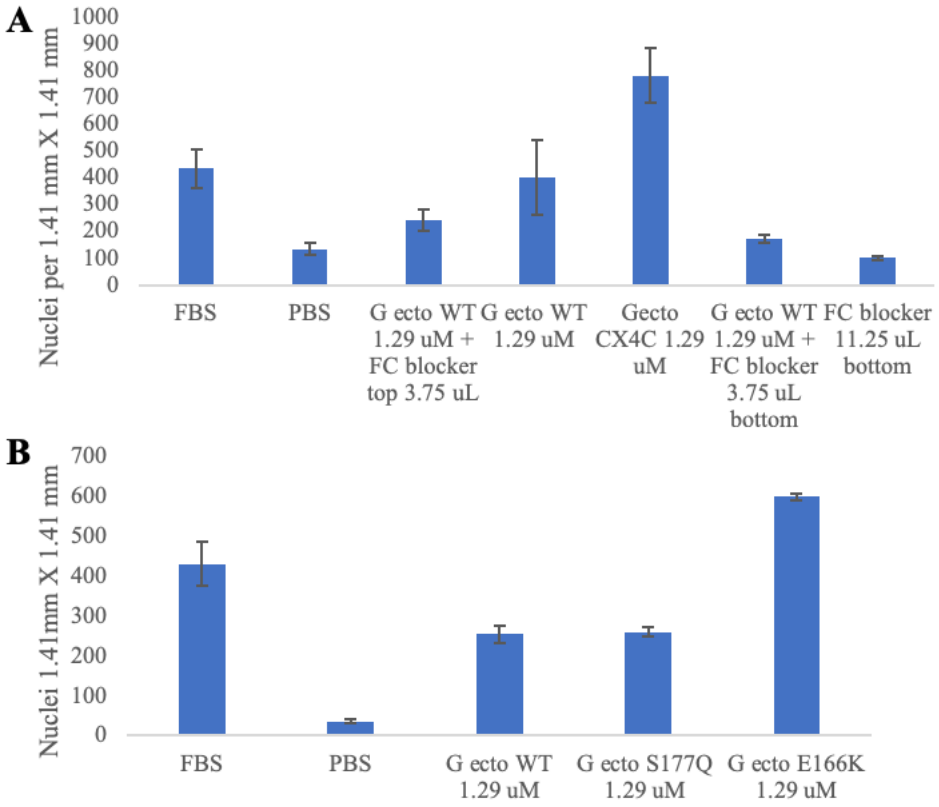

Figure 17: Fc blocker in the bottom chamber reduces RSV G^{ecto} WT induced chemotaxis of THP1 cells more than in the top chamber, and RSV G^{ecto} S177Q, E166K, and CX4C still induce chemotaxis of THP1 cells.

FBS was used as a positive control and PBS was used as a negative control. A) Fc blocker alone in the bottom chamber was used as an additional negative control. RSV G^{ecto} WT was used at 1.29 uM alone, with Fc blocker in the top chamber, or the bottom chamber. RSV G^{ecto} CX4C was used at 1.29 uM. Samples were done in triplicate and error bars represent SD. B) RSV G^{ecto} WT, S177Q, and E166K were used at 1.29 uM. Samples were done in triplicate and error bars represent SD.

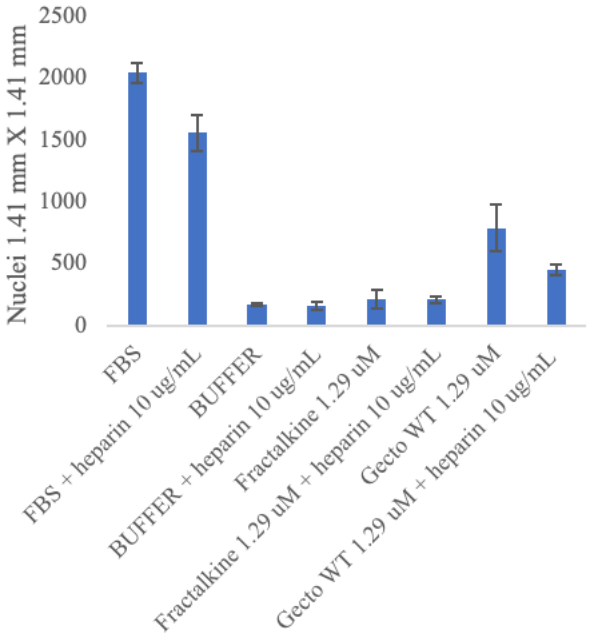

Figure 18: Heparin sodium salts from porcine (heparin) reduces RSV G^{ecto} WT induced chemotaxis of THP1 cells, and Fractalkine does not induce chemotaxis.

Heparin was used at 10 ug/mL. FBS was used as a positive control with and without heparin. Buffer (1X HBSS) was used as a negative control with and without heparin. Fractalkine and RSV G^{ecto} WT were used at 1.29 uM with and without heparin. Samples were done in quadruplicates and error bars represent SD.

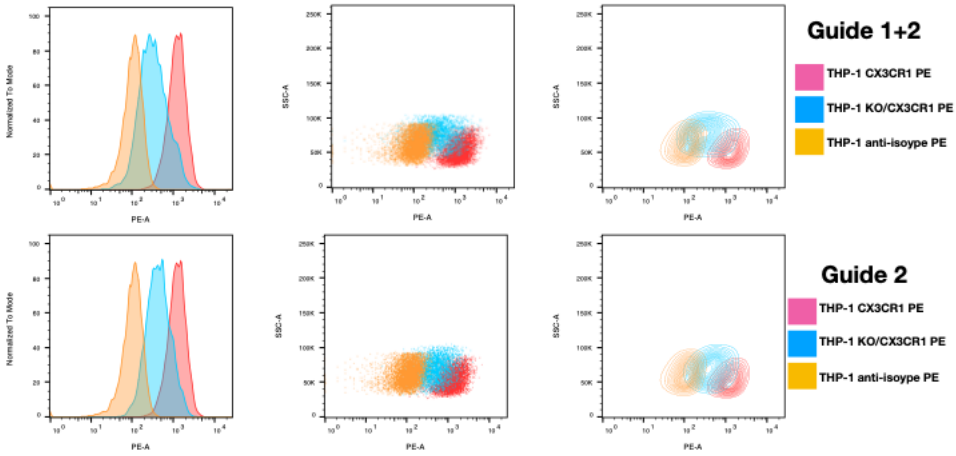

Figure 19: CX3CR1 is slightly knocked down in THP1 cells.

Two cell lines were grown with one (named Guide 2) or two (named Guide 1 + 2) RNA guides to knockdown CX3CR1. Experiments, data, and figure by Dr. Sara

O'Rourke. "Lines were treated for 72 hours with 4 ug/mL of puromycin, 1 mM sodium butyrate at 34C then returned to 2 ug/mL puromycin at 37C to induce Cas9 production." THP1 cells were stained for CX3CR1 using PE rat anti-human CX3CR1 clone 2A9-1 isotype rat IgG2b, k and with PE rat anti-mouse Valpha2 TCR as an isotype negative control. Stained THP1 cells shown in red, knockdown THP1 cells shown in blue, and THP1 cells stained with the isotype control shown in yellow.

Table 3: RNA guides for CX3CR1 Knockdown in THP1 cells

1	F7 non-targeting control guide	F7 non-targeting control guide
2	F12 non-targeting control guide	CCGGTGATGCTACCAGACTA
3	anti-CX3CR1 guide#1	CACGATGTCCCCAATATAAC
4	anti-CX3CR1 guide#2	TTGGCTGAGGCCTGTTATAT
5	anti-CX3CR1 guide#3	AAACTTTGAGTACGATGATT
6	anti-CX3CR1 guide#4	CATCAGCATTGATAGGTACC
7	anti-CX3CR1 guide#5	AACAACCGGACCGTGCAGCA
8	anti-CX3CR1 guide#6	ATGCCTTGGTGACTACCCCG
9	anti-CX3CR1 guide#7	TGCTTTGTGAACATGAACTG
10	anti-CX3CR1 guide#8	GAGAACCACCTTGTTGGTAAATGTCGGTGACACTCTGTTTAAGAGCTATGCTGGAAACAG

11	anti-CX3CR1 guide#9	GAGAACCACCTTGTTGGTGACGCCATGCTGCACGGTCGTTTAAGAGCTATGCTGGAAACA
12	anti-CX3CR1 guide#10	GAGAACCACCTTGTTGGTGACTACCCCGAGGTCCTCCGTTTAAGAGCTATGCTGGAAACAG
13	anti-CX3CR1 guide#11	GAGAACCACCTTGTTGGACAGTCAGCTCTCATTAATG GTTTAAGAGCTATGCTGGAAACA
14	anti-CX3CR1 guide#12	GAGAACCACCTTGTTGGGACTTCTTCCACCATGAGCGTTTAAGAGCTATGCTGGAAACA
15	anti-CX3CR1 guide#13 (Guide 1)	GTTTCCACATTGCGGAGCAC
16	anti-CX3CR1 guide#14 (Guide 2)	ATTGGGGACATCGTGGTCTT

3.3.5 Conclusion

RSV G is thought to interact with CX3CR1 on epithelial and immune cells *in vivo* for virus attachment. RSV G^{ecto} WT has been shown to induce chemotaxis of THP-1 cells a monocyte-like cell line that expresses CX3CR1 in a transwell assay. However anti-G antibodies and an anti-CX3CR1 antibody did not completely block chemotaxis. Additionally, adding Fc blocker to the top of the transwell with the cells or bottom chamber partially blocked chemotaxis of THP-1 cells induced by RSV G^{ecto}. These data suggest that RSV G^{ecto} WT may be inducing chemotaxis of THP-1 cells through a receptor other than or in addition to CX3CR1.

There have been three attempts to create a CRISPR CX3CR1 knockout of THP-1 cells (one attempt by Dr. Sergio Covarrubias, one attempt by me, and one attempt by Dr. Sara O'Rourke). These attempts to create the knockout cell line used

12 guide RNAs in total and were done through lentivirus transduction (Table 1). Dr. O'Rourke worked on a fourth attempt at creating this cell line through electroporation of THP-1 cells of the Cas9 and guide RNA plasmids (Table 1). The new guide RNA plasmids have a human U6 promoter as opposed to a murine U6 promoter that was used in the lentivirus transductions. The guides that were used are from a commercial THP-1 CX3CR1 knockout cell line and an available commercial plasmid (Table 1). Dr. O'Rourke has shown that THP-1 cells can be electroporated and has shown partial knockdown of CD44 as a control and CX3CR1, however the cells were not able to be sorted with the FACS Aria Ilu. because the instrument got clogged.

3.4 cAMP assay

3.4.1 Rationale

I chose to pursue a different cellular assay to test the activation of CX3CR1 because the chemotaxis assay counting chemotaxed cells using trypan blue and a hemocytometer resulted in too much variability. The cAMP assay was being developed before the other counting methods for the chemotaxis assay.

CX3CR1 is a GPCR with a Gαi subunit. Activation of GPCRs with a Gαi subunit inhibit cAMP induction. Forskolin is a small molecule that can increase levels of cAMP in cells. I stimulated THP-1 cells with forskolin (reconstituted in DMSO) and measured cAMP inhibition by attempting to activate CX3CR1 with RSV G^{ecto}. cAMP inhibition was measured by fluorescence and luminescence using a plate reader.

The fluorescence measurement of cAMP levels was taken using the Bride-It cAMP all in one Fluorescence Assay from Mediomics. For this assay, two fluorescence signals are introduced as hangovers of double stranded DNA. CAP, a bacterial DNA binding protein, is active in the presence of cAMP and binds the DNA to quench the fluorescence probes to give off fluorescence as a measure of cAMP levels. Activity of CX3CR1 is inversely proportional to fluorescence signals because it decreases cAMP levels. 10X KRB-IBMX Buffer (10X Krebs-Ringers Bicarbonate Buffer containing 7.5 mM of phosphodiesterase inhibitor IBMX) is used to inhibit intracellular phosphodiesterase breakdown of cAMP.

The luminescence measurement of cAMP levels was taken using the cAMP-Glo Assay from Promega. When CX3CR1 is activated, the alpha subunit dissociates from the GPCR and is free to inhibit cAMP. Meanwhile, free cAMP can bind to inactive protein kinase A holoenzyme. The binding of cAMP to this protein causes the catalytic subunit to be free thus have an active protein kinase A, which can be phosphorylated by the terminal phosphate of ATP. ATP levels are measured using the luciferase-based Kinase-Glo reagent. The levels of cAMP are inversely proportional to ATP levels thus luminescence levels because higher levels of cAMP cause ATP to be consumed, which results in lower luminescence levels. Active CX3CR1 decreased cAMP levels which should result in high luminescence levels.

3.4.2 Materials and methods fluorescence measurements

THP1 cells were washed twice with warm (37C) DPBS by centrifuging 1000 xg, two and a half minutes, at room temperature. Cells were resuspended in KRB-IBMX

buffer for 15,000 cells in 10 uL per well and incubated at room temperature for 15 minutes. Cells were added to a black 384 well plate. Samples were added including forskolin, and the plate was incubated for 20 minutes rotating at room temperature. An aliquot of 10 uL of "cAMP all in one solution" (one tube of Solution A mixed with one tube of 10X lysis buffer) was added to each well. The plate was covered with foil paper and incubated for 30 minutes rotating at room temperature. Fluorescence measurements were taken using the Perkin Elmer EnVision Xcite plate reader with excitation at 485nm and emission at 540 nm.

3.4.3 Fluorescence reading data

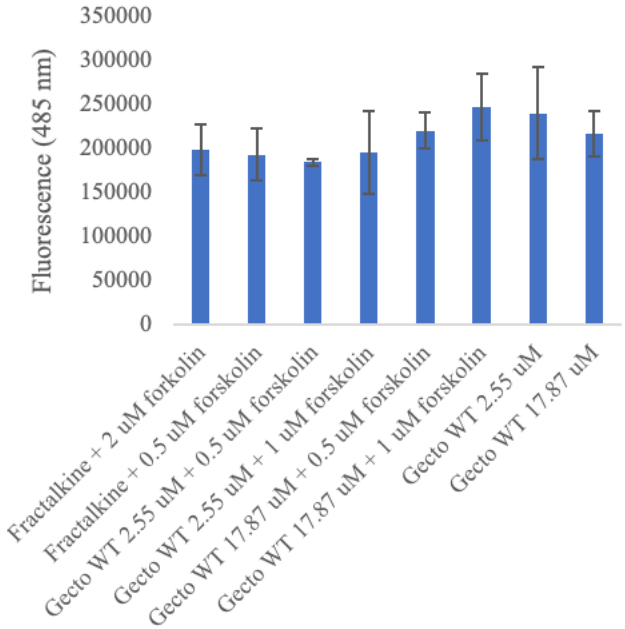

Figure 20: Fractalkine or RSV G^{ecto} WT do not fully inhibit cAMP levels.

Fractalkine was incubated with 2 or 0.5 uM of forskolin. RSV G^{ecto} WT was used at 2.55 or 17.85 uM with and without 0.5 or 1 uM of forskolin. Fluorescence measurements were taken at 485 nm. Samples were done in triplicate and error bars represent SD.

3.4.4 Materials and methods luminescence measurements

THP1 cells were washed twice with KRB IBMX buffer (buffer) by centrifuging at 2000 rcf for two minutes at room temperature. Cells were resuspended in buffer for 15,000 cells in 10 uL per well. An aliquot of 10 uL of cells were added to a 96 well white, clear bottom plate. Samples were added to the cells and incubated for 1 hour at room temperature. Forskolin was added to the cells and incubated for 45 minutes at room temperature. In the dark, 20 uL of cAMP Glo lysis buffer was added to each well and incubated for 20 minutes at room temperature. 40 uL of cAMP Detection Solution (2.5 uL Protein Kinase A, 1 mL cAMP-Glo Reaction buffer) were added to each well and incubated for 20 minutes at room temperature. 80 uL of Kinase-Glo reagent were added to each well and incubated for 10 minutes at room temperature. Luminescence was measured using Perkin Elmer EnVision Xcite plate reader.

3.4.5 Luminescence reading data

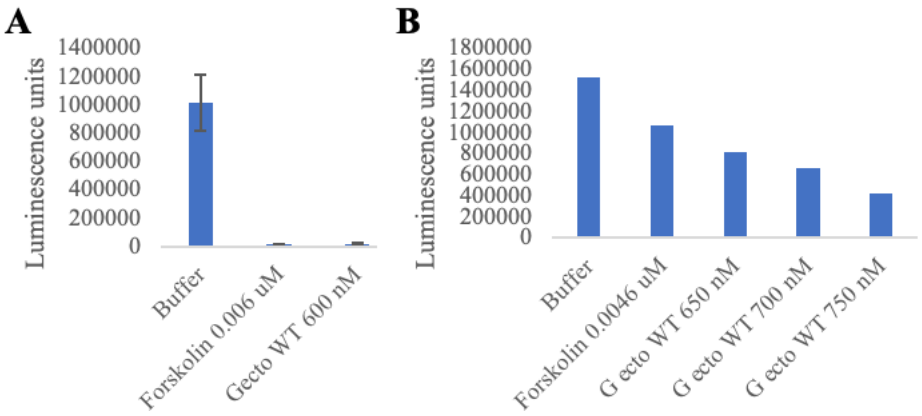

Figure 21: RSV G^{ecto} WT does not seem to inhibit cAMP levels thus does not activate CX3CR1.

KRB IBMX (Buffer) was added to the cells alone as a negative control. A) Forskolin at 0.006 uM alone was used as a positive control for high cAMP levels. RSV G^{ecto} WT was used at 600 nM. Samples were done in triplicate and and error bars represent

SD. B) Forskolin alone was used at 0.0046 uM as a positive control for high cAMP levels. RSV G^{ecto} WT was used at 650, 700, or 750 nM. One replicate per sample.

3.4.6 Conclusion

There was variation in the induction of cAMP by forskolin. Higher concentrations of forskolin alone reduced fluorescence. These data indicate that instead of inducing cAMP levels, forskolin reduced cAMP levels resulting in less fluorescence quenching by CAP and lower fluorescence levels overall. Forskolin was reconstituted in DMSO. It is possible that the higher levels of forskolin was inadvertently higher levels of DMSO that the cells could not handle resulting in lower overall cAMP levels.

There was a lot of variability in the luminescence experiments in whether forskolin reduced luminescence by inducing cAMP levels or if RSV G^{ecto} WT induced luminescence by inhibiting cAMP and maintaining the cell's ATP levels.

Appropriate positive and negative controls for cAMP induction and inhibition are needed to be able to accurately interpret results of the differences seen for forskolin alone compared to RSV G^{ecto} WT or RSV G^{ecto} WT with forskolin. The slight differences seen in some of these samples are not able to be interpreted without such controls.

3.5 Binding Assay

3.5.1 Rationale

CX3CR1 has been thought to interact with RSV G *in vivo* for virus attachment. THP-1 cells are a monocyte-like cell line that expresses CX3CR1, and our collaborators, Dr. Ralph Tripp's lab in Athens, Georgia, has made a stable cell line of HEK293 cells

that overexpress CX3CR1 (HEK293.CX3CR1). Since activation of CX3CR1 by RSV G has not been measured by the calcium flux, chemotaxis, or cAMP assays, I thought that RSV G may bind to CX3CR1, but not activate it.

To test binding of RSV G to CX3CR1, I created an RSV G CCD (aa 157-197 or 157-191) protein fused to GFP to test binding to THP1 or HEK.CX3CR1 cells using the FITC channel on the FACS LSR II. I have also tried measuring binding of RSV G^{ecto} to these cells by probing with an anti-His antibody conjugated to a fluorophore to measure fluorescence thorough FACS LSR II and the FITC channel. Additionally, I have expressed and purified RSV G^{ecto} with an Avi tag that I biotinylated and have tried to measure binding by FACS LSR II using fluorescent Streptactin and Streptavidin that bind to biotinylated proteins (see conclusions in section 3.5.6).

3.5.2 Binding using GFP fusion (157-197 & 157-191) materials and methods

THP1 cells were washed twice by centrifuging at 0.5 rcf, for five minutes at room temperature. Cells were resuspended in 1X RPMI for 500,000 cells in 25 uL per well. An aliquot of 25 uL of cells was added to a 96 well black plate. Samples were added to the cells in 25 uL. The plate was incubated for 1 hour at 37C, 5% CO2. Cells were washed twice with DPBS and resuspended in DPBS at 500 uL per sample. Binding was detected using the FACS LSR II using the FITC channel. DPBS and GFP alone were used as a negative controls. RSV G 157-197 was fused to GFP to create the GFP-G 157-197 and 157-191 fusion proteins.

3.5.2.1 Binding using GFP fusion (157-197 & 157-191) data

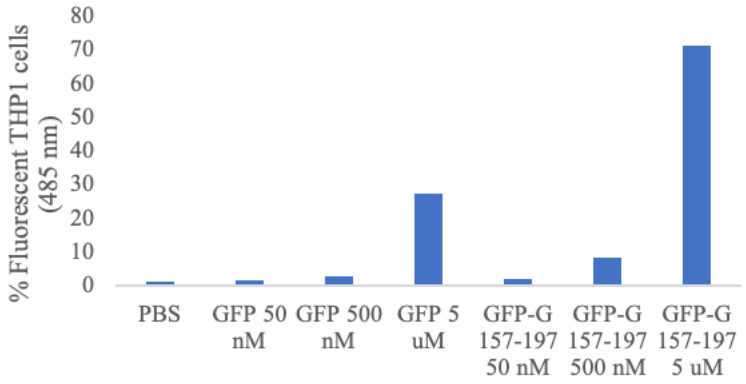

Figure 22: RSV GFP-G 157-197 binds to THP1 cells.

PBS and GFP at 50 and 500 nM and 5 uM were used as negative controls. RSV GFP-G 157-197 was used at 50 and 500 nM and 5 uM. Fluorescence was measured using the FITC channel. One replicate per sample.

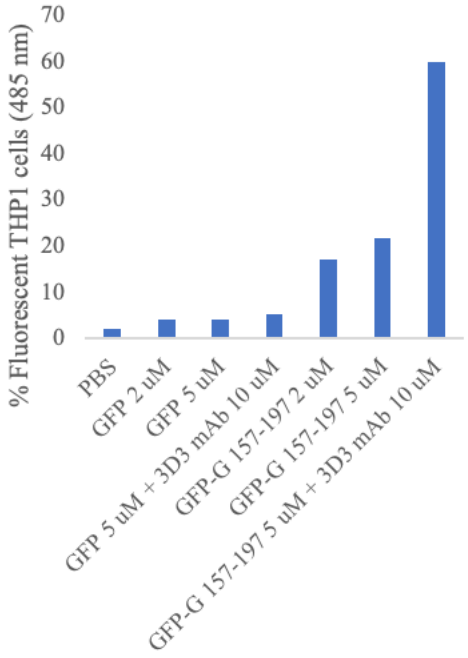

Figure 23: RSV G 157-197 binds to THP1 cells and anti-RSV G mAb 3D3 increases this binding.

PBS and GFP at 2 and 5 uM were used as negative controls. GFP at 5 uM with 3D3 mAb at 10 uM was used as an additional negative control. RSV GFP-G 157-197 was

used at 2 and 5 uM. RSV G 157-197 was also used at 5 uM with 10 uM of 3D3 mAb. Fluorescence was measured using the FITC channel on the LSR II. One replicate per sample.

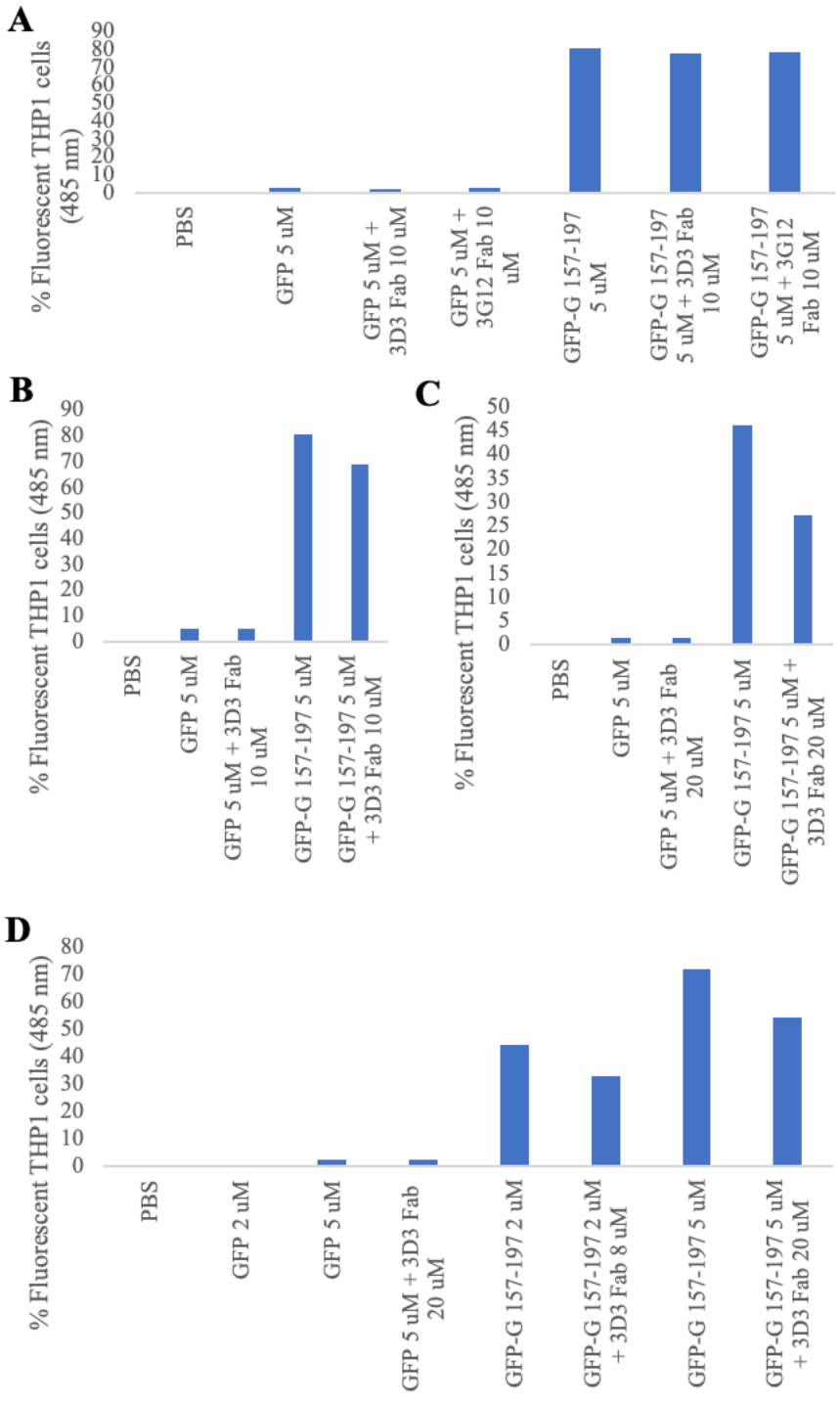

Figure 24: Anti-RSV G Fab 3D3 slightly reduces RSV G 157-197 binding to THP1 cells.

PBS was used as a negative control and GFP at 2 or 5 uM with and without 3D3 Fab at 10 or 20 uM were used as negative controls. One replicate per sample. A) GFP at 5 uM with 10 uM of 3G12 Fab was used as an additional control. RSV GFP-G 157-197 was used at 5 uM with and without 3D3 and 3G12 Fab at 10 uM. B) RSV GFP-G 157-197 was used at 5 uM with and without 3D3 Fab at 10 uM. C) RSV GFP-G 157-197 was used at 5 uM with and without 20 uM of 3D3 Fab. D) RSV GFP-G 157-197 was used at 2 and 5 uM alone and with 8 uM or 20 uM of 3D3 Fab respectively.

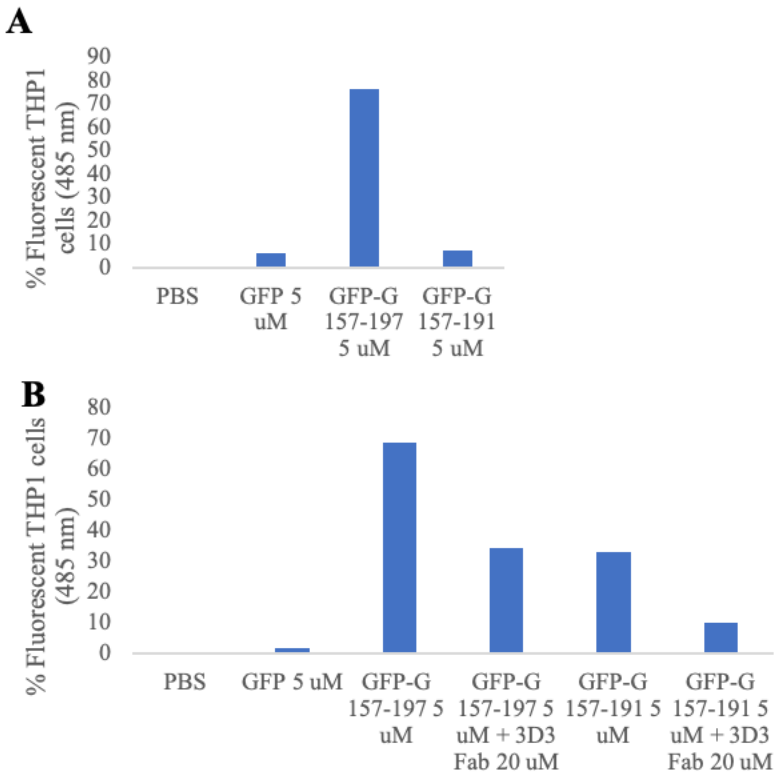

Figure 25: RSV GFP-G 157-191 reduces binding to THP1 cells.

PBS and GFP at 5 uM were used as negative controls. One replicate per sample. A) RSV GFP-G 157-197 and 157-191 were used at 5 uM. B) RSV GFP-G 157-197 and 157-191 were used at 5 uM with and without 20 uM of 3D3 Fab.

3.5.3 Binding using anti-His antibody

Given that the RSV GFP-G 157-191 construct led to much lower binding to THP1 cells, full length RSV G (RSV G^{ecto}) was tested for binding to THP1 cells. RSV G^{ecto}

contained a 6X His tag that was used to measure fluorescence using a fluorescent anti-His antibody.

3.5.3.1 Materials and methods

THP1 cells were washed and resuspended in 1X HBSS to get 500,000 cells in 100 uL per well. Cells were added to a 96 well plate and RSV G^{ecto} WT was incubated with the cells for 1 hour either at 37C at 5% CO2 or 4C. Cells were washed and resuspended in HBSS. Mouse monoclonal IgG2b anti-His-FITC was added either at 1:500 for 1 hour at 37C, 5% CO2 or 1:100 dilution for 20 minutes at 4C. Cells incubated at 37C were washed and resuspended in 500 uL HBSS. Cells incubated at 4C were centrifuged and resuspended in 500 uL HBSS. Fluorescence was measured using the FITC channel on the FACS LSR II.

3.5.3.2 Data

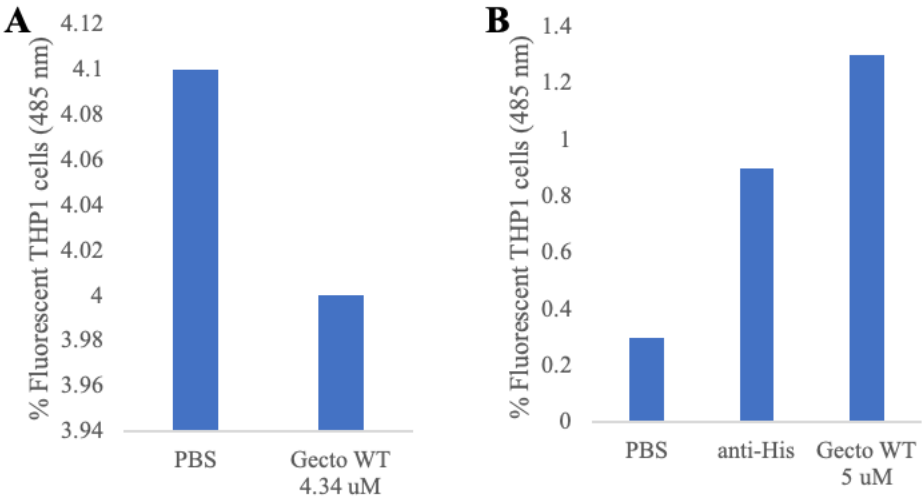

Figure 26: There is some binding of RSV G^{ecto} to THP1 cells at 4C.

PBS was used as a negative control. One replicate per sample. A) Cells were incubated at 37C, 5% CO2. RSV G^{ecto} WT was used at 4.34 uM. B) Cells were incubated at 4C. Anti-His Ab at 1:100 dilution was used as an additional negative control. RSV G^{ecto} WT was used at 5 uM.

3.5.4 Binding using Fluorescent Streptactin

Detecting RSV G^{ecto} WT binding to THP1 cells using an anti-His antibody led to high background; however, cells were not washed after the addition of the anti-His Ab in Figure 23B. Due to the high fluorescence background, a different approach was taken to measure RSV G^{ecto} binding to THP1 or HEK.CX3CR1 cells. RSV G^{ecto} contains two Strep tags. Fluorescent Streptactin binds to Strep tags and can be used to measure binding of RSV G^{ecto} to THP1 or HEK.CX3CR1 cells.

3.5.4.1 Materials and methods

RSV G^{ecto} was mixed with Fluorescent Streptactin XT DY 488 (IBS 2-1562-050) on ice for 1 hour. THP1, HEK.CX3CR1, or HEK293 cells were washed twice with PBS, 1% BSA and resuspended in PBS, 1% BSA for 500,000 cells in ~125 uL. RSV G^{ecto} + Streptactin were added to the ells and incubated on ice for 1 hour. Cells were centrifuged and resuspended in 500 uL of PBS, 1% BSA. Fluorescence was measured using the FITC channel on the FACS LSR II.

3.5.4.2 Data

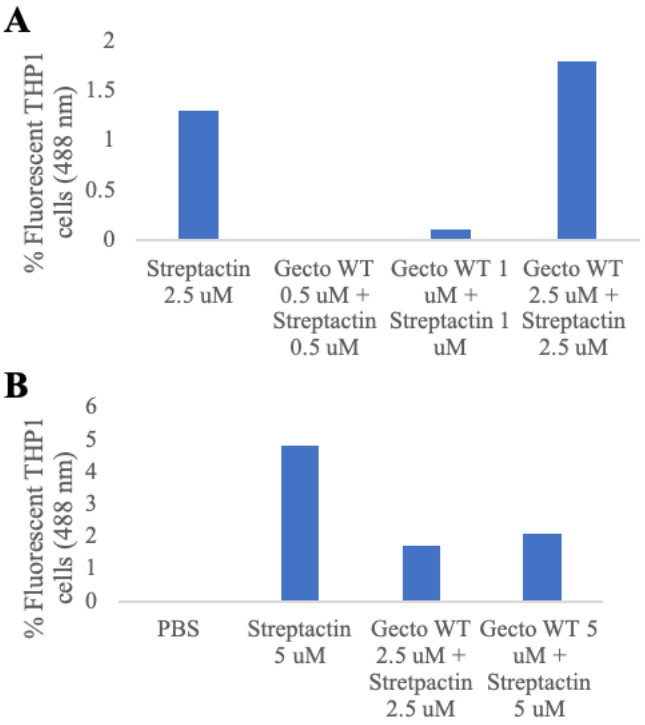

Figure 27: RSV G^{ecto} does not bind THP1 cells.

PBS or Streptactin at 2.5 or 5 uM were used as negative controls. One replicate per sample. A) RSV G^{ecto} was used at 0.5, 1, and 2.5 uM with and without equal concentrations of fluorescent streptactin. B) RSV G^{ecto} was used at 2.5 or 5 uM with and without equal concentrations of fluorescent streptactin.

3.5.5 Binding using Fluorescent Streptavidin

Measuring binding of RSV G^{ecto} to THP1 or HEK.CX3CR1 cells by measuring fluorescence of cells incubated with fluorescent streptactin did not detect binding. Streptactin binds to Strep tags, however the affinity of Streptactin to Strep tags is lower compared to that of Streptavidin to biotin. RSV G^{ecto} was recloned to contain an Avi tag. The Avi tag of RSV G^{ecto} was biotinylated and this protein was used in a

binding assay. Fluorescent streptavidin was used to measure binding of RSV G^{ecto} to THP1 or HEK.CX3CR1 cells.

3.5.5.1 Materials and methods

THP1 cells were washed three times in 1X RPMI 1640. Cells were resuspended in RPMI for 1,000,000 cells in 100 uL per well. Samples (RSV G^{ecto} WT with fluorescent streptavidin) were added to cells and incubated at 37C, 5% CO2 for 1 hour. Cells were centrifuged and resuspended in 500 uL PBS, 1% BSA per tube. Fluorescence was measured using the FITC channel and FACS LSR II.

For a different approach, THP1 or HEK.CX3CR1 cells were washed three times with cold PBS, 1% BSA. Cells were resuspended in PBS, 1% BSA for 500,000 cells in 90 uL per sample. Protein was incubated with 10 ug/ mL heparin sodium salts from porcine (Sigma Aldrich 11339) for 1 hour on ice before adding to cells. Samples were added to cells and incubated for 1 hour on ice. Cells were washed once in PBS, 1% BSA and resuspended in PBS, 1% BSA. Fluorescent streptavidin or streptactin was added to the cells and incubated for 45 minutes on ice. Cells were washed twice and resuspended in 500 uL PBS, 1% BSA. Fluorescence was measured using the FITC channel on the FACS LSR II.

3.5.5.2 Data

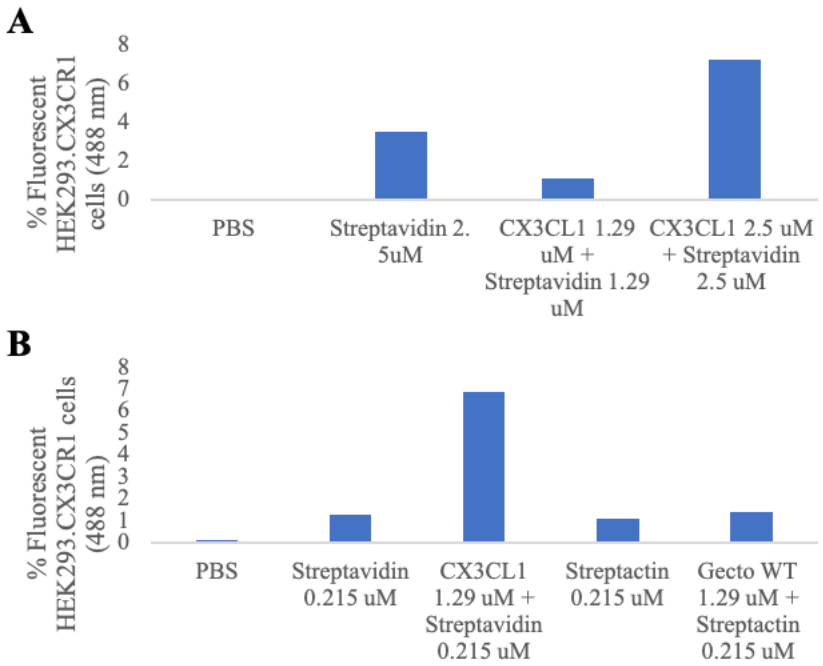

Figure 28: There is slight binding of CX3CL1 but not RSV G^{ecto} WT to HEK.CX3CR1 cells.

A) PBS and streptavidin at 2.5 uM were used as negative controls. CX3CL1 were used at 1.29 and 2.5 uM with equal concentrations of streptavidin. One replicate per sample. B) PBS and streptavidin and streptactin at 0.215 uM were used as negative controls. CX3CL1 was used at 1.29 uM with 0.215 uM of streptavidin and RSV G^{ecto} WT was used at 1.29 uM with 0.215 uM of streptactin. One replicate per sample.

3.5.6 Conclusion

I was able to detect binding using the RSV GFP-G 157-197 fusion protein. Anti-RSV G 3D3 Fab slightly reduced this binding, and deletion of four lysine amino acids at the end of this construct to create RSV GFP-G 157-191 dramatically reduced binding. These results indicate that the binding observed with RSV GFP-G 157-197 was due to the heparin binding domain.

Binding of RSV G^{ecto} WT to THP1 cells was not detected using an anti-His fluorescent antibody. The cells were not washed after adding the antibody, which could be why the background fluorescence was high. Adding some washes after adding this antibody could reduce background fluorescence. It is also possible that CX3CR1 is endocytosed when RSV G^{ecto} WT binds which would lead to detecting no binding.

There was less than 1% of fluorescent THP1 cells incubated with CX3CL1 and about 3-6 % fluorescent HEK.CX3CR1 cells indicating slight binding of CX3CL1 to these cells, however fluorescence of cells incubated with RSV G^{ecto} WT was not above background. It is possible that more washes are needed after incubation with fluorescent streptactin or streptavidin to reduce background fluorescence and more accurately measure binding of CX3CL1 or RSV G^{ecto} WT. It is also possible that RSV G^{ecto} WT binding will be more difficult to detect considering that Bergeron et al. 2021 detected only about 20% binding of RSV G^{ecto} WT to HEK.CX3CR1 cells.

3.6 Presto Tango assay

3.6.1 Rationale

We received a plasmid with a hemagglutinin signal sequence and a Flag tag encoding CX3CR1 that is fused to a V2 tail (to promote arrestin recruitment) and a tetracycline transactivator (tTA) with a TEV cleavage site and a HEK 293T cell line that stably expresses a tTA-dependent luciferase reporter and a Beta-arrestin2-TEV fusion gene (the cell line is called HTLA) from the Roth lab in the University of North Carolina at

Chapel Hill. HTLA cells were transfected with the CX3CR1 plasmid using effectene transfection reagent, however expression of this plasmid was poor.

Activation of CX3CR1 leads to beta-arretstin and TEV protease to be recruited to the V2 tail. TEV protease cleaves at the TEV cleavage site to release the transcription factor tTA. The tTA then enters the nucleus to transcribe the luciferase gene in the HTLA cells and luminescence can be measured using a plate reader.

Since HTLA cells are a derivative of HEK293T cells, they express heparan sulfate proteoglycans (HSPGs) that RSV G uses to non-specifically attach to immortalized cell lines. Heparin sodium (Fisher Scientific 9041-08-1) or heparin sodium salt from porcine (Sigma Aldrich H3393-25KU) were used in some samples to prevent RSV G from interacting with the HTLA cells through the HSPGs.

The Presto Tango assay is completed in five days. Human CX3CL1 *E. coli* derived (R&D systems cat 362-CX/CF 10/13/17) and human CX3CL1 NSO derived (mouse myeloma) (R&D systems cat 365-FR) were used as positive controls for CX3CR1 activation. Recombinant Fractalkine expressed in Chinese Hamster Ovary cells was also used as a positive control for CX3CR1 activation.

3.6.2 Materials and methods

On day one, HTLA cells were plated out in a 12 well plate at 100,000 cells/ mL in 2 mLs of DMEM, 10% FBS, 2 mM glutamax, 1X Pen/Strep (media) per well. The plate was incubated at 37C, 5% CO2. On day two, the media of the HTLA cells was changed one hour before transfection. Cells were transfected with 1 ug of CX3CR1 DNA per well using effectene transfection reagent. One to three wells were left

untransfected. A 96 well white, clear bottom plate was coated with 50 ug/mL of poly-D-lysine and parafilmed and stored at 4C. On day three, the transfected cells were pooled and the untransfected cells were pooled. Cells were plated out in the poly-D-lysine coated 96 well plate at 50,000 cells per well in 100 uL of media. The plate was incubated at 37C, 5% CO2. On day four, the media was changed one hour before adding samples to the cells to 90 uL of DMEM, 10% dialyzed FBS, 2 mM glutamax, 1X Pen/Strep. For samples with heparin, the sample was incubated with heparin on ice for one hour before adding to cells. Samples were added to cells in 10 uL and incubated for 18 to 24 hours at 37C, 5% CO2. On day five, the media and protein were removed from the cells and 100 uL of 1:10 diluted Promega solution (in 1X HBSS, 20 mM HEPES, pH 7.4) was added to each well and incubated at room temperature for 15 minutes. Luminescence was measured using the Perkin Elmer EnVision Xcite plate reader with a 384 well aperture.

3.6.3 Data

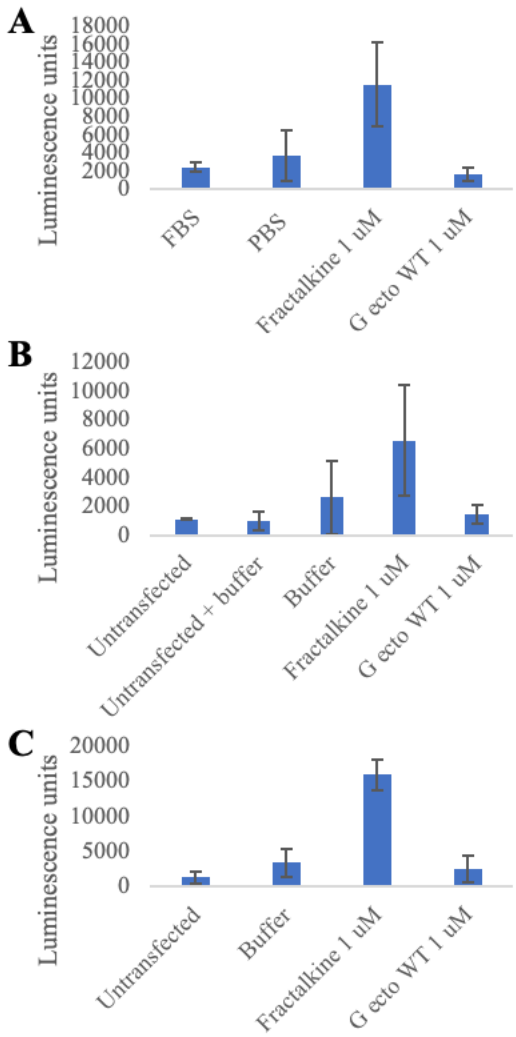

Figure 29: Fractalkine but not RSV G^{ecto} activates CX3CR1.

Fractalkine chemokine domain and RSV G^{ecto} WT were used at 1 uM. A) Cells were transfected using five ug of CX3CR1 DNA. FBS and PBS were used as negative controls. Samples were done in triplicate and error bars represent SD. B) Cells were transfected using calcium phosphate with 600 ng of CX3CR1 DNA. Untransfected HTLA cells with and without 1X HBSS, 20 mM HEPES, pH 7.4 (buffer) were used as negative controls. Buffer alone was used as an additional negative control. Samples were done in triplicate and error bars represent SD. C) Untransfected cells and buffer alone were used as negative controls. Samples were done in replicates of six and error bars represent SD.

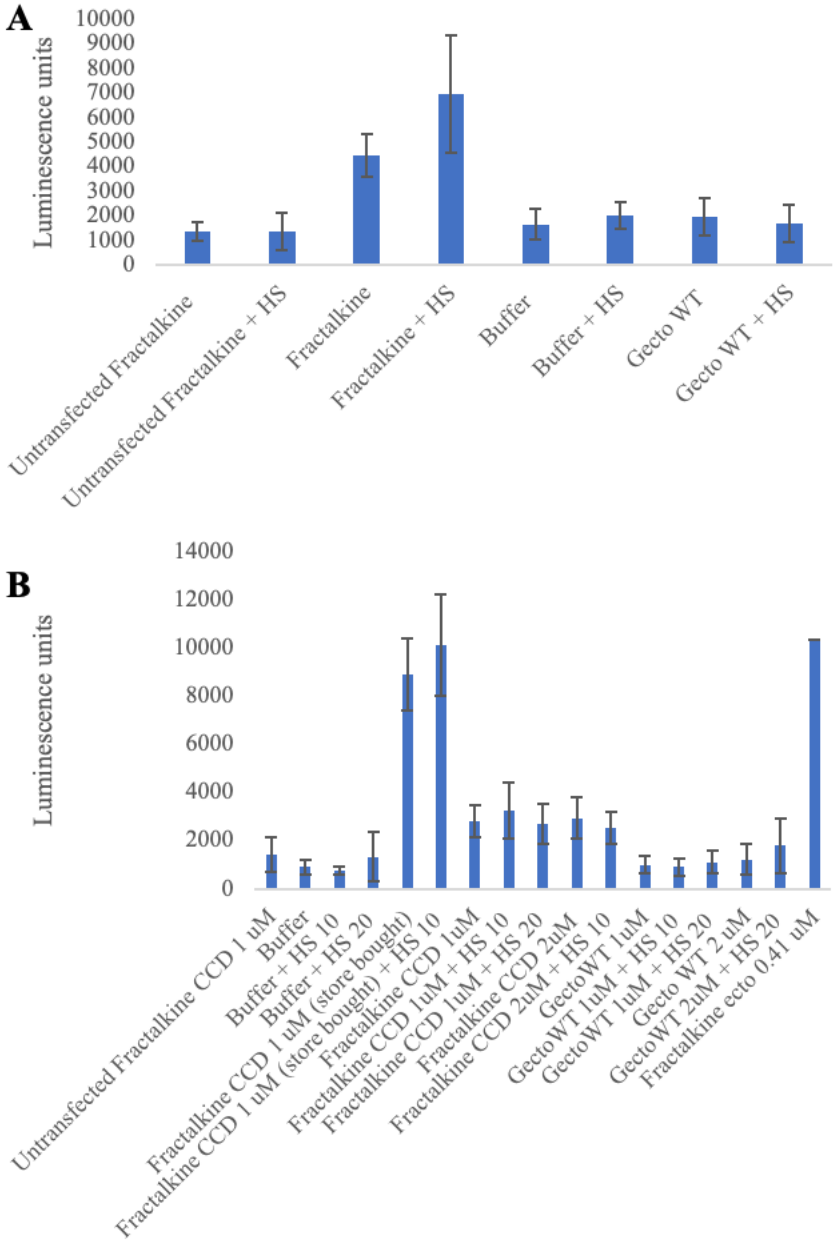

Figure 30: The chemokine domain and full length Fractalkine activates CX3CR1 in the presence and absence of heparin sodium salts, however RSV G^{ecto} does not.

Untransfected cells alone, with 1 uM of Fractalkine, buffer (1X HBSS, 20 mM HEPES, pH 7.4), or heparin sodium salts from porcine (HS) at ug/ mL concentrations

were used as negative controls. Buffer alone or with various concentrations of HS were used as additional negative controls. A) Fractalkine and RSV G^{ecto} WT were used at 1 uM. HS was used at 10 ug/mL. Samples were done in replicates of six and error bars represent SD.

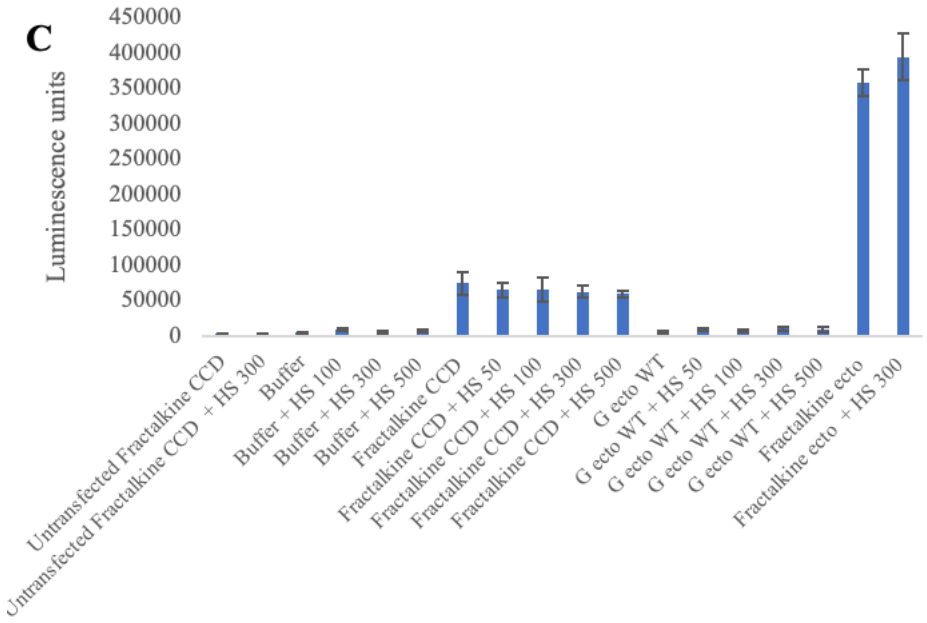

B) The chemokine domain (CCD) of Fractalkine and RSV G^{ecto} WT were used at 1 and 2 uM. Full length Fractalkine (ecto) was used at 0.41 uM. HS was used at 10 or 20 ug/mL as indicated in the axis. Samples were done in replicates of six except Fractalkine CCD store bought (five replicates), and Fractalkine ecto did not have replicates and error bars represent SD. C) Fractalkine and RSV G^{ecto} WT were used at 1 uM. HS was used at 50, 100, 300, or 500 ug/mL. All samples except the untransfected controls (triplicates) were done in replicates of six and error bars represent SD.

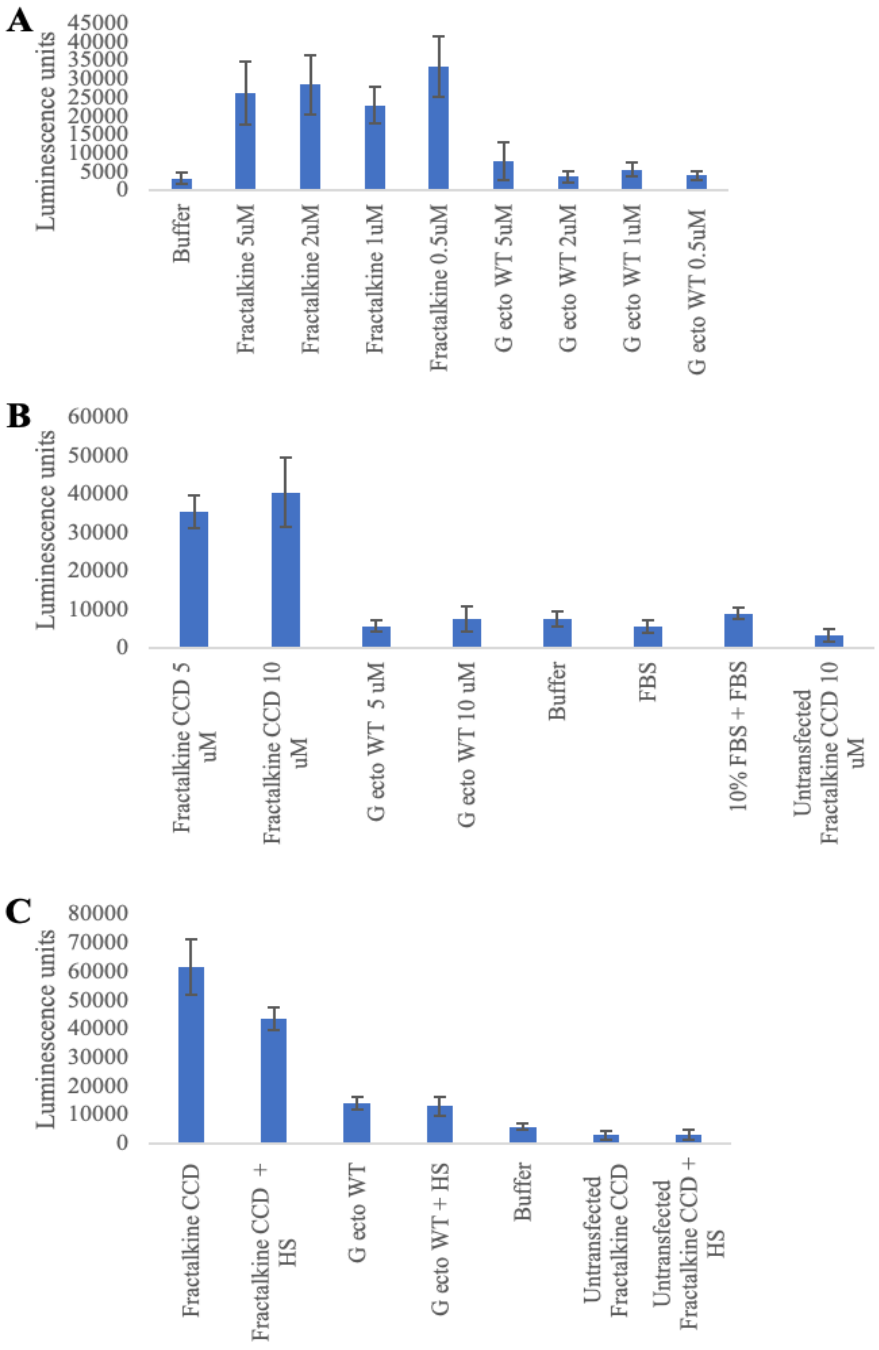

Figure 31: Fractalkine but not RSV G^{ecto} activates CX3CR1 at 5 or 10 uM.

Buffer (1X HBSS, 20 mM HEPES, pH 7.4) was used as a negative control. A) Fractalkine (CCD) and RSV G^{ecto} were used at 5, 2, 1, 0.5 uM. Samples were done in

replicates of six and error bars represent SD. B) Untransfected HTLA cells with Fractalkine CCD were used as negative controls. Buffer, FBS, and 10% FBS added to cells in media containing FBS were used as additional negative controls. Fractalkine CCD and RSV G^{ecto} WT were used at 5 and 10 uM. Samples were done in replicates of six and error bars represent SD. C) Untransfected HTLA cells with Fractalkine CCD or Fractalkine and heparin sodium salt (HS) were used as negative controls. Fractalkine CCD and RSV G^{ecto} WT were used at 10 uM with and without 500 ug/mL of HS. Samples were done in replicates of six and error bars represent SD.

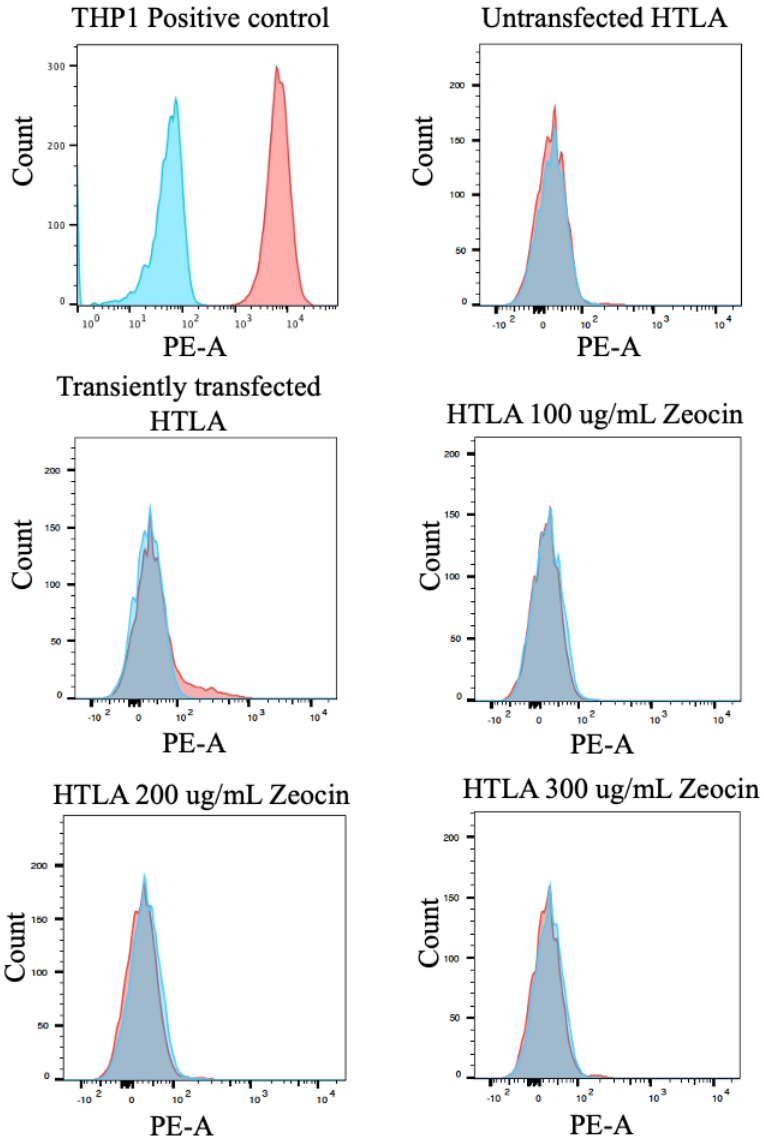

Figure 32: CX3CR1 is expressed in transiently transfected HTLA cells, but poorly expressed in stably transfected cells.

THP1 (positive control) or HTLA cells were stained for CX3CR1 using PE rat anti-human CX3CR1 clone 2A9-1 (isotype rat IgG2b,k) antibody shown in red or using an isotype control antibody PE rat anti-mouse Valpha2 TCR shown in blue. Stably transfected HTLA cells were grown in 100, 200, or 300 ug/mL of zeocin.

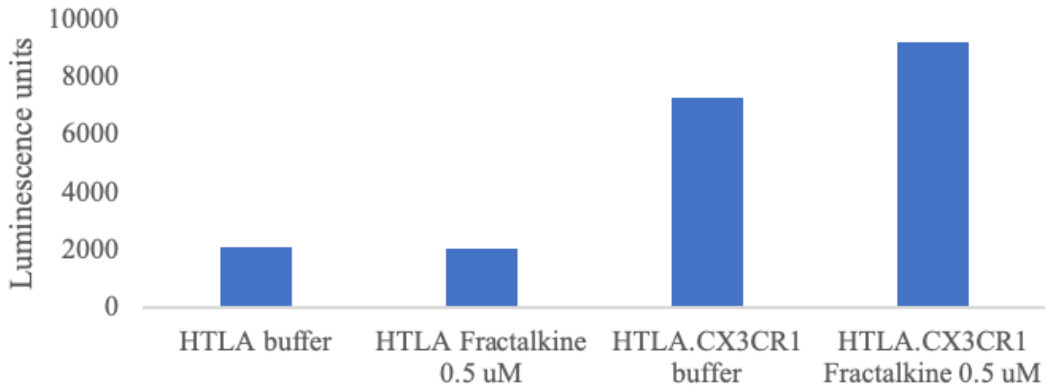

Figure 33: Fractalkine does not activate CX3CR1 of stably transfected HTLA cells.

Untransfected HTLA cells with buffer (1X HBSS, 20 mM HEPES, pH 7.4) or Fractalkine at 0.5 uM were used as controls. Stably transfected HTLA cells (HTLA.CX3CR1, grown in 300 ug/mL zeocin) were incubated with buffer or 0.5 uM Fractalkine. One replicate per sample.

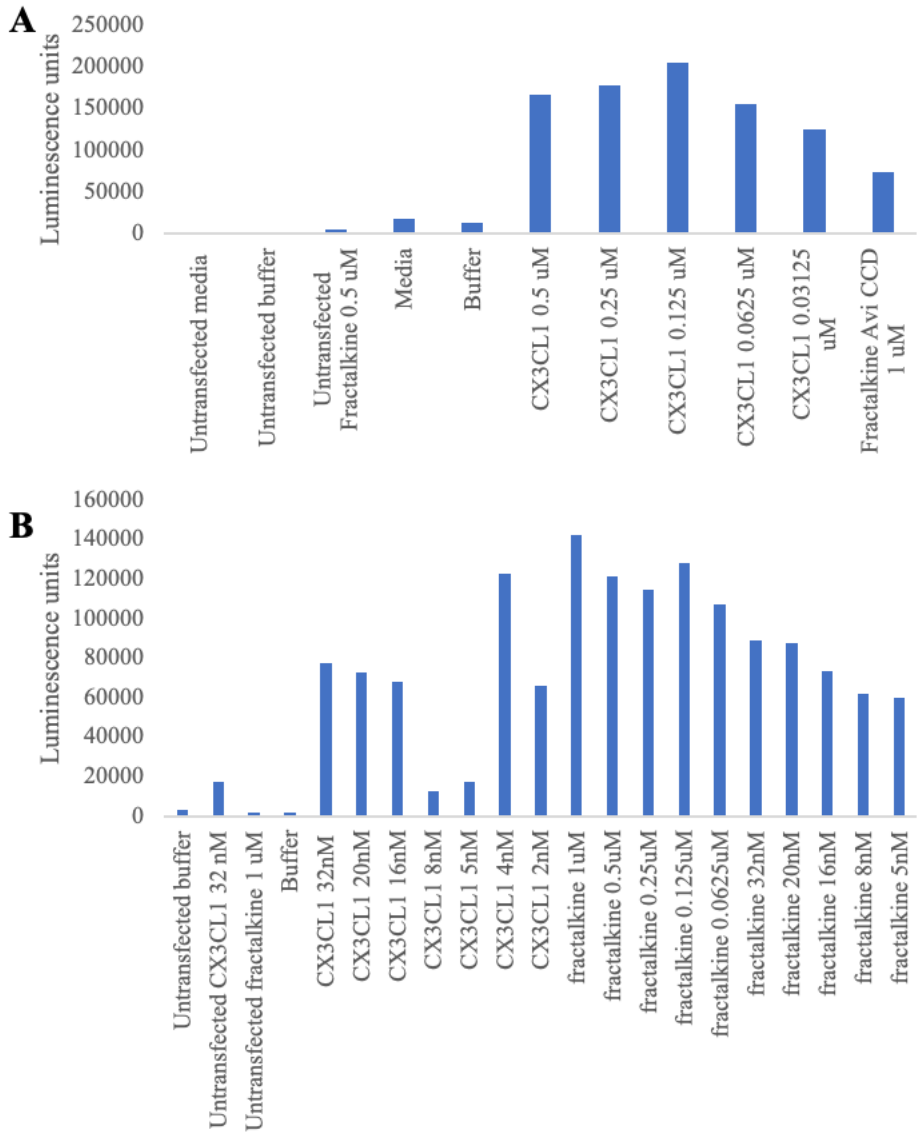

Figure 34: Activation of CX3CR1 by store bought and home-made Fractalkine is concentration dependent.

Untransfected HTLA cells alone, with buffer (1X HBSS, 20 mM HEPES, pH 7.4), with store bought Fractalkine (CX3CL1) or home-made Fractalkine were used as negative controls. Media alone and buffer were used as additional negative controls. A) CX3CL1 was used starting at 0.5 uM and serially diluted 1:2 to 0.03125 uM.

Fractalkine chemokine domain (CCD) with an Avi tag was used at 1 uM. B) CX3CL1 was used starting at 32 nM and serially diluted by half to 2 nM. Home-made Fractalkine was used starting at 1 uM and serially diluted by half to 5 nM. One replicate per sample.

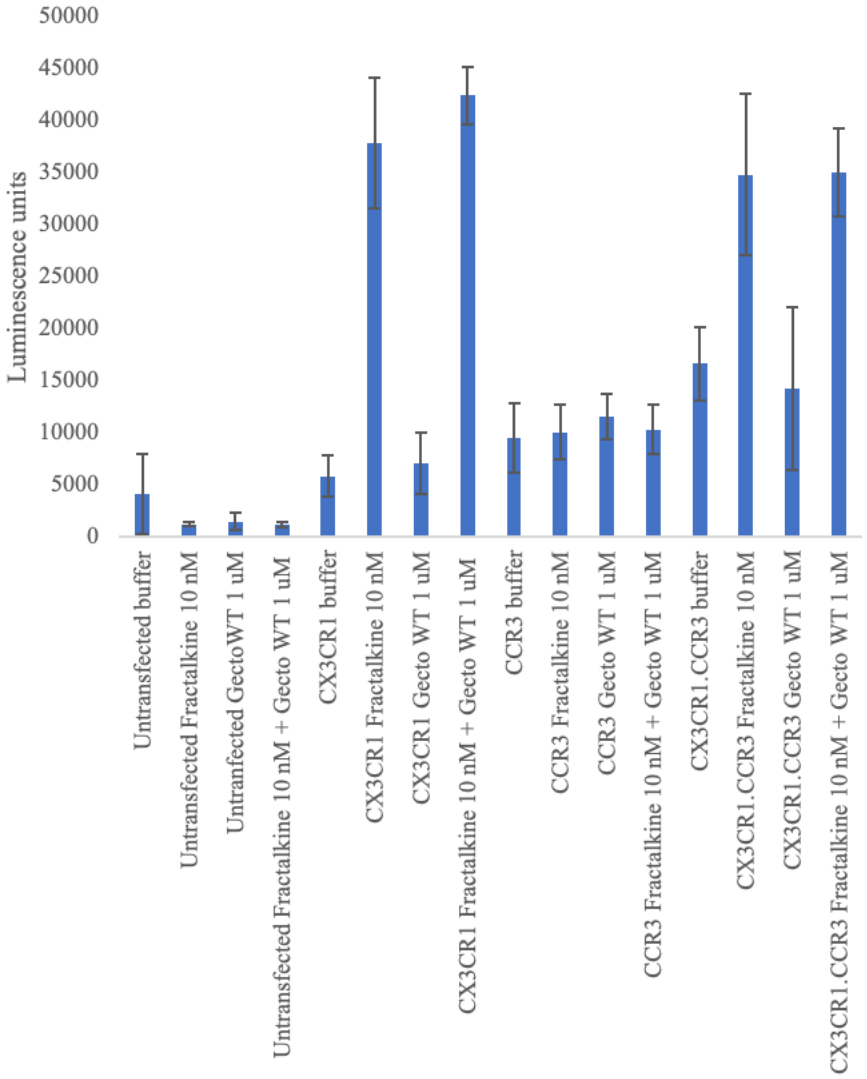

Figure 35: RSV G^{ecto} does not prevent Fractalkine from activating CX3CR1, and CCR3 is not activated by Fractalkine or RSV G^{ecto}.

Untransfected HTLA cells with buffer (1X HBSS, 20 mM HEPES, pH 7.4), Fractalkine, RSV G^{ecto} WT or both proteins were used as negative controls. HTLA cells transfected with CX3CR1 are labeled as CX3CR1 and HTLA cells transfected

with CCR3 are labled CCR3. HTLA cells transfected with CX3CR1 and CCR3 DNA are labeled CX3CR1.CCR3. Transfected cells incubated with buffer were used as additional negative controls. Fractalkine was used at 10 nM and RSV G^{ecto} WT was used at 1 uM. Fractalkine at 10 nM and RSV G^{ecto} WT at 1 uM were incubated on ice for 30 minutes before adding to cells for samples with both proteins. Samples were done in triplicate and error bars represent SD.

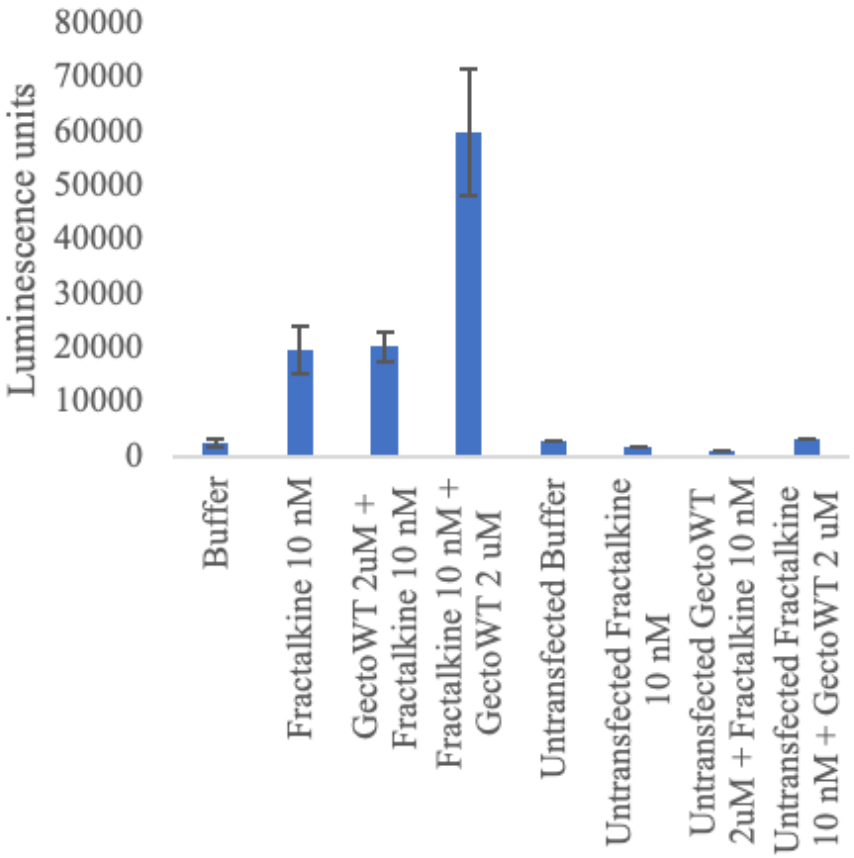

Figure 36: Adding RSV G^{ecto} WT or Fractalkine five hours apart does not prevent Fractalkine from activating CX3CR1.

Untransfected HTLA cells with buffer (1X HBSS, 20 mM HEPES, pH 7.4), Fractalkine, or RSV G^{ecto} WT first or Fractalkine first were used as negative controls. Transfected cells incubated with buffer were used as an additional negative control. Fractalkine was used at 10 nM and RSV G^{ecto} WT was used at 2 uM. For samples with both proteins, the proteins were added five hours apart. Samples were done in triplicate except the untransfected controls (had one sample each) and error bars represent SD.

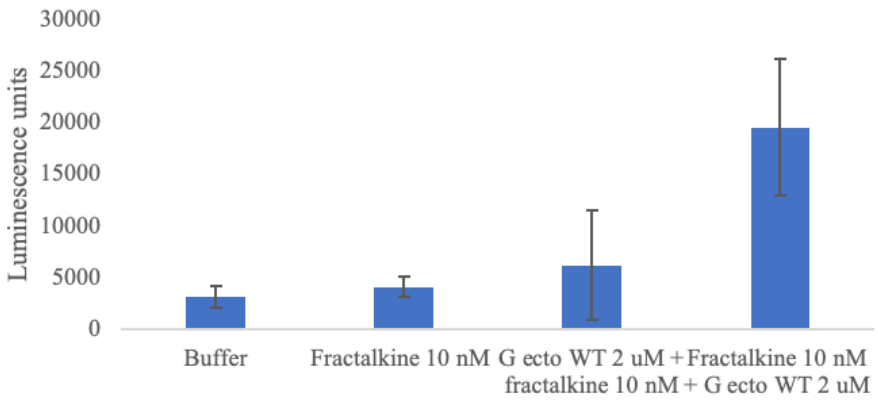

Figure 37: Heparin sodium salts from porcine reduces the activation of CX3CR1 by Fractalkine, however RSV G^{ecto} WT does not.

Transfected cells incubated with buffer (1X HBSS, 20 mM HEPES, pH 7.4) were used as negative controls. Heparin sodium salt from porcine was used at 5 ug/mL. Fractalkine was used at 10 nM and RSV G^{ecto} WT was used at 2 uM. For samples with both proteins, the proteins were added five hours apart with half of the heparin in one sample and the other half of the heparin in the second sample. Samples were done in triplicate and error bars represent SD.

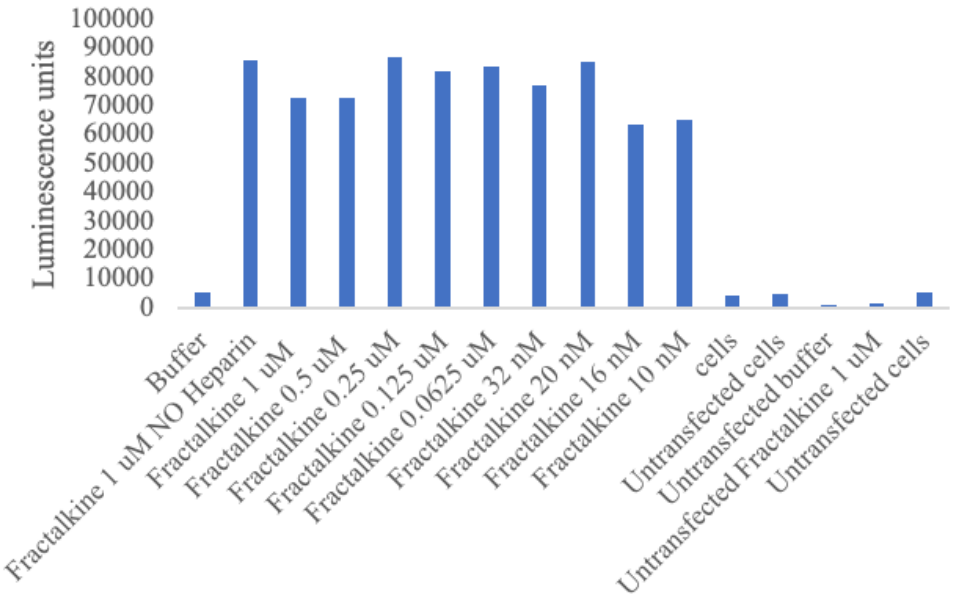

Figure 38: Fractalkine activates CX3CR1 even in the presence of heparin sodium salt from porcine.

Untransfected HTLA cells incubated with media (DMEM, 10% FBS, 2 mM glutamax), buffer (1X HBSS, 20 mM HEPES, pH 7.4), or Fractalkine were used as negative controls. Transfected cells incubated with media (cells), buffer, or 1 uM of Fractalkine with no heparin were used as additional negative controls. Fractalkine was used at 1 uM and serially diluted to 10 nM. Heparin at 5 ug/mL was incubated with protein on ice 1 hour before adding to cells. One replicate per sample.

3.6.4 Conclusion

CX3CR1 was transfected in the HTLA cell line and Fractalkine (the native ligand for CX3CR1) induced luciferase expression. Fractalkine did not induce expression of luciferase of untransfected HTLA cells. RSV G^{ecto} WT did not induce expression of luciferase in transfected HTLA cells (luminescence levels were similar to the negative control). The data suggest that RSV G^{ecto} WT did not activate CX3CR1, which indicates that another receptor that is not present in HEK293T cells may be required for RSV G^{ecto} WT to activate CX3CR1. I have attempted to create an HTLA

cell line that stably expresses CX3CR1, however the cells poorly express the receptor and are not able to be sorted.

3.7 Summary

RSV uses the attachment glycoprotein RSV G to interact with the human chemokine receptor CX3CR1 on host cells. CX3CR1 is a GPCR with an i alpha subunit. GPCR's are involved in the calcium flux pathway. Attempts were made to measure calcium influx into THP1 cells, which are monocyte-like cells that express CX3CR1. Calcium influx was measured by measuring fluorescence of Fluo-4AM through plate reader and FACS, however, I hypothesize the peak of calcium influx was missed due to lag time of measurements, thus other experiments to analyze the interaction between RSV G and CX3CR1 were explored.

Various methods were used to count chemotaxed THP1 cells including trypan blue and a hemocytometer, calcein dye, and hoescht stain. Chemotaxis of THP1 cells was induced by RSV G^{ecto} (full length protein), however was not induced by the Central Conserved Domain (CCD, aa 157-197) of RSV G when the protein was expressed in *E. coli* in its soluble form or refolded from cell pellets. Soluble RSV G CCD induced some chemotaxis of THP1 cells possibly due to the *E. coli* contaminants in the protein samples. RSV G mutant proteins (S177Q, S177R, S177W, E166K, and CX4C) still induced chemotaxis of THP1 cells. Anti-RSV G Fabs, an anti-CX3CR1 polyclonal antibody, Fc blocker alone, and heparin salts reduced RSV G induced chemotaxis of THP1 cells.

We attempted to knockout CX3CR1 from THP1 cells because anti-RSV G Fabs and the anti-CX3CR1 antibody did not fully block chemotaxis, and Fc blocker alone reduced chemotaxis. The CX3CR1 knockdowns were attempted by Dr. Sergio Covarrubias, myself, and Dr. Sara O'Rourke. RNA guides that were used for these attempts are in Table 1. Dr. Sara O'Rourke created two cell lines that had CX3CR1 knocked down, however the cells were not able to be sorted and were frozen down.

Measuring cAMP levels was another approach taken to investigate the activation of CX3CR1 on THP1 cells by RSV G. cAMP levels were measured by fluorescence and luminescence readings. Fluorescence and luminescence readings were inversely proportional to cAMP levels. Forskolin, a small molecule, was used to induce cAMP levels in the cells. Inducing cAMP levels with forskolin was variable, and controls for high cAMP and reduced cAMP levels were needed to properly analyze the data.

Since measuring CX3CR1 activation by RSV G proved difficult, binding of RSV G to THP1 or HEK293 T cells that overexpress CX3CR1 was measured using RSV G fusion proteins with GFP (RSV GFP-G), a fluorescent anti-His antibody, fluorescent Streptactin and fluorescent Streptavidin. RSV GFP-G 157-197 bound to THP1 cells and anti-RSV G Fabs reduced this binding. RSV GFP-G 157-191 (three lysines from the heparin binding domain cut out) dramatically reduced binding, which suggests the binding measured from RSV GFP-G 157-197 was due to the heparin binding domain. Binding of RSV G measured by fluorescent anti-His antibody was not observed when incubated at 37 or 4C, however it is possible that cells were not

washed enough times before measuring fluorescence which could have led to high background fluorescence. Binding of full-length RSV G was also not observed when measuring fluorescence by fluorescent Streptactin or Streptavidin. Similarly, to measuring with the anti-His antibody, high background fluorescence was observed. More washes could have also helped reduce background fluorescence in these samples to more accurately measure binding.

Finally, the last assay to measure CX3CR1 activation by RSV G was the Presto Tango assay. For this assay, CX3CR1 was transfected into HTLA cells and activity was measured by luminescence reading using a plate reader. Fractalkine, the natural ligand for CX3CR1, activated CX3CR1, however RSV G did not. Heparin salts reduced the activation of CX3CR1 by fractalkine, however did not have any effect on RSV G. Adding RSV G five hours before Fractalkine or fractalkine five hours before RSV G did not have any effect on the activation of CX3CR1 by fractalkine. I attempted to create a stable HTLA cell line that expresses CX3CR1, however CX3CR1 expression was poor and cells were not able to be sorted. Another GPCR, CCR3, was transfected into HTLA cells to test whether it could be a potential co-receptor for RSV G activation, however CCR3 activation was not observed.

3.8 Future directions

There is a commercial THP1 cell line with CX3CR1 knocked out, this cell line should be tested in the chemotaxis assay to test activity of RSV G. If RSV G^{ecto} does induce chemotaxis of THP1 $CX3CR1^{-/-}$ cells, those results would indicate that RSV G's immune modulation may be happening through a different receptor. T cells

are a better model for chemotaxis to test activity of CX3CR1 by RSV G because T cells are present in the immune response induced by RSV G and monocytes (THP1 cells) are not as relevant. Furthermore, bovine serum albumin was required for Fractalkine to induce chemotaxis of THP1 cells in Fedechkin et al., 2018, and I did not see chemotaxis of THP1 cells induced by Fractalkine suggesting this is not the best chemotaxis model.

It seems as though binding of RSV G to CX3CR1 expressing cells will be a small percentage. In order to capture this binding, many washes of the cells will be required to reduce background fluorescence, and experiments should be done at 4C to prevent endocytosis of CX3CR1.

For the Presto Tango assay, other isoforms of CX3CR1 should be transfected into the HTLA cells to test activity of CX3CR1, and other receptors should be considered that may be potential co-receptors required for RSV G to activate CX3CR1.

3.9 References

1. Shi T, Balsells E, Wastnedge E, Singleton R, Rasmussen ZA, Zar HJ, Rath BA, Madhi SA, Campbell S, Vaccari LC, Bulkow LR, Thomas ED, Barnett W, Hoppe C, Campbell H, Nair H. 2015. Risk factors for respiratory syncytial virus associated with acute lower respiratory infection in children under five years: Systematic review and meta–analysis. J Glob Health 5.
2. Scheltema NM, Gentile A, Lucion F, Nokes DJ, Munywoki PK, Madhi SA, Groome MJ, Cohen C, Moyes J, Thorburn K, Thamthitiwat S, Oshitani H,

Lupisan SP, Gordon A, Sánchez JF, O'Brien KL, Gessner BD, Sutanto A, Mejias A, Ramilo O, Khuri-Bulos N, Halasa N, de-Paris F, Pires MR, Spaeder MC, Paes BA, Simões EAF, Leung TF, da Costa Oliveira MT, de Freitas Lázaro Emediato CC, Bassat Q, Butt W, Chi H, Aamir UB, Ali A, Lucero MG, Fasce RA, Lopez O, Rath BA, Polack FP, Papenburg J, Roglić S, Ito H, Goka EA, Grobbee DE, Nair H, Bont LJ, James Nokes D, Munywoki PK, Madhi SA, Groome MJ, Cohen C, Moyes J, Thorburn K, Thamthitiwat S, Oshitani H, Lupisan SP, Gordon A, Sánchez JF, O KL, Khuri-Bulos N, Halasa N, de-Paris F, Rosane Pires M, Spaeder MC, Paes BA, F Simões EA, Leung TF, Tereza da Costa Oliveira M, Cecília de Freitas Lázaro Emediato C, Bassat Q, Butt W, Chi H, Bashir Aamir U, Ali A, Lucero MG, Fasce RA, Lopez O, Rath BA, Polack FP, Papenburg J, Roglić S, Ito H, Goka EA, Grobbee DE, Nair H, Bont LJ. 2017. Global respiratory syncytial virus-associated mortality in young children (RSV GOLD): a retrospective case seriesThe Lancet Global Health.

3. Hall CB, Weinberg GA, Iwane MK, Blumkin AK, Edwards KM, Staat MA, Auinger P, Griffin MR, Poehling KA, Erdman D, Grijalva CG, Zhu Y, Szilagyi P. 2009. The Burden of Respiratory Syncytial Virus Infection in Young Children. Pediatr Biostat https://doi.org/10.1056/NEJMoa0804877.

4. Li Y, Wang X, Blau DM, Caballero MT, Feikin DR, Gill CJ, Madhi SA, Omer SB, F Simões EA, Campbell H, Bermejo Pariente A, Bardach D, Bassat Q, Casalegno J-S, Chakhunashvili G, Crawford N, Danilenko D, Anh Ha Do L, Echavarria M, Gentile A, Gordon A, Heikkinen T, Sue Huang Q, Jullien S,

Krishnan A, Luis Lopez E, Markić J, Mira-Iglesias A, Moore HC, Moyes J, Mwananyanda L, James Nokes D, Noordeen F, Obodai E, Palani N, Romero C, Salimi V, Satav A, Seo E, Shchomak Z, Singleton R, Stolyarov K, Stoszek SK, von Gottberg A, Wurzel D, Yoshida L-M, Fu Yung C, Zar HJ. 2022. Global, regional, and national disease burden estimates of acute lower respiratory infections due to respiratory syncytial virus in children younger than 5 years in 2019: a systematic analysis. www.thelancet.com 399.

5. Branche AR, Ann Falsey BR. 2015. Respiratory Syncytial Virus Infection in Older Adults: An Under-Recognized Problem. Drugs Aging https://doi.org/10.1007/s40266-015-0258-9.
6. Satakel M, Coligan2 JE, Elango3 N, Norrby4 E, Venkatesan5 S. 1985. Respiratory syncytial virus envelope glycoprotein (G) has a novel structure. Nucleic Acids Res 13:7795–7812.
7. Mclellan JS, Ray WC, Peeples ME. 2013. Structure and Function of RSV Surface Glycoproteins https://doi.org/10.1007/978-3-642-38919-1_4.
8. Tripp RA, Power UF, Openshaw PJM, Kauvar LM. 2017. Respiratory Syncytial Virus: Targeting the G Protein Provides a New Approach for an Old Problem. J Virol 92:e01302-17.
9. Graham BS. 2017. Vaccine development for respiratory syncytial virus This review comes from a themed issue on Preventive and therapeutic vaccines Epidemiology and vaccine target populations. Curr Opin Virol 23:107–112.
10. Jorquera PA, Tripp RA. 2017. Expert Review of Respiratory Medicine

Respiratory syncytial virus: prospects for new and emerging therapeutics Respiratory syncytial virus: prospects for new and emerging therapeutics https://doi.org/10.1080/17476348.2017.1338567.

11. Higgins D, Trujillo C, Keech C. 2016. Advances in RSV vaccine research and development – A global agenda. Vaccine 34:2870–2875.
12. RSV Vaccine and mAb Snapshot | PATH.
13. Olchanski N, Hansen RN, Pope E, D 'cruz B, Fergie J, Goldstein M, Krilov LR, Mclaurin KK, Nabrit-Stephens B, Oster G, Schaecher K, Shaya FT, Neumann PJ, Sullivan SD. 2018. Palivizumab Prophylaxis for Respiratory Syncytial Virus: Examining the Evidence Around Value. Open Forum Infect Dis https://doi.org/10.1093/ofid/ofy031.
14. Perk Y, Özdil M. 2018. Cite this article as: Perk Y, Özdil M. Respiratory syncytial virüs infections in neonates and infants. Turk Pediatr Ars 53:63–70.
15. Rezaee F, Linfield DT, Harford TJ, Piedimonte G. 2017. Ongoing developments in RSV prophylaxis: a clinician's analysis. Curr Opin Virol.
16. Simoes EAF, Bont L, Manzoni P, Fauroux B, Paes B, Figueras-Aloy J, Checchia PA, Carbonell-Estrany X. 2018. Past, Present and Future Approaches to the Prevention and Treatment of Respiratory Syncytial Virus Infection in Children. Infect Dis Ther 7.
17. Resch B. 2017. Product review on the monoclonal antibody palivizumab for prevention of respiratory syncytial virus infection https://doi.org/10.1080/21645515.2017.1337614.

18. Fedechkin SO, George NL, Wolff JT, Kauvar LM, Dubois RM. 2018. Structures of respiratory syncytial virus G antigen bound to broadly neutralizing antibodies. Sci Immunol 3:1–8.

19. Chirkova T, Lin S, P Oomens AG, Gaston KA, Boyoglu-Barnum S, Meng J, Stobart CC, Cotton CU, Hartert T V, Moore ML, Ziady AG, Anderson LJ, Larry Anderson CJ. 2015. CX3CR1 is an important surface molecule for respiratory syncytial virus infection in human airway epithelial cells. J Gen Virol https://doi.org/10.1099/vir.0.000218.

20. Jeong K-I, Piepenhagen PA, Kishko M, Dinapoli JM, Groppo RP, Zhang L, Almond J, Kleanthous H, Delagrave S, Parrington M. 2015. CX3CR1 Is Expressed in Differentiated Human Ciliated Airway Cells and Co-Localizes with Respiratory Syncytial Virus on Cilia in a G Protein-Dependent Manner. PLoS One https://doi.org/10.1371/journal.pone.0130517.

21. Johnson SM, Mcnally BA, Ioannidis I, Flano E, Teng MN, Oomens AG, Walsh EE, Peeples ME. 2015. Respiratory Syncytial Virus Uses CX3CR1 as a Receptor on Primary Human Airway Epithelial Cultures. PLoS Pathog 11.

22. Hijano DR, Kalergis AM, Kauvar LM, Tripp RA, Polack FP, Cormier SA. 2019. Role of Type I Interferon (IFN) in the Respiratory Syncytial Virus (RSV) Immune Response and Disease Severity. Front Immunol | www.frontiersin.org 1:566.

23. Tripp RA, Jones LP, Haynes LM, Zheng HQ, Murphy PM, Anderson LJ. 2001. CX3C chemokine mimicry by respiratory syncytial virus G glycoprotein. Nat

Immunol 2:732–738.

24. Harcourt J, Alvarez R, Jones LP, Henderson C, Anderson LJ, Tripp RA. 2006. Respiratory Syncytial Virus G Protein and G Protein CX3C Motif Adversely Affect CX3CR1 T Cell Responses. J Immunol 176:1600–1608.

25. Arnold R, Kfnig B, Werchau H, Kfnig W. 2004. Respiratory syncytial virus deficient in soluble G protein induced an increased proinflammatory response in human lung epithelial cells. Virology https://doi.org/10.1016/j.virol.2004.10.004.

26. Haynes LM, Jones LP, Barskey A, Anderson LJ, Tripp RA. 2003. Enhanced disease and pulmonary eosinophilia associated with formalin-inactivated respiratory syncytial virus vaccination are linked to G glycoprotein CX3C-CX3CR1 interaction and expression of substance P. J Virol 77:9831–9844.

27. Collarini EJ, Lee FE-H, Foord O, Park M, Sperinde G, Wu H, Harriman WD, Carroll SF, Ellsworth SL, Anderson LJ, Tripp RA, Walsh EE, Keyt BA, Kauvar LM. 2009. Potent High-Affinity Antibodies for Treatment and Prophylaxis of Respiratory Syncytial Virus Derived from B Cells of Infected Patients. J Immunol 183:6338–6345.

28. Han J, Takeda K, Wang M, Zeng W, Jia Y, Shiraishi Y, Okamoto M, Dakhama A, Gelfand EW. 2014. Effects of Anti-G and Anti-F Antibodies on Airway Function after Respiratory Syncytial Virus Infection. Am J Respir Cell Mol Biol 51.

29. Caidi H, Miao C, Thornburg NJ, Tripp RA, Anderson LJ, Haynes LM. 2018.

Anti-respiratory syncytial virus (RSV) G monoclonal antibodies reduce lung inflammation and viral lung titers when delivered therapeutically in a BALB/c mouse model. Antivir Res 154:149–157.

30. Capella C, Chaiwatpongsakorn S, Gorrell E, Risch ZA, Ye F, Mertz SE, Johnson SM, Moore-Clingenpeel M, Ramilo O, Mejias A, Peeples ME. 2017. Prefusion F, Postfusion F, G Antibodies, and Disease Severity in Infants and Young Children With Acute Respiratory Syncytial Virus Infection. J Infect Dis ® 1398:1398–406.

31. Shaw CA, Ciarlet M, Cooper BW, Dionigi L, Keith P, O 'brien KB, Rafie-Kolpin M, Dormitzer PR, O'Brien KB, Rafie-Kolpin M, Dormitzer PR. 2013. The path to an RSV vaccine. Curr Opin Virol 3:332–342.

32. Chanock RM, Jensen K, Parrott RH. 1969. Respiratory Syncytial Virus Disease in Infants 89:422–434.

33. Villafana T, Falloon J, Griffin MP, Zhu Q, Esser MT. 2017. Expert Review of Vaccines Passive and active immunization against respiratory syncytial virus for the young and old Passive and active immunization against respiratory syncytial virus for the young and old https://doi.org/10.1080/14760584.2017.1333425.

34. Johnson TR, Graham BS. 1999. Secreted Respiratory Syncytial Virus G Glycoprotein Induces Interleukin-5 (IL-5), IL-13, and Eosinophilia by an IL-4-Independent Mechanism. J Virol 73:8485–8495.

35. Johnson TR, Teng MN, Collins PL, Graham BS. 2004. Respiratory Syncytial

Virus (RSV) G Glycoprotein Is Not Necessary for Vaccine-Enhanced Disease Induced by Immunization with Formalin-Inactivated RSV. J Virol 78:6024–6032.

36. Knudson CJ, Hartwig SM, Meyerholz DK, Varga SM. 2015. RSV Vaccine-Enhanced Disease Is Orchestrated by the Combined Actions of Distinct CD4 T Cell Subsets. PLOS Pathog https://doi.org/10.1371/journal.ppat.1004757.

37. Acosta PL, Caballero MT, Polack FP. 2016. Brief History and Characterization of Enhanced Respiratory Syncytial Virus Disease https://doi.org/10.1128/CVI.00609-15.

38. Fuentes S, Klenow L, Golding H, Khurana S. 2017. Preclinical evaluation of bacterially produced RSV-G protein vaccine: Strong protection against RSV challenge in cotton rat model. Sci Rep 7:1–13.

39. Tripp RA. 2004. Pathogenesis of Respiratory Syncytial Virus InfectionVIRAL IMMUNOLOGY.

40. Fuentes S, Coyle EM, Golding H, Khurana S. 2015. Nonglycosylated G-Protein Vaccine Protects against Homologous and Heterologous Respiratory Syncytial Virus (RSV) Challenge, while Glycosylated G Enhances RSV Lung Pathology and Cytokine Levels. J Virol 89:8193–8205.

41. Li C, Zhou X, Zhong Y, Li C, Dong A, He Z, Zhang S, Wang B. 2016. A Recombinant G Protein Plus Cyclosporine A–Based Respiratory Syncytial Virus Vaccine Elicits Humoral and Regulatory T Cell Responses against Infection without Vaccine-Enhanced Disease. J Immunol.

42. Johnson TR, Johnson JE, Roberts SR, Wertz GW, Parker RA, Graham BS. 1998. Priming with Secreted Glycoprotein G of Respiratory Syncytial Virus (RSV) Augments Interleukin-5 Production and Tissue Eosinophilia after RSV ChallengeJOURNAL OF VIROLOGY.

43. Johnson TR, Varga SM, Braciale TJ, Graham BS. 2004. Vβ14 + T Cells Mediate the Vaccine-Enhanced Disease Induced by Immunization with Respiratory Syncytial Virus (RSV) G Glycoprotein but Not with Formalin-Inactivated RSV . J Virol 78:8753–8760.

44. Jorquera PA, Anderson L, Tripp RA. 2015. Expert Review of Vaccines Understanding respiratory syncytial virus (RSV) vaccine development and aspects of disease pathogenesis Understanding respiratory syncytial virus (RSV) vaccine development and aspects of disease pathogenesis https://doi.org/10.1586/14760584.2016.1115353doi.org/10.1586/14760584.2016.1115353.

45. Jones HG, Ritschel T, Pascual G, Brakenhoff JPJ, Keogh E, Furmanova-Hollenstein P, Lanckacker E, Wadia JS, Gilman MSA, Williamson RA, Roymans D, Van 't Wout AB, Langedijk JP, Mclellan JS. 2018. Structural basis for recognition of the central conserved region of RSV G by neutralizing human antibodies. PLOS Pathog https://doi.org/10.1371/journal.ppat.1006935.

46. Radu GU, Caidi H, Miao † Congrong, Tripp RA, Anderson LJ, Haynes LM. 2010. Prophylactic Treatment with a G Glycoprotein Monoclonal Antibody Reduces Pulmonary Inflammation in Respiratory Syncytial Virus (RSV)-

Challenged Naïve and Formalin-Inactivated RSV-Immunized BALB/c Mice. J Virol 84:9632–9636.

47. Caidi H, Harcourt JL, Tripp RA, Anderson LJ, Haynes LM, Varga SM. 2012. Combination Therapy Using Monoclonal Antibodies against Respiratory Syncytial Virus (RSV) G Glycoprotein Protects from RSV Disease in BALB/c Mice. PLoS One https://doi.org/10.1371/journal.pone.0051485.

48. Haynes LM, Caidi H, Radu GU, Miao C, Harcourt JL, Tripp RA, Anderson LJ. 2009. Therapeutic Monoclonal Antibody Treatment Targeting Respiratory Syncytial Virus (RSV) G Protein Mediates Viral Clearance and Reduces the Pathogenesis of RSV Infection in BALB/c Mice. J Infect Dis 200:439–486.

49. Miao C, Radu GU, Caidi H, Tripp RA, Anderson LJ, Haynes LM. 2009. Treatment with respiratory syncytial virus G glycoprotein monoclonal antibody or F(ab9) 2 components mediates reduced pulmonary inflammation in mice. J Gen Virol https://doi.org/10.1099/vir.0.009308-0.

50. Boyoglu-Barnum S, Gaston KA, Todd SO, Boyoglu C, Chirkova T, Barnum TR, Jorquera P, Haynes LM, Tripp RA, Moore ML, Anderson LJ. 2013. A Respiratory Syncytial Virus (RSV) Anti-G Protein F(ab=) 2 Monoclonal Antibody Suppresses Mucous Production and Breathing Effort in RSV rA2-line19F-Infected BALB/c Mice. J Virol https://doi.org/10.1128/JVI.01164-13.

51. Boyoglu-Barnum S, Chirkova T, Todd SO, Barnum TR, Gaston KA, Jorquera P, Haynes LM, Tripp RA, Moore ML, Anderson LJ. 2014. Prophylaxis with a Respiratory Syncytial Virus (RSV) Anti-G Protein Monoclonal Antibody

Shifts the Adaptive Immune Response to RSV rA2-line19F Infection from Th2 to Th1 in BALB/c Mice. J Virol https://doi.org/10.1128/JVI.01503-14.

52. Boyoglu-Barnum S, Todd SO, Chirkova T, Barnum TR, Gaston KA, Haynes LM, Tripp RA, Moore ML, Anderson LJ. 2015. An anti-G protein monoclonal antibody treats RSV disease more effectively than an anti-F monoclonal antibody in BALB/c mice HHS Public Access. Virology 483:117–125.

53. Lee H-J, Lee J-Y, Park M-H, Kim J-Y, Chang J. 2017. Monoclonal Antibody against G Glycoprotein Increases Respiratory Syncytial Virus Clearance In Vivo and Prevents Vaccine- Enhanced Diseases. PLoS One https://doi.org/10.1371/journal.pone.0169139.

54. Hammitt LL, Dagan R, Yuan Y, Baca Cots M, Bosheva M, Madhi SA, Muller WJ, Zar HJ, Brooks D, Grenham A, Wählby Hamrén U, Mankad VS, Ren P, Takas T, Abram ME, Leach A, Griffin MP, Villafana T. 2022. Nirsevimab for Prevention of RSV in Healthy Late-Preterm and Term Infants. N Engl J Med 386:837–846.

55. Boyoglu-Barnum S, Todd SO, Meng J, Barnum TR, Chirkova T, Haynes LM, Jadhao SJ, Tripp RA, Oomens AG, Moore ML, Anderson LJ. 2017. Mutating the CX3C Motif in the G Protein Should Make a Live Respiratory Syncytial Virus Vaccine Safer and More Effective. J Virol https://doi.org/10.1128/JVI.02059-16.

56. Jung Y-J, Lee Y-N, Kim K-H, Lee Y, Jeeva S, Park BR, Kang S-M. 2020. Recombinant Live Attenuated Influenza Virus Expressing Conserved G-

Protein Domain in a Chimeric Hemagglutinin Molecule Induces G-Specific Antibodies and Confers Protection against Respiratory Syncytial Virus. Vaccines https://doi.org/10.3390/vaccines8040716.

57. Tian P, Xu D, Huang Z, Meng F, Fu J, Wei H, Chen T. 2018. Evaluation of truncated G protein delivered by live attenuated Salmonella as a vaccine against respiratory syncytial virus. Microb Pthogenes 115:299–303.

58. Kim A-R, Lee D-HD-H, Lee S-H, Rubino I, Choi H-JH-J, Quan F-S. 2018. Protection induced by virus-like particle vaccine containing tandem repeat gene of respiratory syncytial virus G protein. PLoS One 13:1–14.

59. Lee S, Quan F-S, Kwon Y, Sakamoto K, Kang S-M, Compans RW, Moore ML. 2014. Additive Protection Induced by Mixed Virus-like Particles Presenting Respiratory Syncytial Virus Fusion or Attachment Glycoproteins. Antivir Res 111:129–135.

60. Ha B, Yang JE, Chen X, Jadhao SJ, Wright ER, Anderson LJ. 2020. Two RSV Platforms for G, F, or G+F Proteins VLPs. Viruses https://doi.org/10.3390/v12090906.

61. Blanco JCG, Pletneva LM, Mcginnes-Cullen L, Otoa RO, Patel MC, Fernando LR, Boukhvalova MS, Morrison TG. 2018. Efficacy of a respiratory syncytial virus vaccine candidate in a maternal immunization model. Nat Commun https://doi.org/10.1038/s41467-018-04216-6.

62. Hwang HS, Kim K-H, Lee Y, Lee Y-T, Ko E-J, Park S, Lee JS, Lee B, Kwon Y-M, Moore ML, Kang S-M. 2017. Virus-like particle vaccines containing F

or F and G proteins confer protection against respiratory syncytial virus without pulmonary inflammation in cotton rats. Hum Vaccin Immunother 13:1031–1039.

63. Wang D, Phan S, Distefano DJ, Citron MP, Callahan CL, Indrawati L, Dubey SA, Heidecker GJ, Govindarajan D, Liang X, He B, Espeseth AS. 2017. A Single-Dose Recombinant Parainfluenza Virus 5-Vectored Vaccine Expressing Respiratory Syncytial Virus (RSV) F or G Protein Protected Cotton Rats and African Green Monkeys from RSV Challenge. J Virol https://doi.org/10.1128/JVI.

64. Liang B, Kabatova B, Kabat J, Dorward DW, Liu X, Surman S, Liu X, Park Moseman A, Buchholz UJ, Collins PL, Munir S, Liang CB, Terence Dermody ES. 2019. Effects of Alterations to the CX3C Motif and Secreted Form of Human Respiratory Syncytial Virus (RSV) G Protein on Immune Responses to a Parainfluenza Virus Vector Expressing the RSV G Protein Downloaded fromjvi.asm.org 1 Journal of Virology.

65. Binjawadagi B, Ma Y, Binjawadagi R, Brakel K, Harder O, Peeples M, Li J, Niewiesk S. 2021. Mucosal Delivery of Recombinant Vesicular Stomatitis Virus Vectors Expressing Envelope Proteins of Respiratory Syncytial Virus Induces Protective Immunity in Cotton Rats https://doi.org/10.1128/JVI.

66. Brakel KA, Binjawadagi B, French-Kim K, Watts M, Harder O, Ma Y, Li J, Niewiesk S. 2021. Coexpression of respiratory syncytial virus (RSV) fusion (F) protein and attachment glycoprotein (G) in a vesicular stomatitis virus

(VSV) vector system provides synergistic effects against RSV infection in a cotton rat model https://doi.org/10.1016/j.vaccine.2021.10.042.

67. Sawada A, Ito T, Yamaji Y, Nakayama T, Henry O. 2021. Chimeric Measles Virus (MV/RSV), Having Ectodomains of Respiratory Syncytial Virus (RSV) F and G Proteins Instead of Measles Envelope Proteins, Induced Protective Antibodies against RSV https://doi.org/10.3390/vaccines9020156.

68. Ura T, Okuda K, Shimada M. 2014. Developments in Viral Vector-Based Vaccines 2:624–641.

69. Jorquera PA, Oakley KE, Powell TJ, Palath N, Boyd JG, Tripp RA. 2015. Layer-By-Layer Nanoparticle Vaccines Carrying the G Protein CX3C Motif Protect against RSV Infection and Disease. Vaccines 3:829–849.

70. Qiao L, Zhang Y, Chai F, Tan Y, Huo C, Pan Z. 2016. Chimeric virus-like particles containing a conserved region of the G protein in combination with a single peptide of the M2 protein confer protection against respiratory syncytial virus infection. Antiviral Res 131:131–140.

71. Yang J, Ma C, Zhao Y, Fan A, Zou X, Pan Z, Yang CJ. 2020. Hepatitis B Virus Core Particles Containing a Conserved Region of the G Protein Combined with Interleukin-35 Protected Mice against Respiratory Syncytial Virus Infection without Vaccine-Enhanced Immunopathology 94:7–20.

72. Lei L, Qin H, Luo J, Tan Y, Yang J, Pan Z. 2021. Construction and immunological evaluation of hepatitis B virus core virus-like particles containing multiple antigenic peptides of respiratory syncytial virus. Virus Res

298:198410.

73. Mcgill JL, Kelly SM, Kumar P, Speckhart S, Haughney SL, Henningson J, Narasimhan B, Sacco RE. 2018. Efficacy of mucosal polyanhydride nanovaccine against respiratory syncytial virus infection in the neonatal calf OPEN. Sci Rep https://doi.org/10.1038/s41598-018-21292-2.

74. Power UF, Nguyen TN, Rietveld E, De Swart RL, Groen J, Osterhaus ADME, De Groot R, Corvaia N, Beck A, Bouveret-Le-Cam N, Bonnefoy J-Y. 2001. Safety and Immunogenicity of a Novel Recombinant Subunit Respiratory Syncytial Virus Vaccine (BBG2Na) in Healthy Young Adults. J Infect Dis.

75. Nguyen TN, Power UF, Robert A, Haeuw J-F, Helffer K, Perez A, Asin M-A, Corvaia N, Libon C. 2012. The Respiratory Syncytial Virus G Protein Conserved Domain Induces a Persistent and Protective Antibody Response in Rodents. PLoS One 7.

76. Zhang S, Zhao G, Su C, Li C, Zhou X, Zhao W, Zhong Y, He Z, Peng H, Dong A, Wang B. 2020. Neonatal priming and infancy boosting with a novel respiratory syncytial virus vaccine induces protective immune responses without concomitant respiratory disease upon RSV challenge. Hum Vaccines Immunother 16:664–672.

77. Lee JY, Chang J. 2017. Universal vaccine against respiratory syncytial virus A and B subtypes. PLoS One 12:1–19.

78. Cheon IS, Shim B-SS, Park S-MM, Choi Y, Jang JE, Jung DI, Kim J-OO, Chang J, Yun C-HH, Song MK, Cheon S, Shim B-SS, Park S-MM, Choi Y,

Jang JE, Jung DI, Kim J-OO, Chang J, Yun C-HH, Song K. 2014. Development of safe and effective RSV vaccine by modified CD4 epitope in g protein core fragment (GcF). PLoS One 9:1–10.

79. Kim S, Joo D-H, Lee J-B, Shim B-S, Cheon IS, Jang J-E, Song H-H, Kim K-H, Song K, Chang J. 2012. Dual Role of Respiratory Syncytial Virus Glycoprotein Fragment as a Mucosal Immunogen and Chemotactic Adjuvant. PLoS One 7.

80. Jo Y-M, Kim J, Chang J. 2019. Vaccine containing G protein fragment and recombinant baculovirus expressing M2 protein induces protective immunity to respiratory syncytial virus. Clin Exp Vaccine Res 43–53.

81. Li N, Zhang L, Zheng B, Li W, Liu J, Zhang H, Zeng R. 2019. RSV recombinant candidate vaccine G1F/M2 with CpG as an adjuvant prevents vaccine-associated lung inflammation, which may be associated with the appropriate types of immune memory in spleens and lungs https://doi.org/10.1080/21645515.2019.1596710.

82. Bergeron HC, Murray J, Nuñez Castrejon AM, Dubois RM, Tripp RA, Mccormick C. 2021. Respiratory Syncytial Virus (RSV) G Protein Vaccines With Central Conserved Domain Mutations Induce CX3C-CX3CR1 Blocking Antibodies. Viruses 13.

83. Zhang W, Choi Y, Haynes LM, Harcourt JL, Anderson LJ, Jones LP, Tripp RA. 2010. Vaccination To Induce Antibodies Blocking the CX3C-CX3CR1 Interaction of Respiratory Syncytial Virus G Protein Reduces Pulmonary

Inflammation and Virus Replication in Mice. J Virol 84:1148–1157.

84. Rey GU, Miao C, Caidi H, Trivedi SU, Harcourt JL, Tripp RA, Anderson LJ, Haynes LM. 2013. Decrease in Formalin-Inactivated Respiratory Syncytial Virus (FI-RSV) Enhanced Disease with RSV G Glycoprotein Peptide Immunization in BALB/c Mice https://doi.org/10.1371/journal.pone.0083075.

85. Khan IU, Huang J, Li X, Xie J, Zhu N. 2018. Nasal immunization with RSV F and G protein fragments conjugated to an M cell-targeting ligand induces an enhanced immune response and protection against RSV infection https://doi.org/10.1016/j.antiviral.2018.10.001.

86. Khan IU, Ahmad F, Zhang S, Lu P, Wang J, Xie J, Zhu N. 2018. Respiratory syncytial virus F and G protein core fragments fused to HBsAg-binding protein (SBP) induce a Th1-dominant immune response without vaccine-enhanced disease. Int Immunol 31:199–209.

87. Lee J, Klenow L, Coyle EM, Golding H, Khurana S. 2018. Protective antigenic sites in respiratory syncytial virus G attachment protein outside the central conserved and cysteine noose domains. PLoS One https://doi.org/10.1371/journal.ppat.1007262.

88. Nuñez Castrejon AM, O'Rourke SM, Kauvar LM, DuBois RM. 2022. Structure-Based Design and Antigenic Validation of Respiratory Syncytial Virus G Immunogens. J Virol 96.

89. G Blanco JC, Boukhvalova MS, Morrison TG, Vogel SN. 2018. A Multifaceted Approach to RSV Vaccination. Hum Vaccin Immunother 0.

90. Bont LJ, Nunes C, Mejias A, Falsey AR, Kragten-Tabatabaie L, Baraldi E, Papadopoulos NG, Polack FP, Stein RT, Mazur NI, Higgins D, Nunes MC, Melero JA, Langedijk AC, Horsley N, Buchholz UJ, Openshaw PJ, Mclellan JS, Englund JA, Mejias A, Karron RA, Simões EA, Knezevic I, Ramilo O, Piedra PA, Chu HY, Falsey AR, Nair H, Kragten-Tabatabaie L, Greenough A, Baraldi E, Papadopoulos NG, Vekemans J, Polack FP, Powell M, Satav A, Walsh EE, Stein RT, Graham BS, Bont LJ. 2018. The respiratory syncytial virus vaccine landscape: lessons from the graveyard and promising candidates. Lancet Infect Dis https://doi.org/10.1016/S1473-3099(18)30292-5.

91. Samy N, Reichhardt D, Schmidt D, Chen LM, Silbernagl G, Vidojkovic S, Meyer TP, Jordan E, Adams T, Weidenthaler H, Stroukova D, De Carli S, Chaplin P. 2020. Safety and immunogenicity of novel modified vaccinia Ankara-vectored RSV vaccine: A randomized phase I clinical trial https://doi.org/10.1016/j.vaccine.2020.01.055.

92. Jordan E, Lawrence SJ, Meyer TPH, Schmidt D, Schultz S, Mueller J, Stroukova D, Koenen B, Gruenert R, Silbernagl G, Vidojkovic S, Chen LM, Weidenthaler H, Samy N, Chaplin P. 2020. Broad Antibody and Cellular Immune Response From a Phase 2 Clinical Trial With a Novel Multivalent Poxvirus-Based Respiratory Syncytial Virus Vaccine. J Infect Dis ® 223:1062–72.

93. Hendricks DA, Baradaran K, Mclntosh K, Patterson ~' JL. 1987. Appearance of a Soluble Form of the G Protein of Respiratory Syncytial Virus in Fluids of

Infected Cells. J gen Virol 68:1705–1714.

94. Hendricks,' DA, Mcintosh K, Patterson2' JL. 1988. Further Characterization of the Soluble Form of the G Glycoprotein of Respiratory Syncytial Virus. J Virol 62:2228–2233.

95. Roberts,' Drew Lichtenstein SR, Ball,' And LA, Wertz' GW. 1994. The Membrane-Associated and Secreted Forms of the Respiratory Syncytial Virus Attachment Glycoprotein G Are Synthesized from Alternative Initiation Codons. J Virol 68:4538–4546.

96. Barr FE, Pedigo H, Johnson TR, Shepherd VL. 2000. Surfactant Protein-A Enhances Uptake of Respiratory Syncytial Virus by Monocytes and U937 MacrophagesAm. J. Respir. Cell Mol. Biol.

97. Hickling TP, Malhotra R, Bright H, Mcdowell W, Blair ED, Sim RB. 2000. Lung Surfactant Protein A Provides a Route of Entry for Respiratory Syncytial Virus into Host CellsVIRAL IMMUNOLOGY.

98. Hickling TP, Bright H, Wing K, Gower D, Martin SL, Sim RB, Malhotra R. 1999. A recombinant trimeric surfactant protein D carbohydrate recognition domain inhibits respiratory syncytial virus infection in vitro and in vivo. Eur J Immunol 29:3478–3484.

99. Levine AM, Elliott J, Whitsett JA, Srikiatkhachorn A, Crouch E, Desilva N, Korfhagen T. 2004. Surfactant Protein-D Enhances Phagocytosis and Pulmonary Clearance of Respiratory Syncytial Virus. Am J Respir Cell Mol Biol 31:193–199.

100. Ehl S, Bischoff R, Ostler T, Vallbracht S, Schulte-Mönting J, Poltorak A, Freudenberg M. 2004. The role of Toll-like receptor 4 versus interleukin-12 in immunity to respiratory syncytial virus. Eur J Immunol 34:1146–1153.

101. Lizundia R, Sauter K-S, Taylor G, Werling D. 2008. Host species-specific usage of the TLR4–LPS receptor complex. Innate Immun https://doi.org/10.1177/1753425908095957.

102. Marchant D, Singhera GK, Utokaparch S, Hackett TL, Boyd JH, Luo Z, Si X, Dorscheid DR, Mcmanus BM, Hegele RG. 2010. Toll-Like Receptor 4-Mediated Activation of p38 Mitogen-Activated Protein Kinase Is a Determinant of Respiratory Virus Entry and Tropism. J Virol 84:11359–11373.

103. Marr N, Turvey SE. 2012. Role of human TLR4 in respiratory syncytial virus-induced NF-iB activation, viral entry and replication. Innate Immun https://doi.org/10.1177/1753425912444479.

104. Malhotra R, Ward M, Bright H, Priest R, Foster MR, Hurle M, Blair E, Bird M. 2003. Isolation and characterisation of potential respiratory syncytial virus receptor(s) on epithelial cells. Microbes Infect.

105. Arnold R, König W. 2005. Respiratory Syncytial Virus Infection of Human Lung Endothelial Cells Enhances Selectively Intercellular Adhesion Molecule-1 Expression. J Immunol 174:7359–7367.

106. Liu X, Qin X, Xiang Y, Liu H, Gao G, Qin L, Liu C, Qu X. 2013. Progressive Changes in Inflammatory and Matrix Adherence of Bronchial Epithelial Cells with Persistent Respiratory Syncytial Virus (RSV) Infection (Progressive

Changes in RSV Infection). Int J Mol Sci 14:18024–18040.

107. Behera AK, Matsuse H, Kumar M, Kong X, Lockey RF, Mohapatra SS. 2001. Blocking Intercellular Adhesion Molecule-1 on Human Epithelial Cells Decreases Respiratory Syncytial Virus Infection. Biochem Biophys Res Commun 280.

108. Lingemann M, Mccarty T, Liu X, Buchholz Id UJ, Surman S, Martin SE, Collins PL, Munir Id S. 2019. The alpha-1 subunit of the Na + ,K +-ATPase (ATP1A1) is required for macropinocytic entry of respiratory syncytial virus (RSV) in human respiratory epithelial cells. PLOS Pathog https://doi.org/10.1371/journal.ppat.1007963.

109. Wellemans V, Benhassou HA, Fuselier E, Bellesort F, Dury S, Lebargy F, Dormoy V, Fichel C, Naour R Le, Gounni AS, Lamkhioued B. 2021. Role of CCR3 in respiratory syncytial virus infection of airway epithelial cells. iScience 24.

110. Fong AM, Alam SM, Imai T, Haribabu B, Patel DD. 2002. CX 3 CR1 Tyrosine Sulfation Enhances Fractalkine-induced Cell Adhesion*. J Biol Chem 277.

111. Johnson PR, Spriggs MK, Olmsted RA, Collins PL. 1987. The G glycoprotein of human respiratory syncytial viruses of subgroups A and B: Extensive sequence divergence between antigenically related proteins (viral attachment protein/O-linked glycosylation/protein structure). Biochemistry 84:5625–5629.

112. Green G, Johnson SM, Costello H, Brakel K, Harder O, Oomens AG, Peeples

ME, Moulton HM, Niewiesk S. 2021. CX3CR1 Is a Receptor for Human Respiratory Syncytial Virus in Cotton Rats. J Virol 95.

113. Johnson CH, Miao C, Blanchard EG, Caidi H, Radu GU, Hartcourt JL, Haynes LiM. 2012. Effect of Chemokine Receptor CX3CR1 Deficiency in a Murine Model of Respiratory Syncytial Virus Infection. Comp Med 62:14–20.

114. Das S, Raundhal M, Chen J, Oriss TB, Huff R, Williams J V, Ray A, Ray P. 2017. Respiratory syncytial virus infection of newborn CX3CR1-deficient mice induces a pathogenic pulmonary innate immune response. JCI insight https://doi.org/10.1172/jci.insight.94605.

115. Cepika AM, Gagro A, Bace A, Tjesic-Drinkovic D, Kelecic J, Baricic-Voskresensky T, Matic M, Drazenovic V, Marinic I, Mlinaric-Galinovic G, Tjesic-Drinkovic D, Vrtar Z, Rabatic S. 2008. Expression of chemokine receptor CX3CR1 in infants with respiratory syncytial virus bronchiolitis. Pediatr Allergy Immunol 19:148–156.

116. Zhivaki D, Bastien Lemoine S, Lim A, Zhang X, Tissiè P, Lo R, Correspondence M. 2017. Respiratory Syncytial Virus Infects Regulatory B Cells in Human Neonates via Chemokine Receptor CX3CR1 and Promotes Lung Disease Severity. Immunity https://doi.org/10.1016/j.immuni.2017.01.010.

117. Anderson CS, Chu C-Y, Wang Q, Mereness JA, Ren Y, Donlon K, Bhattacharya S, Misra RS, Walsh EE, Pryhuber GS, Mariani TJ. 2019. CX3CR1 as a respiratory syncytial virus receptor in pediatric human lung.

Pediatr Res https://doi.org/10.1038/s41390-019-0677-0.

118. Anderson CS, Chirkova T, Slaunwhite CG, Qiu X, Walsh EE, Anderson LJ, Mariani TJ. 2021. CX3CR1 Engagement by Respiratory Syncytial Virus Leads to Induction of Nucleolin and Dysregulation of Cilium-Related Genes. J Virol 95.

119. Fedechkin SO, George NL, Castrejon AMN, Dillen JR, Kauvar LM, Dubois RM. 2020. Conformational Flexibility in Respiratory Syncytial Virus G Neutralizing Epitopes. J Virol 94.

Appendix Co-authorship

A version of this paper was published in Journal of Virology

A1: Conformational Flexibility in Respiratory Syncytial Virus G Neutralizing Epitopes Fedechkin et al. 2020

I expressed RSV G^{ecto} and RSV G^{ecto} F170P and showed purity by SDS-PAGE. I used biolayer interferometry to test binding of these proteins to 3D3 and 3G12 monoclonal anti-RSV G antibodies. I showed that mutating phenylalanine at position 170 to proline to restrict the flexibility of RSV G prevented its binding to 3G12 mAb.

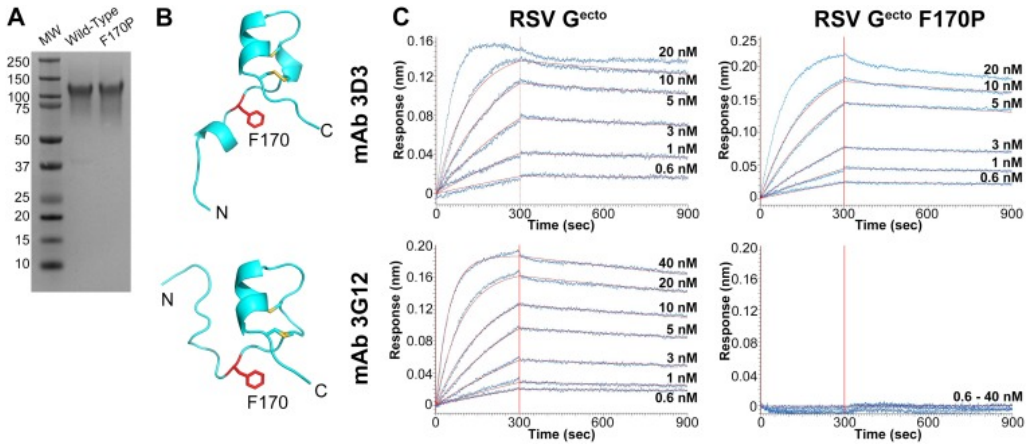

Figure 39: Differences in bnmAb 3G12 and bnmAb 3D3 binding to RSV G^{ecto} F170P.

(A) Coomassie-stained SDS-polyacrylamide gel of RSV G^{ecto} (wild type) and RSV G ecto F170P (F170P). Molecular weight (MW) ladder values (in kilodaltons) are labeled. (B) Structure of the RSV G CCD when bound to bnmAb 3D3 (top) and bnmAb 3G12 (bottom). F170 is in red. (C) Biolayer interferometry traces (blue) and curve fits (red) for binding of bnmAb 3D3 (top) and bnmAb 3G12 (bottom) to RSV G^{ecto} and RSV G^{ecto} F170P. Concentrations of G^{ecto} used for each trace are shown. The vertical red line indicates the transition of the biosensors from the association step to the dissociation step. Binding on-rates, off-rates, dissociation constants, and curve fit statistics are shown in Table 2.

Expression and purification of RSV G^{ecto} and RSV G^{ecto} F170P. A codon-optimized synthetic gene encoding RSV G (strain A2) amino acids 64 to 298 (UniProtKB accession number P03423) was cloned into pCF in frame with an N-terminal CCR5 signal sequence, a C-terminal His tag, and Twin-Strep purification tags. The F170P mutation was introduced by Phusion site-directed mutagenesis and verified by Sanger sequencing. Recombinant RSV G^{ecto} and RSV G^{ecto} F170P were produced by transient transfection in HEK293F cells with Effectene transfection reagent (Qiagen). After 5 days, cell medium was supplemented with BioLock (IBA) and 20 mM Tris-HCl (pH 8.0) and 0.22-?m filtered. RSV G^{ecto} and RSV G^{ecto} F170P

were batch purified from medium with Strep-Tactin resin (IBA), washed, and eluted with Strep-Tactin elution buffer (50 mM Tris [pH 8.0], 150 mM NaCl, 1 mM EDTA, 2.5 mM desthiobiotin). RSV G^{ecto} and RSV G^{ecto} F170P were concentrated and dialyzed into phosphate-buffered saline (PBS) using 10-kDa spin concentrators. Protein purity was evaluated by SDS-polyacrylamide gel electrophoresis.

Binding affinity analyses. An Octet RED96e biolayer interferometry instrument was used to evaluate the binding of bnmAbs 3G12 and 3D3 to RSV G^{ecto} and RSV G^{ecto} F170P. Antibody 3G12 or 3D3 at 1 ug/ml in Octet buffer (phosphate-buffered saline [pH 7.4], 0.05% Tween 20, 1% bovine serum albumin [BSA]) was loaded onto anti-human IgG Fc capture (AHC) biosensors, and 2-fold serially diluted RSV G^{ecto} or RSV G^{ecto} F170P, from 40 nM to 0.625 nM, was assessed for binding. Red lines are the fit of global association and dissociation with a 1:1 model, with at least 5 curves used to determine binding on- and off-rates and to calculate dissociation constants.

A version of this paper was published in Viruses

A2: Respiratory Syncytial Virus (RSV) G Protein Vaccines With Central Conserved Domain Mutations Induce CX3C-CX3CR1 Blocking Antibodies

Bergeron et al 2021

I expressed and purified RSV G^{ecto} WT, S177Q, S177R, and CX4C. I used SDS-PAGE to test for purity and Coot to overlay the RSV G structure with the 2D10, 3G12, and 3D3 anti-RSV G monoclonal antibodies and model the mutant proteins. These immunogens were used to immunize mice. Mice were challenged with RSV and antibody levels of these mice were measured before and after RSV challenge.

These antibodies were also used to block the interaction of RSV G and CX3CR1 on HEK293 cells that over express CX3CR1. RSV G S177Q was measured to elicit higher levels of antibodies compared to wild-type RSV G or the other mutant proteins, and it lowered BAL cell influx into the lungs of immunized challenged mice.

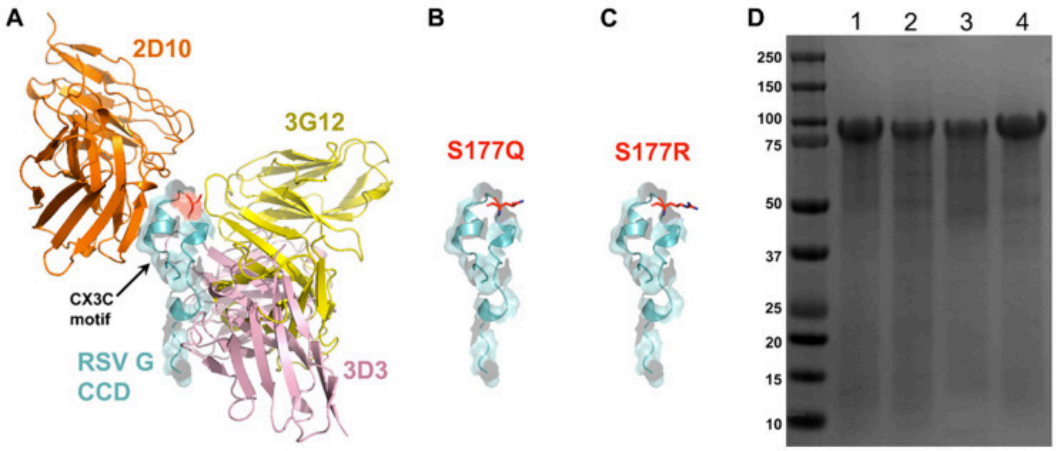

Figure 40: Rational design and expression of RSV G protein immunogens.

(A) RSV G protein central conserved domain (CCD) (cyan) with CX3C motif highlighted, and sites of anti-G protein mAb binding: 2D10 (orange), 3G12 (yellow), and 3D3 (magenta). Serine 177 mutations modeled with (B) glutamine and (C) arginine. (D) Coomassie-stained SDS-PAGE gel of RSV G protein immunogens at ~90kDa. Lane 1: wild-type, lane 2: CX4C, lane 3: 177R, lane 4: 177Q.

2.2. Immunogens A synthetic gene encoding RSV strain A2 (RSV/A2) G protein amino acids 64 to 298 (UnitProtKB entry P03423) was cloned into pCF in-frame with an N-terminal TPA signal sequence and C-terminal tandem 6-histidine and Twin-Strep purification tags. Recombinant RSV G protein was produced by transient-transfection in CHO-S cells (Thermo Fisher Scientific, Waltham, MA, USA #R800-07) and secreted RSV G protein was affinity purified on a StrepTrap column (GE

Healthcare Bio-Sciences, Uppsala, Sweden). Mutants were produced by Phusion site-directed mutagenesis and verified by Sanger sequencing. The CX4C mutant contained an insertion of an alanine within the CX3C motif, making it to 182CWAIAC187. Mutants S177Q and S177R contained serine177 substitution with glutamine or arginine, respectively. All proteins were concentrated and dialyzed into PBS. Proteins were flash-frozen in liquid nitrogen and stored at −80 ◦C until use. SDS-polyacrylamide gel electrophoresis was used to evaluate protein purity.

A3: Overall Thesis Summary

Respiratory syncytial virus is the leading cause of death of children world-wide and contributes to respiratory disease in immunocompromised and elderly populations. Currently there are no FDA approved vaccines or anti-virals to protect against RSV infection. Palivizumab, an anti-RSV F antibody, is the only prophylaxis available and it does reduce hospitalizations, however a more effective vaccine or prophylaxis is urgently needed.

RSV G is an important antigen to consider in vaccine developmental strategies. While RSV G has been shown to induce a Th2 response and eosinophilia in RSV infected animals, antibodies against RSV have been shown to be protective *in vivo* thus a vaccine that can induce anti-RSV G antibodies could potentially be more effective than Palivizumab (as some studies have shown) (Chapter one).

I produced an RSV G vaccine immunogen with a single point mutation using the published structures of RSV G bound to neutralizing antibodies. I showed through biolayer interferometry, ELISA, and X-ray crystallography that the single point

mutation did not disrupt epitopes on RSV G for neutralizing antibodies. I also showed that it is important to keep the structure in mind when developing a vaccine immunogen as the RSV G mutant protein CX4C that was developed before the structure of RSV G was solved had disrupted epitopes. Furthermore, I showed that the RSV G S177Q mutant protein is a promising vaccine immunogen (Chapter two).

I also analyzed the interaction between RSV G and CX3CR1 through various cell-based assays. I found that GFP fused to RSV G bound to THP1 cells (that express CX3CR1), however removing part of the heparin binding domain of RSV G reduced binding. I also found that RSV G is chemotactic but it is not clear if the activity is through the CX3CR1 chemokine receptor. Finally, I showed that the natural ligand of CX3CR1 called Fractalkine was able to activate CX3CR1 in a cell-based assay called Presto Tango, however RSV G did not activate CX3CR1. These data show that the interaction between RSV G and CX3CR1 needs further investigation (Chapter three).

Finally, I contributed to two published papers. In the first paper, Fedechkin et al., 2020 (section A1), I showed that mutating phenylalanine at position 170 of RSV G to proline restricted the flexibility of RSV G and prevented its binding to 3G12 mAb. In the second paper, Bergeron et al., 2021 (section A2), I produced the wild-type RSV G and mutant proteins that were used as vaccine immunogens.